

The Study of Plume Activity and Cloud Environment
Jupiter Aerocapture Mission
(SPACE-JAM)

Robert Aaron, Stan Barlow, Jacob Killelea, Yu-Hsuan Kuo, Jacob Margulies,
Adam New, Jacob Rehmeier, Annika Rollock, Timothy Sullivan, Logan Thompson

May 13, 2019

Contents

1	Introduction	5
2	PDR Success Criteria	5
2.1	RFA Closure	6
3	Mission Overview	7
3.1	Specific Terminology	7
3.2	Mission Objectives	7
3.3	Requirements	8
3.3.1	Change Requests	8
3.3.2	Level I Requirements	8
3.3.3	Level II Requirements	9
3.4	Concept of Operations	9
4	System Level	11
4.1	Level III Spacecraft Requirements and Compliance Summary	11
4.2	Summary of Error Budgets	11
4.3	System-Level Performance Metrics	12
4.4	System-Level Trade Studies	13
5	Subsystem Level	13
5.1	Mission Design	13
5.1.1	Trajectories to Jupiter	13
5.1.2	Baseline Mission Design	14
5.1.3	Jupiter Aerocapture	17
5.1.4	Jupiter Science Orbit Design	21
5.1.5	Cruise Simulation	22
5.1.6	Jupiter Orbit Simulation	24
5.1.7	Delta-V Budget	24
5.1.8	Earth Re-entry	24
5.1.9	Risk Assessment	25
5.2	Flight Software	26
5.2.1	Critical Events	28
5.2.2	Robustness	29
5.3	Environment	29
5.3.1	Solar Flux and Power Source Choices	30
5.3.2	Magnetic and Radiation Fields	30
5.3.3	Radiation Doses	31
5.4	Structure and Mechanical System	32
5.4.1	Structure subsystem Level IV Requirements	32
5.4.2	Aerocapture Method Trade Study	32
5.4.3	Material Selection	33
5.4.4	Orbital Stage Design	34
5.4.5	Entry Stage Design	38
5.4.6	Cruise Stage Design	39
5.4.7	Separation Mechanism	40
5.4.8	Simulation Results	41
5.4.9	Risk	42
5.5	Thermal System	42
5.5.1	Thermal Level IV Requirements	43
5.5.2	Operating Temperature	44
5.5.3	Thermal Environment	44
5.5.4	Thermal Design	45
5.5.5	Thermal Analysis	46
5.5.6	Thermal Risks and Mitigation Plan	47
5.6	Electric and Power System	48
5.6.1	Requirements	48

5.6.2	Power Selection	48
5.6.3	RTG Performance	49
5.6.4	System Overview	50
5.6.5	Power Distribution Unit	50
5.6.6	Power Budget	51
5.6.7	Battery Sizing	53
5.6.8	Risk	53
5.7	Command and Data Handling	54
5.7.1	Requirements	54
5.7.2	Trade Study	56
5.7.3	Memory Allocation	57
5.7.4	Risk Assessment	57
5.8	Attitude Determination and Control System	57
5.8.1	ADCS Requirements	58
5.8.2	Design Options and Trades	60
5.8.3	ADCS PDR Configuration	61
5.8.4	Pointing Control	63
5.8.5	Pointing Error	65
5.8.6	Detumbling	65
5.8.7	Entry Guidance	66
5.8.8	Entry Guidance Block Diagram	66
5.9	Propulsion System	67
5.9.1	Propulsion Subsystem Level IV Requirements	67
5.9.2	ΔV Requirements	68
5.9.3	Propellant Selection	68
5.9.4	Propellant and Tank Sizing	69
5.9.5	Pressurant and Tank Sizing	71
5.9.6	Thruster Selection	72
5.9.7	Propulsion Plumbing	73
5.9.8	Risk	74
5.10	Telecommunications	75
5.10.1	Component Overview	77
5.10.2	Cruise Phase Operations	77
5.10.3	Orbital Phase Operations	78
5.10.4	HGA Link Performance	79
5.10.5	MGA Link Performance	79
5.10.6	Telecommunications Risk	80
5.11	Operations and Ground Support	81
6	System-level Risks and Mitigation Plan	81
6.1	Red Risk Items	82
6.2	Yellow Risk Items	82
6.2.1	RTG Cost	82
6.2.2	Aerocapture Failure	82
6.2.3	Aerocapture Apojoove Target Failure	82
6.3	Green or Grey Risk Items	82
6.3.1	Failure to Raise Perijove	83
6.3.2	Launch Failure	83
7	Development Cost and Schedule	83
7.1	Cost Breakdown	83
7.1.1	Discussion of Cost Estimate Methods	84
7.1.2	Discussion of Labor Costs	84
7.1.3	Discussion of RTG Cost	85
7.1.4	Discussion of Cost Risk	85
7.2	Schedule	85
8	TBR Requirement Resolution	87

9 Appendix	87
9.1 Imaging Frequency calculations	87
9.2 Carrier Link and Data Rate Calculations	89
10 Acknowledgements	89

1 Introduction

This document defines the Study of Plume Activity and Cloud Environment Jupiter Aerocapture Mission (SPACE-JAM) mission requirements, as well as the pre-phase A design. The initial mission constraints fix the launch date within the 2023 opportunity and state that the spacecraft must arrive before 2030. The spacecraft must then complete the science mission within 3 years of arrival and ensure planetary protection following mission completion. These requirements and the subsequent design flowdown are addressed throughout the following document.

2 PDR Success Criteria

As defined in the NASA Systems Engineering Handbook [1], the success criteria for the Preliminary Design Review (PDR) can be defined as follows:

PDR Success Criteria	
Criteria	Resolution
1. The top-level requirements—including mission success criteria, TPMs, and any sponsor-imposed constraints—are agreed upon, finalized, stated clearly, and consistent with the preliminary design.	See section 3.3.2 for details on the level 1 requirements that address both the sponsor-imposed constraints and section 3.3.1 for the change requests regarding these requirements. Requests for Action (RFAs) from the Concept Design Review (CoDR) are addressed within this section.
2. The flowdown of verifiable requirements is complete and proper or, if not, an adequate plan exists for timely resolution of open items. Requirements are traceable to mission goals and objectives.	Sections 3.3.3 and 4.1 detail the flowdown of high level mission goals to subsequent level I and II requirements. Specific subsystem requirements can be found in the specific subsystem sections under section 5.
3. The preliminary design is expected to meet the requirements at an acceptable level of risk.	Individual subsystem risks can be found under their respective sections in section 5. The spacecraft risk mitigation plan can be found in section 6.
4. Definition of the technical interfaces is consistent with the overall technical maturity and provides an acceptable level of risk.	Technical interfaces, block diagrams, subsystem requirements, and risks can be found under their respective subsystem sections under section 5. The level IV requirements are consistent with the level of fidelity expected at PDR and can also be found under 5.
5. Adequate technical interfaces are consistent with the overall technical maturity and provide an acceptable level of risk.	See block diagrams and level IV requirements at the subsystem levels in section 5.
6. Adequate technical margins exist with respect to TPMs.	Design margins have been considered, calculated in accordance with the subsystem factors and conventions, and added to the spacecraft design. Details on specific subsystem margins can be found in 5.

7. Any required new technology has been developed to an adequate state of readiness, or backup options exist and are supported to make them a viable alternative.	All of the technology in this spacecraft design has been flight tested and successfully flown at the outer planets, with an exception for the technology specifically for the aerocapture event. As an aerocapture maneuver has never been flown before, this is a critical risk for the mission and is discussed further in section 6.
8. The project risks are understood and have been credibly assessed, and plans, a process, and resources exist to effectively manage them.	The risk mitigation plan is discussed in detail in section 6.
9. SMA (e.g., safety, reliability, maintainability, quality, and EEE parts) has been adequately addressed in preliminary designs and any applicable SMA products (e.g., PRA, system safety analysis, and failure modes and effects analysis) have been approved.	SMA was a driving factor behind every design decision, and is discussed further in each subsystem section as well as section 6.
10. The operational concept is technically sound, includes (where appropriate) human factors, and includes the flowdown of requirements for its execution.	The operational concept is detailed in section 3.4 and 5.1. The requirement flowdown from this concept is included in the level I-IV requirements that are further detailed in sections 3.3.2, 3.3.3, 4.1, and 5.

2.1 RFA Closure

Following the CoDR presentation, four RFAs were expressed and have subsequently been closed in the work leading to PDR. These closures are summarized in the table below.

RFA Closure	
RFA #	Resolution
1. Description: The entry interface conditions were well defined, but the entry corridor was ill-defined. Action: Extend the entry interface definition to include the aerocapture corridor for safe/successful aerocapture pass.	The entry corridor was refined as more design knowledge was acquired. In order to successfully simulate entry, the vehicle's general size and mass properties, as well as arrival velocity, had to be known. As a result, the entry corridor is now defined as the range of vehicle flight path angles that will result in successful aerocapture. This range is between 8.3-8.4 (TBR) degrees.
2. Description: Requirements derivation includes both function and performance. Performance allocations are missing and decomposition of Level II requirements into Level III. Action: Develop companion performance requirements and allocation values with TBRs to be resolved by PDR and decompose Level II requirements into the complete set of Level III requirements.	See subsequent requirement breakdowns in section 3.3.3 and 4.1 for refined requirements and added performance allocation.

<p>3. Description: ADCS block diagram and other subsystem block diagrams are missing key components.</p> <p>Action: Update ADCS block diagram to reflect proper selection of components.</p>	<p>See section 5.8 and other subsystem sections in section 5 for complete block diagrams.</p>
<p>4. Description: Division of roles and responsibilities for Systems Engineering (SE) efforts is unorthodox and has the potential to miss important connections across the system.</p> <p>Action: Monitor approach, adjust as necessary and measure the success. Report findings.</p>	<p>The unconventional team structure will be discussed further in the PDR presentation with the PIs.</p>

3 Mission Overview

The aim of this mission is to utilize an aerocapture pass around Jupiter in order to enable a plume study of the four Galilean moons: Io, Europa, Ganymede, and Callisto. The science requirements and subsequent spacecraft requirements will be detailed in the following sections.

3.1 Specific Terminology

As this mission includes multiple phases and overall spacecraft configurations, it is necessary to define some terminology that will be used throughout the document. These terms are listed here for convenience and initial clarification.

The term "cruise stage" refers to the configuration of the spacecraft en route to Jupiter. This stage will be detached before the aerocapture pass.

The term "entry stage" refers to the configuration of the spacecraft following cruise separation. This includes the heat shield and back shell, which will protect the spacecraft during the atmosphere pass. The drag skirt will be part of this configuration until jettison.

Within the entry stage, "aeroshell" refers to the encapsulating structure that contains the orbiter, separate from the drag skirt. The "back shell" is the part of this on the back of the spacecraft that will not be flow facing, while the "heat shield" is the front of the entry stage that will be directly in line with the flow.

The term "orbiter" refers to the final configuration of the spacecraft, and will be housed inside the "entry stage" before and during aerocapture, and attached to the "cruise stage" en route to Jupiter.

The term "spacecraft" shall refer vaguely to the final orbiting stage during any point of the mission, whether or not the cruise or entry stages are present and attached.

3.2 Mission Objectives

The mission objectives are as follows:

1. Solve the technical challenges of using aerocapture (not aerobraking) to orbit a gas giant
2. Characterize the upper atmosphere during the aerocapture pass
3. Observe and characterize (frequency and spatial distribution) plume activity on the 4 primary Jovian moons

3.3 Requirements

3.3.1 Change Requests

It is notable that a change request was submitted for the initial requirement OPS-04. The change reflects the resolution of an inconsistency in two conflicting science requirements, and is detailed below.

SPACEJAM Change Requests		
CR #	Summary	Effect
1	Change 10,000 km closest approach distance to 1.5 million km. This satisfies a 10km pixel resolution for the moons + 25% margin, and therefore a total surface resolution of 7.5 km.	This change will primarily effect the science and mission design teams. It will allow more moon passes and observations per orbit, and the mission will be less likely to require an extension to meet the science requirement.

3.3.2 Level I Requirements

Table 3: Level I Requirements

Req. No.	Requirement
MSN-01	The mission shall solve the technical challenges of using Aerocapture to orbit a gas giant.
MSN-02	The mission shall characterize the upper atmosphere of Jupiter during the Aero-capture pass.
MSN-03	The mission shall observe and characterize (frequency, duration and spatial distribution) plume activity on the 4 primary Jovian moons.

3.3.3 Level II Requirements

Table 4: Level II Requirements

Req. No.	Requirement	Rationale
GEN-01	The mission shall include designated payload and Aerocapture concept.	This requirement is driven by the customer and principal investigator.
LS-01	The mission shall launch in 2023.	This requirement is driven by the customer and principal investigator.
FS-01	The reference spacecraft shall arrive at the target body (Jupiter) at or before 2030.	This requirement is driven by the customer and principal investigator.
OPS-01	The mission shall have a 3-year mission duration after arrival at the target body (Jupiter).	This requirement is driven by the customer and principal investigator.
OPS-02	The mission shall provide 7.5 km knowledge of plume origin on the surface.	This requirement is driven by the customer and principal investigator. . *Affected by CR-1
OPS-03	The mission shall fulfill the frequency in number of plumes per day and 1 hr accuracy on duration.	This requirement is driven by the customer and principal investigator.
OPS-04	The mission shall orbit on a trajectory which allows for closest approach distance of 1.5 million km.	This requirement is driven by OPS-02. *Affected by CR-1
OPS-05	The mission shall record acceleration data from aerospace at $1m/s^2$ resolution from 0-40 g's.	This requirement is driven by the customer and principal investigator.
GS-01	The mission shall be capable to communication with ground station, minumin 1 ground station.	This requirement is driven by the customer and principal investigator.

It is note-worth that both OPS-02 and OPS-04 were affected by the change request, as the new distance allowed for a 25% margin on the plume knowledge accuracy.

3.4 Concept of Operations

The concept of operations for this spacecraft flow down from the overarching mission requirements and trajectory design. The target launch window for this mission is centered around May 25th, 2023 out of the Cape Canaveral launch site. The planned trajectory is a Venus-Earth-Mars-Earth flyby series, which will minimize C3 while allowing the spacecraft to arrive at Jupiter before the end of the year in 2030. After orbit insertion via aerocapture, the spacecraft will then begin its three year science mission and moon observation. Following completion of this mission, the spacecraft will be enter a disposal trajectory in accordance with planetary protection.

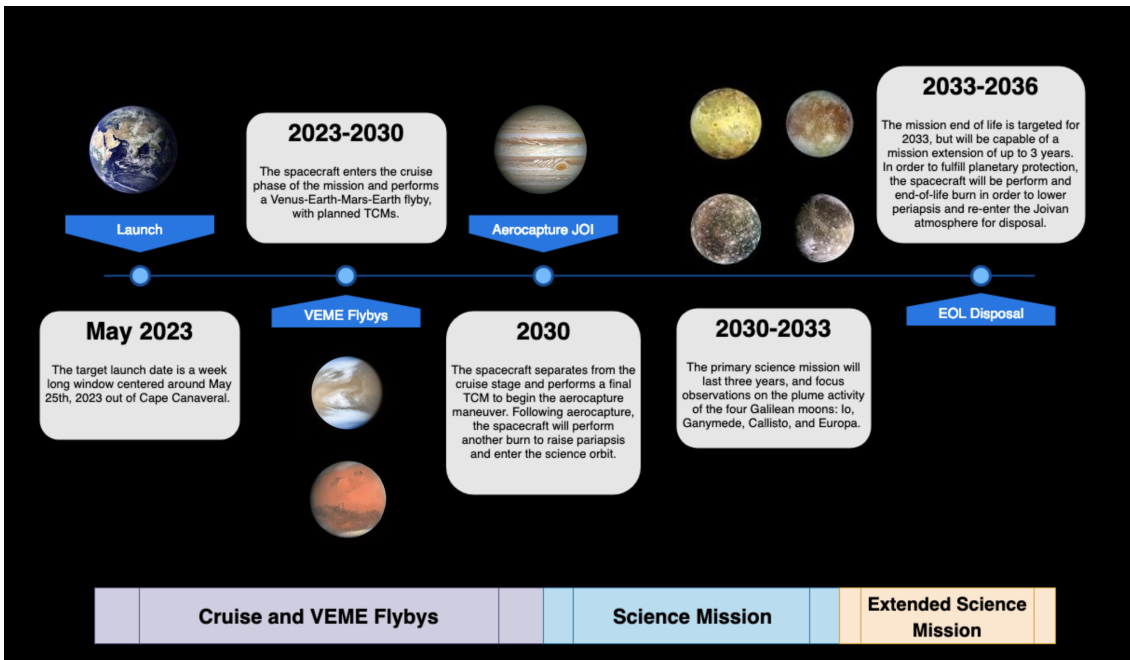


Figure 1: An illustration of the SPACEJAM mission concept of operations, from launch to end of life (EOL) and disposal.

Figure 1 summarizes the high-level concept of operations, which will be explored in more detail within the mission design in section 5.1. A concept of the aerocapture maneuver is provided below:

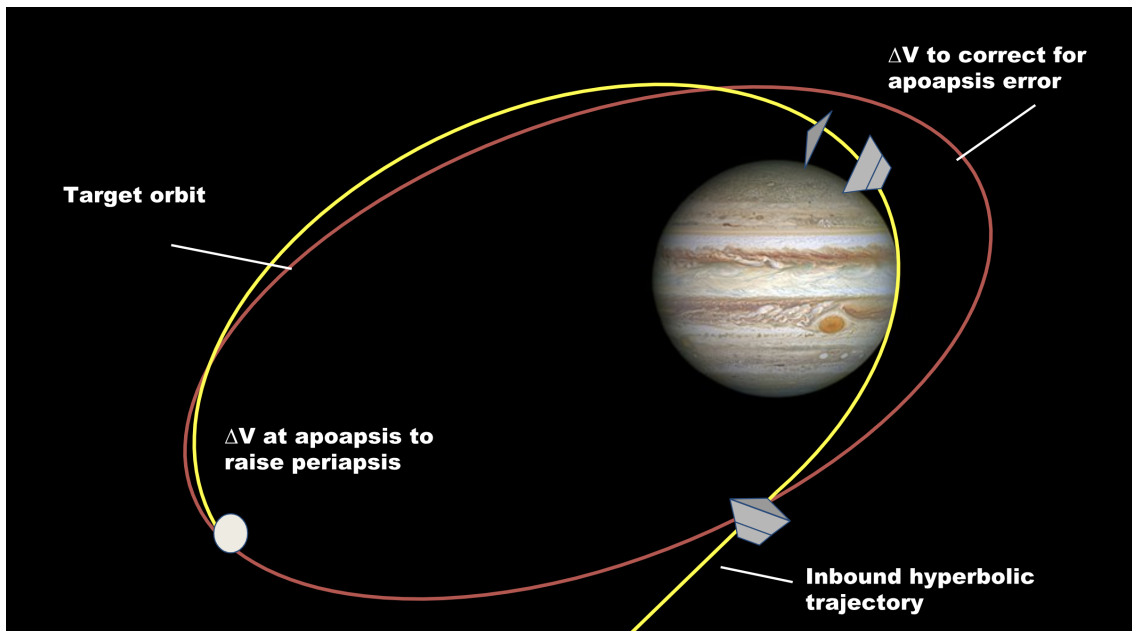


Figure 2: An illustration of the SPACEJAM aerocapture concept of operations.

Figure 2 is a graphical representation of the aerocapture maneuver, and as a result does not show the complete details of the event. For completeness, the specifics of each stage of the aerocapture maneuver are provided in the mission design section 5.1. However, a summary will be provided in this section.

The spacecraft will jettison the cruise stage and place that stage onto a disposal trajectory towards Jupiter. The spacecraft will then enter Jupiter's atmosphere at 60 km/s in its entry configuration

with drag skirt attached. When this velocity takes into account the rotation of the target body, the effective entry velocity will be 72 km/s, with a target entry flight path angle window of 8.1-8.2 degrees from azimuth. Part way through the atmospheric flight, the spacecraft will jettison the drag skirt in order to change its ballistic coefficient and exit the atmosphere at 57.5 km/s. Upon exit of the atmosphere, the spacecraft will jettison the aeroshell - both heat shield and backshell - in order to begin the orbital science phase of the mission.

The spacecraft will then need to re-acquire signal with the Earth and determine the resulting orbit post-aerocapture. In order to avoid re-entering the Jovian atmosphere, the spacecraft must also perform a burn to raise periapsis, which is discussed in later sections.

4 System Level

4.1 Level III Spacecraft Requirements and Compliance Summary

Table 5: Level III Requirement

Req. No.	Requirement	Rationale
SC-01	The reference spacecraft shall maintain 3-axis stabilization and provide desired pointing during the mission.	Functional flowdown and to ensure mission success.
SC-02	The reference spacecraft shall maintain structural stability throughout the entire mission.	Functional flowdown and to ensure mission success.
SC-03	The reference spacecraft shall retain temperature within operation temperature of all the components.	Functional flowdown and to ensure mission success.
SC-04	The reference spacecraft shall be capable to send out command, storage data, manage and monitor each spacecraft system.	Functional flowdown and to ensure mission success.
SC-05	The reference spacecraft shall be power positive in all modes throughout the entire mission.	Functional flowdown and to ensure mission success.
SC-06	The reference spacecraft shall be capable to accelerate and control RCS.	Functional flowdown and to ensure mission success.
SC-07	The reference spacecraft shall be capable of communicating, transiting data, and receiving command with GS through Deep Space Network.	Functional flowdown and to ensure mission success.
SC-08	The reference spacecraft shall have software system to operate mission by following mission schedule.	Functional flowdown and to ensure mission success.

4.2 Summary of Error Budgets

A summary of the error budgets within each subsystem is displayed in Figure 3.

Error Budget				
Subsystem	Parameter	Value	Unit	Notes
Mission Design	Exit V Error	< 1%	m/s	Aerocapture Event
	Entry Speed	500	m/s	
	Entry Height	5000	m	
	ΔV	190	m/s	
Structures	Mass	20%	kg	Margin
Propulsion	ΔV	52%	m/s	Margin
ADCS	Pointing Error	6.00	mrad	3 σ
Telecomm	MGA Link Margin	3.01	dB	
FSW	Memory Margin	1	MB	Regular interval calling
C&DH	Memory	10%	MB	Margin

Figure 3: Error Budget Overview

4.3 System-Level Performance Metrics

A summary of notable performance metrics within each subsystem is displayed in Figure 4.

Performance Metrics					
Subsystem	Parameter	Value		Unit	Notes
Mission Design	Drag Coefficient	0.003			Aerocapture Event
	Exit Velocity	56.9	57.1	km/s	Min/Max
	Initial Apojove	2.1	2.6	Mm	Min/Max
Propulsion	DV Budget, Cruise	155.1		m/s	
	DV Budget, Orbital	429.6		m/s	
	DV Budget, Total	584.7		m/s	
	Fuel	416.2		kg	
Structures	Maximum Load	575,000		N	Aerocapture Event
	Dry Mass, Orbital	924.1		kg	
	Length, Orbital	3.08		m	
	Diameter, Orbital	2.37		m	
	Mass, Entry	1,891.80		kg	Aerocapture Entry Mass
	Diameter, Heat Shield	2.5		m	
	Wet Mass, Cruise	2,417.10		kg	Launch Mass
	Length, Cruise	3.49		m	
	Diameter, Cruise	5		m	
Thermal	Operating Temperature	-20	60	C	Min/Max
EPS	Power, Science	80.9	96.73	W	Nominal / Peak
	Power, Downlink	117.5	132.55	W	Nominal / Peak
	Power, Cruise	84.9	101.53	W	Nominal / Peak
	Battery Size	400		Wh	
	Battery Recharge Time	11.19		h	
	Memory	128	512	MB	RAM / Flash
CDH	Throughput	256		MB/s	SpaceWire Link
Telecomm	Transmit Frequency	8.4		GHz	HGA and MGA
	Range	6.45		AU	HGA and MGA
ADCS	Slew Rate	2		deg/sec	Approx. per axis
	Angular Acceleration	0.04		deg/sec^2	Approx. per axis

Figure 4: Performance Metrics Overview

4.4 System-Level Trade Studies

5 Subsystem Level

This section presents an overview of the design of each subsystem. Each subsection includes Level IV subsystem requirements, system block diagrams, and a risk assessment. Risk assessments are defined by the criteria as described in the Spacecraft Systems Engineering textbook[2]:

Red:	unresolved, likely, imminent and/or severe in effect
Yellow:	potentially severe effects and/or growing likelihood
Green:	small likelihood and/or effect
Grey:	retired risk, no longer a threat

5.1 Mission Design

5.1.1 Trajectories to Jupiter

Several trajectory options to Jupiter were considered in order to meet mission requirements including direct transfer and gravity assist trajectories. As Jupiter's orbital radius is approximately 5.2 AU, an extremely high C3 is required for launch to a direct transfer to Jupiter.

Two gravity assist trajectories exist with launch opportunities in 2023 arriving on or before 2030. The first is a Venus-Venus-Venus (VVV) gravity assist trajectory and the second is an Venus-Earth-Mars-Earth (VEME) gravity assist each departing around May 2023 [3]. The un-optimized starting parameters for these trajectories are listed in Table 6. Since the VEME trajectory is preferable in all measures it was chosen and optimized to reduce the required C3 and minimize the necessary ΔV during TCMs enroute to Jupiter.

Trajectory	Launch	C3 (km^2/s^2)	Arrival V_∞ (km/s)	Duration (years)
Direct	July 2023	80.5	5.8	2.2
VVV	May 2023	30.3	7.0	6.9
VEME	May 2023	10.5	5.6	6.4

Table 6: Initial 2023 Gravity Assist Trajectories

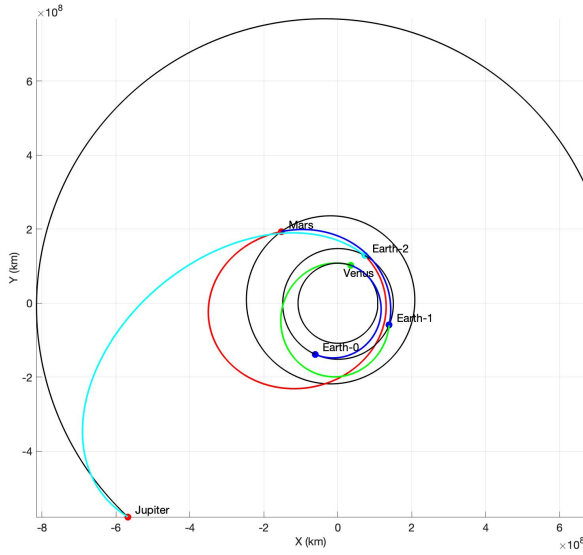


Figure 5: VEME Trajectory

5.1.2 Baseline Mission Design

Interplanetary Trajectory

The lowest energy launch required for the chosen VEME trajectory requires a C3 of about $9.9 \text{ km}^2/\text{s}^2$ occurring around the 26 May 2023. From this date additional launch and flyby dates were explored and an optimal launch date of 25 May 2023 was selected due to its low C3 requirement of $10.03 \text{ km}^2/\text{s}^2$ and low theoretical TCM ΔV requirement of approximately 6 m/s under two body assumptions. Arrival V_∞ were roughly equal between trajectories and all reached Jupiter prior to 2031. From this low-fidelity trajectory, a high-fidelity solution was computed using GMAT resulting in the trajectory depicted in Table 7. The nominal TCM ΔV budget is 91.66 m/s from which the overall TCM ΔV requirements were determined using simulation. The trajectory utilizes TCMs prior to the various flybys which greatly reduces the necessary ΔV required for each maneuver. Due to the required inclination adjustment during the trajectory between Earth and Jupiter, a second large TCM is required to arrive at the correct inclination at Jupiter. Several additional TCMs are scheduled during each section of the trajectory to correct for accumulated errors from the nominal trajectory depicted in Table 7.

Event	Flyby Date	TCM Date	TCM (m/s)	$R_{\text{Periapsis}}$ (km)	Flyby Altitude (km)
VGA	20 Oct 2023	NA	NA	16386.7	10334.7
EGA1	29 Aug 2024	16 Oct 2023	2.692	8648.8	2277.8
MGA	13 Feb 2025	19 Aug 2024	6.428	4939.4	1550.4
EGA2	22 Nov 2026	02 Feb 2025	2.842	7811.1	1440.1
		27 Feb 2025	77.37		
Jupiter	26 Feb 2030	12 Nov 2026	2.323		
Total			91.66		

Table 7: Nominal Trajectory 25 May 2023 Launch

The spacecraft will encounter four solar conjunctions during its cruise to Jupiter in which the sun will come between the Earth and the spacecraft making communication with the spacecraft difficult or impossible. As such, no TCMs are scheduled around these times. The spacecraft's distance from the Sun and Earth is shown in Figure 6 and the maximum conjunction dates are shown in Table 6. After arrival, solar conjunctions will occur roughly once a year.

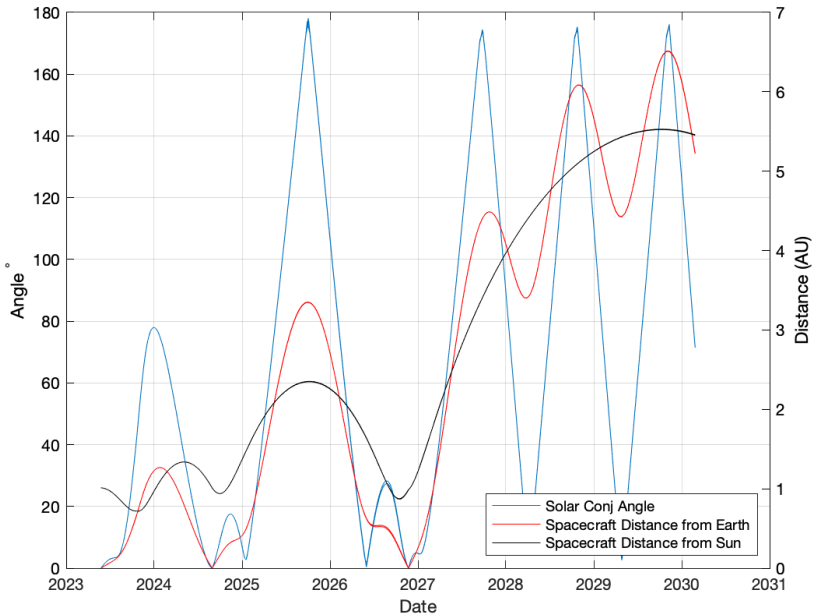


Figure 6: Cruise Spacecraft Distances and Solar Conjunction

Conjunction	Date
1	30 Sep 2025
2	23 Sep 2027
3	17 Oct 2028
4	1 Nov 2029

Table 8: Dates of Solar Conjunction Maximum

Launch

The chosen launch date of 25 May 2023 occurs early during an approximately week-long period in which the C3 necessary to reach Jupiter through the VEME trajectory is around $10 \text{ km}^2/\text{s}^2$. The flight time and V_∞ for this period is fairly constant, making C3 the primary factor in launch window selection, Figure 7.

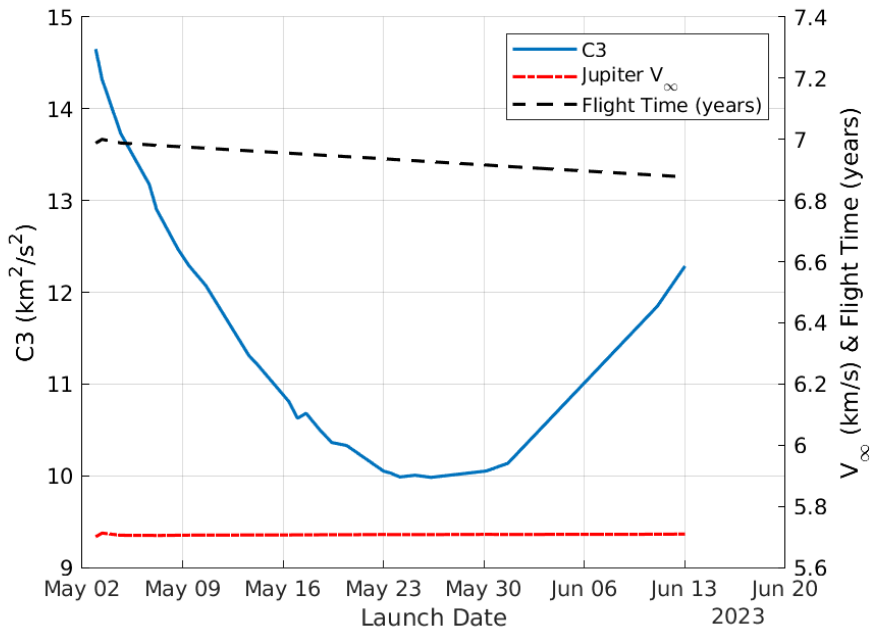


Figure 7: 2023 Launch Opportunity

Since the spacecraft diameter prohibits using an Atlas V 4m fairing and with a spacecraft launch mass below 2500kg (allowing for launch vehicle integration mass of up to 100kg), the proposed launch vehicle for this mission is the Atlas V (521). The spacecraft mass falls outside the capability of the Atlas V (511) and the 531 variant is more powerful than necessary for this mission, see Figure 8. The Atlas V (521) allows for a three-week launch window opening May 16 2023 and closing on June 6 not limited by launch vehicle performance, illustrated in Figure 9.

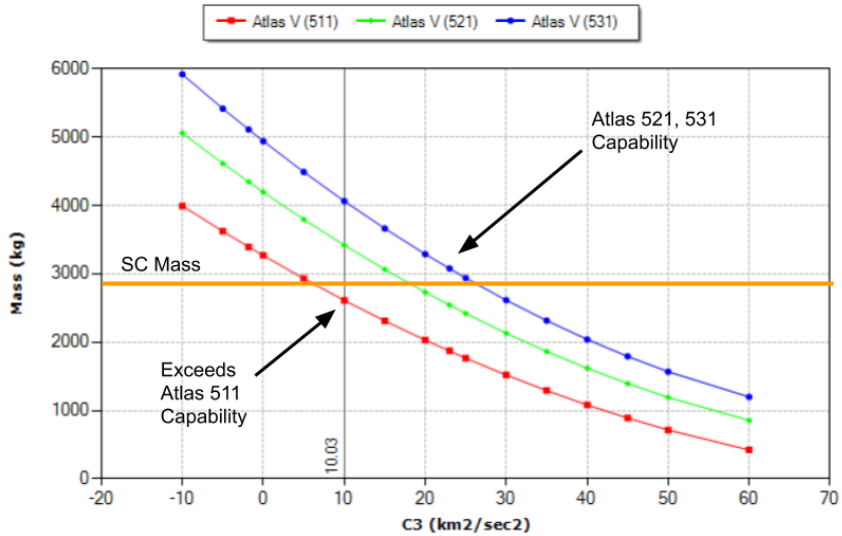


Figure 8: Launch Vehicles

Figure 9 shows the change in required DLA over the launch period in the ecliptic frame which declines as the launch window progresses. All simulations in GMAT were started from a LEO inclined 50° from the equator.

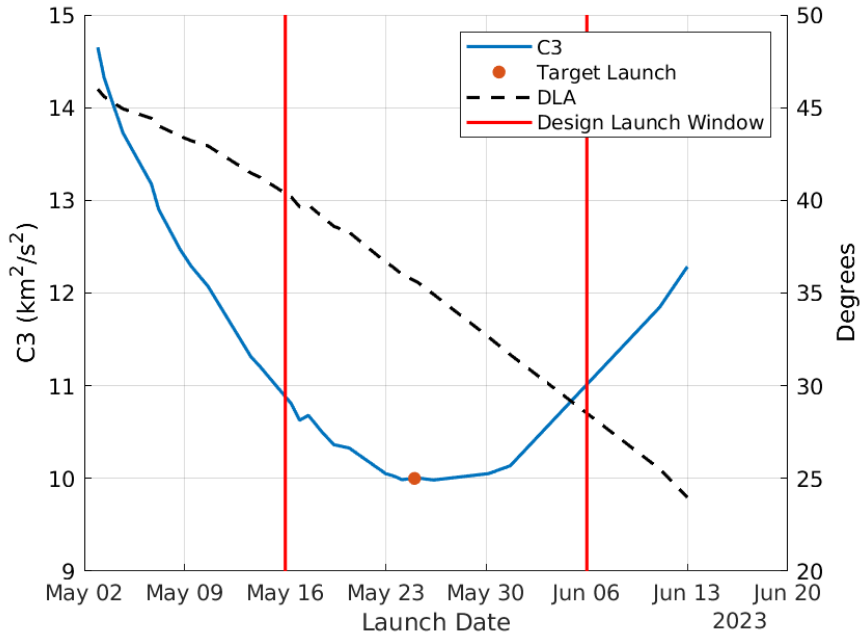


Figure 9: Launch Window and DLA

5.1.3 Jupiter Aerocapture

Overview

The aerocapture maneuver is directly driven by the level 1 mission requirements, MSN-1 and MSN-2. In order to solve the technical challenges of aerocapture and address MSN-1, multiple aerocapture architecture trades were considered.

The trades for entry guidance and TPS material are discussed in the ADCS (5.8) and structures (5.4) sections, respectively. However, the aerocapture maneuver is also highly coupled with both the mission design parameters upon arrival at Jupiter and the resulting orbit following atmospheric exit. This coupling is discussed in later sections in determining the final science orbit parameters.

Entry Corridor and Interface Definition

The entry corridor is the set of flight path angles, measured from the planet's azimuth, that will allow successful aerocapture to a desirable final orbit. This corridor is greatly influenced by the spacecraft mass and the arrival velocity, and as a result, these values will continue to be refined through the project development. In its current configuration, the spacecraft has an entry corridor ranging from 8.52-8.58° from azimuth. This corridor defines the range of entry flight path angles that will allow the spacecraft to reach the desired science orbit. There is a larger range of an additional half degree that will allow successful aerocapture, but will result in an orbit that is too large.

The mission's entry interface is measured from the conventional science definition of the Jovian "surface", and is subsequently defined by matching the atmospheric density to the density of interface on terrestrial planets.

In the science community, the "surface" of gas giants is defined as the location in the planet's atmosphere where the pressure is equal to 1 bar. On Jupiter, this corresponds to a mean radius of 69,911 km from the center of the planet. Because of its oblateness, Jupiter is much wider at the equator than the poles. As a result, the "surface" is at a radius of 142,984 km at the equator.

For the purposes of this mission, the atmospheric interface is defined to be the location in the Jovian atmosphere where the density is roughly less than $2.222 \times 10^{-8} \text{ kg/m}^3$. This density corresponds to the defined entry interface at Earth and Mars. At Jupiter, the atmosphere is believed to drop down below this density at an altitude of 500 km above the "surface". Therefore, the definition of atmospheric interface at Jupiter will be at $r_j + 500\text{km}$ from the center of the planet.

In-Flight Data Acquisition

In accordance with requirements MSN-02 and OPS-05, the spacecraft must be able to characterize the upper Jovian atmosphere during the aerocapture pass as well as record the resulting acceleration data. The Mars Science Laboratory Entry Descent and Landing Instrument (MEDLI) suite used during the Mars Science Laboratory mission includes an atmospheric measurement system.[\[4\]](#) This Mars Entry Atmospheric Data System (MEADS) measures the atmospheric pressure on the heat shield at the seven MEADS locations during entry through the atmosphere. Both of these suites will be retrofitted - and subsequently renamed as JEDLI and JEADS - to be applied to the SPACEJAM mission.

Like MEADS, the JEADS pressure sensors are to be arranged in a special cross pattern. Data from these sensors will be used to determine the spacecraft's orientation and position relative to entry interface during the atmospheric flight. This will provide novel and invaluable data of the Jupiter atmosphere composition.

JISP (JEDLI Integrated Sensor Plugs) is another set of sensors that are heritage from MEDLI, and will also be embedded in the spacecraft's heat shield. These sensors will measure the temperature flux through the heat shield during entry and will allow scientists to determine the atmospheric composition from the temperature and pressure data at different points in the atmosphere.

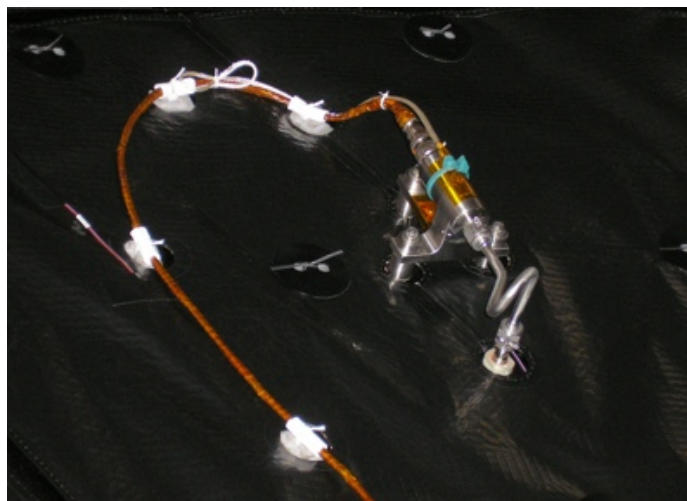


Figure 10: A photo of the MEADS sensors in the spacecraft's head shield.

These instruments will return 0.9-1 MB of raw data, which will be transferred during the first downlink following the aerocapture maneuver.

Post-Aerocapture Orbit Determination

The accuracy of the post-aerocapture orbit is dependant on a number of factors, most of which are unknown before entry. These include atmosphere composition, density, and wind speed, and will heavily influence the drag skirt jettison time as well as the final orbit apoapsis. The method for entry guidance is further discussed in the ADCS section. This poses a severe risk to the spacecraft and mission, which is addressed further in section [6](#).

Simulation and Monte Carlo

Throughout the mission and spacecraft design process, simulations were performed using the CU Boulder Entry Systems Design Laboratory (EsDL) Aeroassist simulation (ASIM) software. ASIM is a Matlab suite that incorporates atmospheric models, multiple guidance modes, 6dof integration, and multi-stage jettison dynamics into a variety of entry, descent, and landing scenarios.

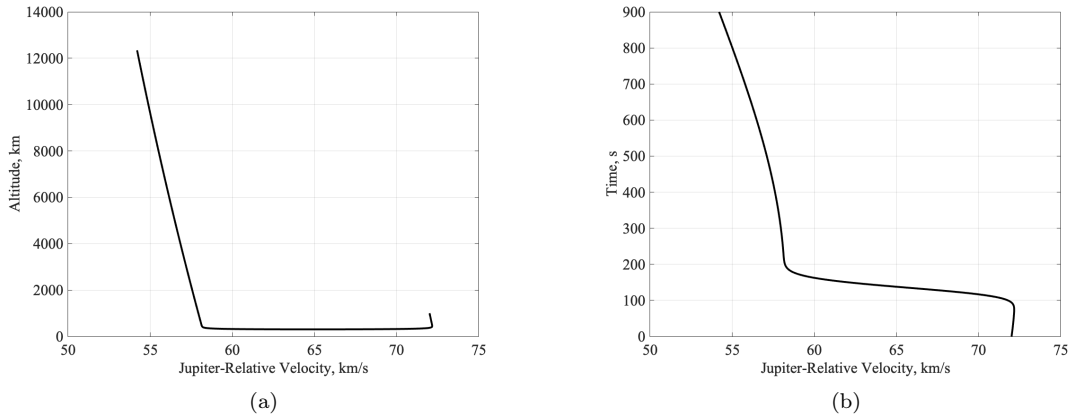


Figure 11: Plots of Jupiter-relative spacecraft velocity vs. altitude (a) and time (b), during the aerocapture event.
Flight path angle = -8.52°

In order to quantify the error in final orbit apoapsis, a Monte Carlo simulation was run with noise injected into the atmospheric conditions. Additional dispersions were added to the entry interface altitude, flight path angle, entry speed, and coordinates of entry.

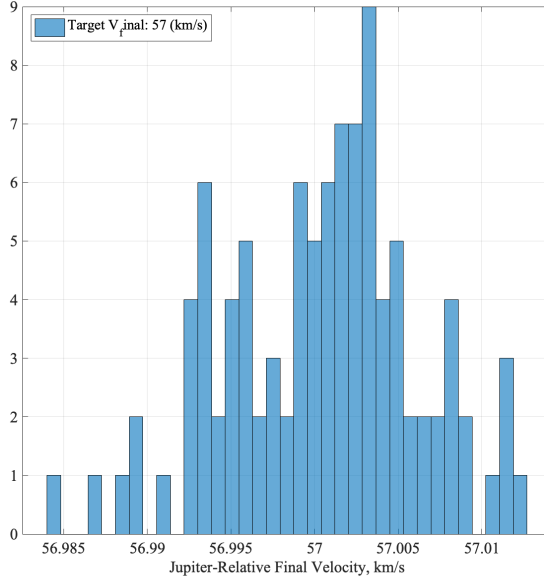


Figure 12: The histogram for aerocapture Monte Carlo, $N = 100$.

The 1σ values used for the dispersions in this simulation are as follows:

1σ Variable	Value
C_d	0.003
v_{atm} (m/s)	500
h_{atm} (m)	5000
Flight path angle (rad)	5e-4
Entry latitude (rad)	5e-4
Entry longitude (rad)	5e-4
Entry azimuth (rad)	5e-4

Table 9: Dispersions applied to each relevant entry variable.

The Jovian atmosphere was dispersed with random noise added proportionally to the magnitude of the exponential atmospheric model at that altitude.

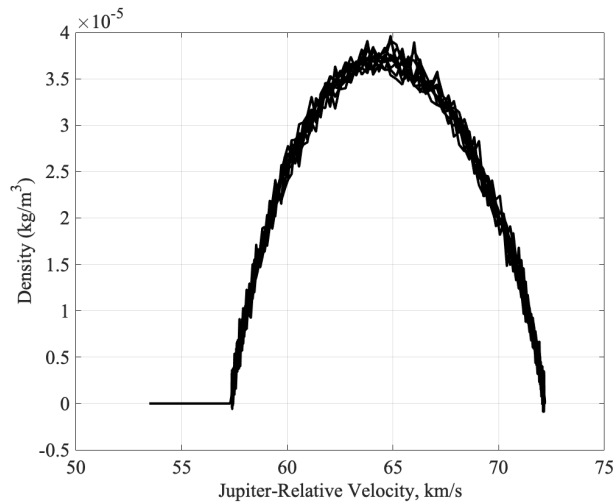


Figure 13: The density of the Jovian atmosphere with noise versus the flight velocity.

As can be seen by figure 13, the aerocapture guidance method is robust despite the unknowns in atmospheric composition.

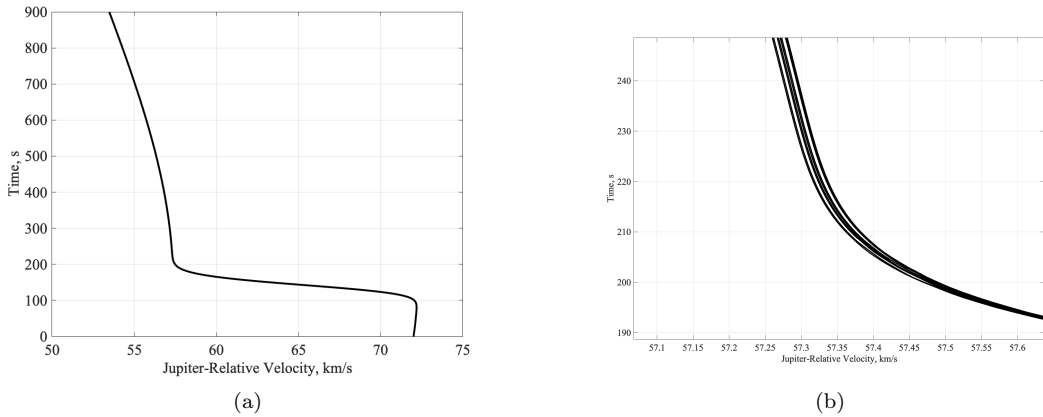


Figure 14: Plots of Jupiter-relative spacecraft velocity following Monte Carlo analysis, $N=10$, with the target velocity at perijove at 57.5 km/s. Figure 11.b) shows the elbow section at higher magnification in order to illustrate the robustness and accuracy of the targeting despite atmospheric dispersion.

On further analysis, it is evident that the variable with the biggest effect on the final velocity of

the spacecraft is the entry flight path angle. If the spacecraft is to enter outside of the targetted corridor, the result will be mission failure. Because of this, it is critical that the spacecraft ensure aerocapture within the entry corridor. However, this is typical of all missions with a portion involving entry and is not an unexpected or exaggerated risk.

5.1.4 Jupiter Science Orbit Design

The post-aerocapture orbit was designed to minimize radiation exposure to the spacecraft and time spent flying through Jupiter's main ring while still achieving the required science objectives. While a near polar orbit (such as that used by Juno) would provide the best radiation environment, aerocapture at a highly inclined trajectory poses difficulty due to the variable wind speeds across Jupiter's atmospheric bands and a post-aerocapture inclination change would be fuel prohibitive. Instead, the spacecraft's trajectory is designed to enter aerocapture with a 10° inclination. An inclination of 10° results in a two order of magnitude reduction in time spent passing through Jupiter's main ring. The initial post-aerocapture orbit is highly uncertain due to the limited knowledge of Jupiter's atmosphere, and this inclination change also reduces the likelihood of collision with a moon immediately following aerocapture.

To determine the size of the target orbit, a series of post-aerocapture exit velocities were run through GMAT to determine the resulting apojove, ΔV requirements, and moon observation time. The results are shown in Tables 10 and 11 and Figure 15. Larger orbits reduce the ΔV required and moon observation time while smaller orbits also provide less time for computation of the perijove raise maneuver. Since the fuel requirements grow significantly for a target exit velocity less than 56.8 km/s without significant science benefit and exit velocities less than 57.2 km/s provide few moon observations comparatively, the exit velocity target of 57 km/s was selected with fuel margin available to reduce the orbit size if desired.

Aerocapture Exit Velocity (km/s)	Apojove (km)	Time to Periapsis Raise (days)	Periapsis Raise ΔV (km/s)	Station- keeping ΔV (km/s)	Disposal ΔV (km/s)	ΔV Total (km/s)
56.6	1,455,437	2.2	0.134	0.038	0.189	0.361
56.8	1,697,522	2.7	0.115	0.025	0.136	0.276
57	2,032,143	3.5	0.098	0.016	0.113	0.228
57.2	2,524,668	4.8	0.079	0.033	0.095	0.207
57.4	3,321,540	7.1	0.060	0.023	0.042	0.126
57.6	4,831,810	12.4	0.044	0.036	0.068	0.148

Table 10: Jupiter Orbit ΔV Requirements

Aerocapture Exit Velocity (km/s)	Apojove (km)	Callisto	Europa	Ganymede	Io	% Time in Moon View	Avg # of Moons in View
56.6	1,455,437	26%	66%	53%	76%	95%	2.21
56.8	1,697,522	26%	57%	48%	62%	90%	1.94
57	2,032,143	26%	44%	41%	41%	78%	1.51
57.2	2,524,668	24%	26%	30%	26%	58%	1.06
57.4	3,321,540	17%	16%	18%	16%	38%	0.66
57.6	4,831,810	6%	8%	8%	9%	17%	0.32

Table 11: Jupiter Orbit Moon Observations

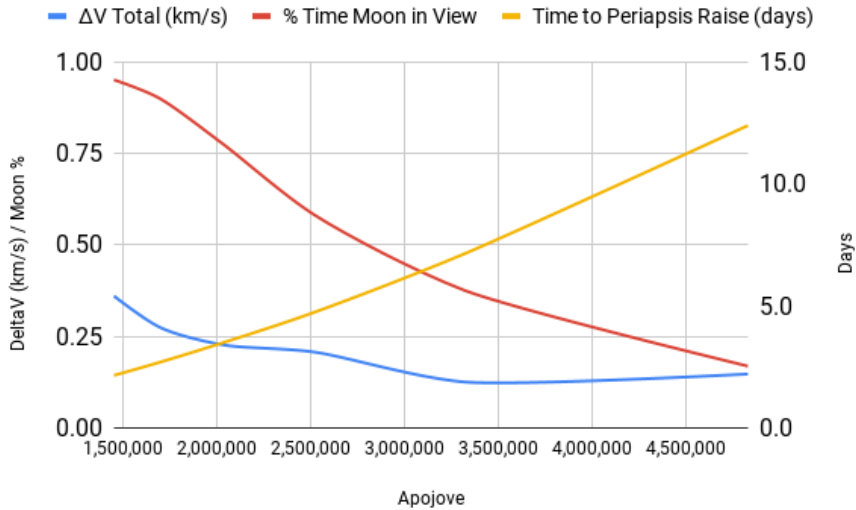


Figure 15: Jupiter Orbit Study

At its first apojove pass, the spacecraft will perform a perijove raise maneuver of approximately 100 m/s (depending on aerocapture exit velocity) in order to increase perijove to a target radius of 80,000 km. This maneuver will reduce the spacecraft's exposure to Jupiter's radiation bands and avoid reentry into the atmosphere. With an instrument requirement of 7.5 km resolution, the spacecraft must be within approximately 1.5 million km of a particular moon's surface in order to capture a photo. This allows for, on average, roughly 1.51 moons to visible at any given time throughout the 3 year mission. The orbit apojove can be reduced with a small burn to bring the time a moon is in view to 90% from the initial 78%. Two station-keeping burns are scheduled after each year to keep the orbit in its desired shape.

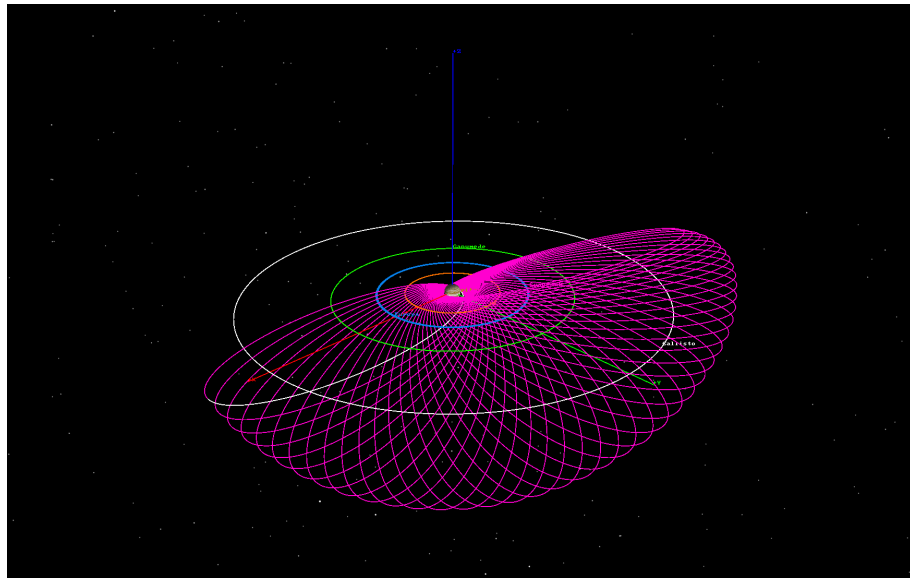


Figure 16: Jupiter Perijove Raise and First Year Orbit

5.1.5 Cruise Simulation

In order to account for errors in trajectory caused by TCMs imperfections, errors from the ADCS and propulsion components were injected into the simulation at each nominal TCM. The simulation used a 3σ burn error of 2% from the nominal ideal burn and a pointing error 3σ of 6 mrad. From

the resulting trajectory, the ΔV cost of a later clean-up maneuver occurring 21 days later was calculated.

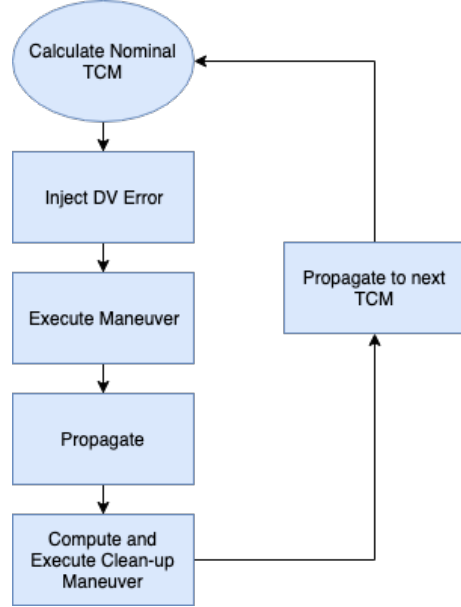


Figure 17: TCM Error Calculation

Parameter	3σ Error
Propulsion	2% Nominal ΔV
Pointing	6 mrad

Table 12: Spacecraft Error Sources

The simulation resulted in the following cruise ΔV TCM distribution with a mean of 113 m/s and standard deviation of 7.7 m/s allocating 136 m/s of ΔV for the cruise TCMs.

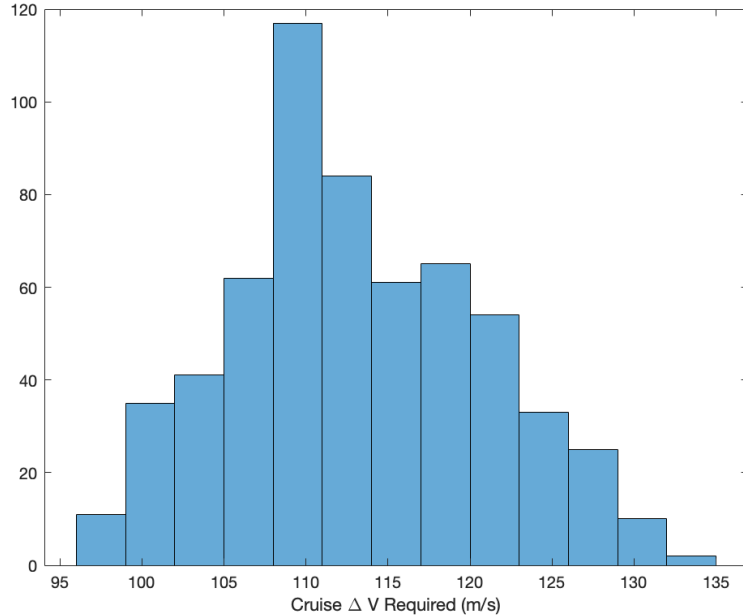


Figure 18: Cruise Monte Carlo Results

5.1.6 Jupiter Orbit Simulation

From the target exit velocity of 57 km/s, aerocapture exit simulations defined an upper and lower bound on the predicted aerocapture exit velocity. Using GMAT to calculate the resulting orbit shape at these limits yielded the following results and ΔV costs in Table 13. As seen earlier, the smaller orbit allows for more moon observations but requires a higher ΔV to maintain.

Parameter	Lower	Upper
Exit Velocity (km/s)	56.9	57.1
Apojove (km)	2095329	2621086
Orbit Period (days)	7.3	10.1
ΔV		
Station Keeping	49.4	11.4
Perijove Raise	93.7	75.4
Disposal	113.2	102.8
ΔV Total (m/s)	256.3	189.6

Table 13: Initial Jupiter Orbit Bounds

5.1.7 Delta-V Budget

Finally, using the cruise and Jupiter simulations the ΔV budget for the mission was established, Figure 14. A launch error budget of 5 m/s was designated based on the launch provider 3σ target. The propellant system comes with additional margin based on tank sizes above the required ΔV budget discussed further in the spacecraft propulsion system section. The ΔV budget includes a contingency 100 m/s allocation to the orbiter stage based on the uncertainty surrounding the aerocapture event should a large maneuver need to be conducted early in the Jupiter mission. Other maneuvers to avoid impacting a moon can be conducted with small phasing maneuvers once the Jupiter orbit is determined.

Stage	Element	Nominal ΔV (m/s)	$3\sigma\Delta V$ (m/s)
Cruise	TCMs	92	136
	Launch Error		5
	Margin		10%
	Total Cruise		155.1
Orbiter	Perijove Raise	98	94
	Station Keeping	16	50
	Contingency	100	100
	Disposal	113	114
	Margin		20%
	Total Orbiter		430
	Total		585

Table 14: ΔV Budget

5.1.8 Earth Re-entry

Due to the ^{238}Pu RTG, particular care must be taken to ensure that the spacecraft has no chance of Earth re-entry during either of the two Earth gravity assists. For an Earth re-entry to occur, the spacecraft would need to be significantly off-course and unresponsive to commands from mission control. As such, the following requirement was established: The spacecraft EGA B-plane uncertainty will not come within 3σ of re-entry at Earth during EGA1 or EGA2. To address this risk the spacecraft will use progressive B-Plane targeting TCMs enroute to EGA1 and EGA2 incrementally adjusting the Earth flyby until the final B-plane coordinates can be targeted while ensuring the OD solution 3σ uncertainty remains outside of an Earth impact. An example sequence for EGA2 is shown in Figure 19.

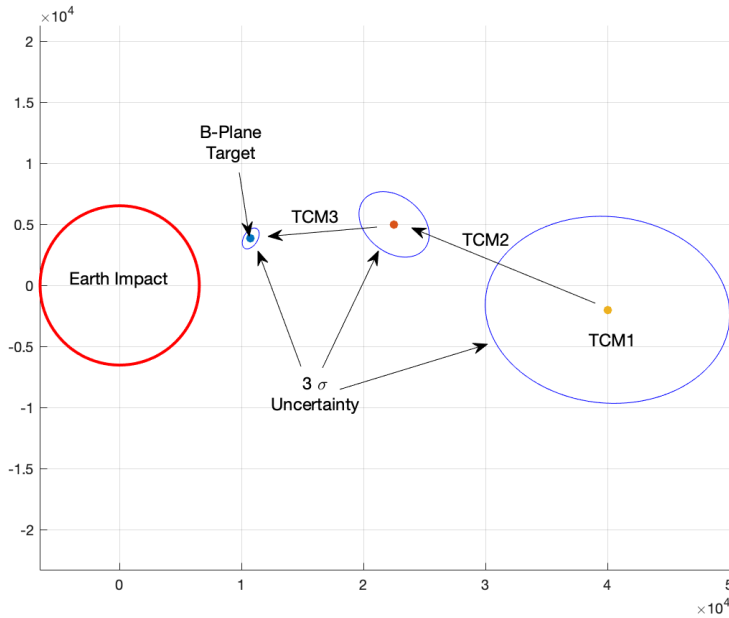


Figure 19: EGA2 Progressive B-Plane Targeting

5.1.9 Risk Assessment

B-plane targeting and orbital determination solutions to adhere to planetary protection requirements and ensure the spacecraft trajectory does not intersect with the Earth are well understood and have been used on previous interplanetary missions. The largest mission design risk arises from the aerocapture event at Jupiter which is not well understood. To mitigate this risk, the target initial orbit is designed to reduce the likelihood of a moon impact and the spacecraft designed to conduct the perijove raise maneuver autonomously, if necessary, which can later be refined by the operations team.

Consequence (Expected Impact to the Mission)	Severe (5)	SC 3σ B-plane solution outside Earth re-entry corridor	Progressive B-Plane Targeting Mitigation Inclined orbit, exit velocity/apojove target	Earth Re-entry Moon Impact		
		Orbit out of Jupiter equatorial plane, apojove beyond Callisto	SC in safe initial orbit Mitigation Exit velocity/apojove target, autonomous perijove raise	Initial Orbit		
Moderate (3)						
Minor (2)						
Negligible (1)						
		Very Unlikely (1)	Unlikely (2)	Possible (3)	Likely (4)	Very Likely (5)
Acceptable		Tolerable	Intolerable	Likelihood (Qualitative)		

Figure 20: Mission Design Risk Mitigation

5.2 Flight Software

Flight software is a complex element of spacecraft design, but can often come later in the process of development. Consequently, the design effort here focused on the functional elements that the software would need to accomplish and the high level requirements, rather than the underlying details of operating systems, hardware interaction, and process scheduling. In addition, flight software does not have many *direct* requirements to satisfy, but rather facilitates the fulfillment of nearly all the other spacecraft requirements by commanding the spacecraft hardware, maintaining attitude, communicating with the ground, performing TCMs, and operating the spacecraft sensors.

The high level flight software requirements can be summarized as follows:

Table 15: Flight Software Subsystem Requirements - Cruise Phase

Req. No.	Requirement	Rationale	Verification
FSW-CR-01	Communicate with ground	The spacecraft must receive attitude and TCM commands from the ground and must transmit any necessary information for the ground operators to calculate these parameters.	Functional test of radio hardware and communication software.
FSW-CR-02	Operate actuators for attitude control	The spacecraft must closely control its attitude in order for TCM maneuvers and injection burns to be completed correctly.	Software-in-the-loop simulation test and functional test of the appropriate actuators.
FSW-CR-03	Sequence TCM and injection burns	TCM and injection burns must occur at precise times, which the spacecraft will need to actuate itself as there may be too much lag for ground operators.	Software-in-the-loop simulation test.
FSW-CR-04	Sequence cruise stage jettison	To prepare for aerocapture, the flight software will need to initiate a physical reconfiguration of the spacecraft.	Software-in-the-loop simulation test and functional test of the appropriate actuators.
FSW-CR-05	Flight software shall maintain enough free memory to serve critical interrupts.	The spacecraft must be able to respond to regular calls to critical software from outside normal control flow.	Software-in-the-loop simulation.

Table 16: Flight Software Subsystem Requirements - Aerocapture Phase

Req. No.	Requirement	Rationale	Verification
FSW-AC-01	Run guidance algorithms to sequence drag skirt actuation and jettison	The drag skirt is the primary method of trajectory control during the aerocapture maneuver. The spacecraft must first actuate it and then jettison at precise times determined by the guidance algorithms.	Software-in-the-loop simulation test and a functional test of the appropriate actuators.
FSW-AC-02	Sequence heatshield and aeroshell jettison	After the spacecraft has exited Jupiter's atmosphere, it must shed extra mass in order to reject heat from its RTG and prepare for the periapsis raise maneuver.	Software-in-the-loop simulation test and functional test of the appropriate actuators.
FSW-AC-03	Flight software shall maintain enough free memory to serve critical interrupts.	The spacecraft must be able to respond to regular calls to critical software from outside normal control flow.	Software-in-the-loop simulation.

Table 17: Flight Software Subsystem Requirements - Orbit Operations Phase

Req. No.	Requirement	Rationale	Verification
FSW-OO-01	Sequence communication with ground	Like in the cruise phase, the spacecraft will need to make trajectory correction maneuvers and receive precise pointing instructions from ground operators. It also needs to acknowledge these instructions and return the science data from the mission's instruments.	Functional test of the radio hardware and software.
FSW-OO-02	Operate actuators for attitude control	In order to collect the science data, the spacecraft must maintain precise attitudes.	Software-in-the-loop simulation test and functional test of the appropriate actuators.
FSW-OO-03	Operate scientific instruments	Acquisition of scientific data is necessary for mission success.	Flatsat test, demonstrating that the flight software can send the correct instructions to the instruments.
FSW-OO-04	Sequence orbit correction burns	Ground operators will be too far away to directly control the spacecraft. Instead, the spacecraft will need to maintain its own sequencing software in order to precisely time these burns.	Software-in-the-loop simulation test and functional test of the appropriate actuators.
FSW-OO-05	Flight software shall maintain enough free memory to serve critical interrupts.	The spacecraft must be able to respond to regular calls to critical software from outside normal control flow.	Software-in-the-loop simulation.

5.2.1 Critical Events

5.2.1.1 Cruise Tasks

During cruise, flight software is primarily concerned with maintaining a thermally stable state and communication with DSN operators on Earth. This requires that the spacecraft be able to point its antennas such that a two way radio link with the Earth can be closed, as well as storing, parsing, and interpreting commands and data sent from the Earth. In addition, the flight software is responsible for receiving, scheduling, and executing TCMs en-route. While the ground operators can calculate the TCM duration and direction in advance, it is up to the spacecraft to align its attitude with the desired direction and burn for the correct duration, at the right time. In order to execute these TCMs properly, the spacecraft will need to maintain precise knowledge of its own attitude relative to the solar system, as well as precise clocks that can both sequence the start of the TCM burn and stop at a precise time.

5.2.1.2 Jupiter Encounter

The Jupiter encounter environment is a highly dynamic environment. Flight software is responsible for sequencing all events during this stage without ground intervention, as a two way radio link is not guaranteed during aerocapture. The lightspeed latency is 43 minutes, and is subsequently too great for ground operators to actively control the spacecraft during this critical maneuver. The spacecraft must instead rely on autonomous operations. Once a final trajectory correction burn has been executed, the flight software will sequence the cruise stage jettison event and monitor for Jupiter atmospheric interface.

Once inside Jupiter's atmosphere, the spacecraft will run continuous numerical simulations in order to determine the optimal times to actuate and then jettison the drag skirt around the aeroshell in order to attempt to capture into a Jovian orbit with the proper apoapsis.

As the spacecraft leaves Jupiter's atmosphere, the flight software will also sequence the heatshield and aeroshell jettison events and rotate the spacecraft for initial acquisition of the orbital stage. Following these events, the spacecraft must then be able to perform a periapsis raise maneuver before the first orbit is complete.

5.2.1.3 Periapsis Raise and Orbit Operations

After leaving the atmosphere, the spacecraft will be in an elliptical orbit with a periapsis inside Jupiter's atmosphere. The spacecraft will not have enough energy to escape the atmosphere if another pass is performed, so a burn is required to raise the orbit's periapsis above Jupiter's atmosphere. The spacecraft is anticipated to be placed into a seven day orbit, so ground operators will have several days to calculate and prepare for the burn and high levels of automation are not anticipated to be required.

However, in order to acquire signal from Earth, flight software will be responsible for switching over telecommunications from the jettisoned cruise stage MGA to the orbital stage HGA. The flight software will also be responsible for sequencing the TWTA and other components of the telecommunications and C&DH subsystems.

After the spacecraft is in a stable orbit, the focus moves to operating the science instruments and storing, processing, and sending science data. In order to operate the cameras, the spacecraft's attitude control is just as important. Using the reaction wheels and attitude control thrusters, the flight software will be responsible for running a closed loop control system to maintain the spacecraft's attitude such that the science instruments can point directly at their targets with the minimum jitter and unintended slew. In addition, because the primary science instruments are cameras, image compression will be an important, but not flight critical, software operation. Many well optimized image compression algorithms already exist, such as JPEG, which is based on a discrete cosine transform function.

5.2.2 Robustness

5.2.2.1 Hardware

Due to Jupiter's harsh radiation environment, all critical hardware components that are radiation sensitive will be placed in a protective vault, if possible. This vault is further detailed in the C&DH section.

5.2.2.2 Computation

Computational robustness is detailed for each guidance mode in the ADCS section.

5.2.2.3 Fault Tolerance

Flight software must be resistant to a variety of undesirable conditions and faults. These include processes that attempt to use all of the processor's computing time, out of bounds memory accesses, unintended access to hardware peripherals, and overwriting memory in other processes. For example, it would be very undesirable for an image compression process to overwrite memory used by the flight guidance process and cause the guidance process to either crash or produce incorrect computational results.

In addition, it is imperative that flight software actually has time to run at regular intervals. It becomes very difficult to reason about the behavior of the software unless this guarantee can be maintained.

While the flight software must be generally well written, one of the most important tools for ensuring that the above concerns are addressed is a preemptively multitasking real time operating system, or RTOS. This software regularly interrupts other running processes and switches the thread of execution in order to serve other processes. In addition, an RTOS can enforce memory boundaries and prevent certain processes accessing certain peripherals. With the addition of a hardware timer connected to a software interrupt, the RTOS can guarantee that guidance software will run at deterministic intervals.

In addition, in the case of critical maneuvers such as aerocapture or periapsis raise, it may actually be desirable to disable features like safe mode, or non-critical processes in order to minimize risk during time sensitive mission periods. For example, a software fault during aerocapture could result in loss of mission unless the spacecraft could very quickly resume the aerocapture guidance software. In this case, it makes sense to disable anything that could interrupt the guidance software.

5.2.2.4 Computing Margins

A properly designed, preemptively multitasking RTOS should be able to keep the spacecraft responsive even under 100% computational loads. However, other resources - particularly memory - may suffer under such conditions. In order to handle unexpected activity, memory should be arranged such that separate regions exist for software call stacks for interrupt routines and other software, and each of these regions should always have enough free memory such that an interrupt can call the main RTOS tick and switch to the guidance software without running out of memory.

5.3 Environment

The near Jupiter environment is characterized by its remoteness from the sun and the intense radiation trapped in Jupiter's magnetic fields. In order to address this environment, all at-risk components were placed inside heritage radiation vaults that have been flight-proven on Juno. These vaults are further discussed in section [5.7](#).

5.3.1 Solar Flux and Power Source Choices

Solar flux proportionally to the square of the distance from the Sun. Jupiter is approximately five times as far away from the Sun as the Earth, and consequently it receives less than 1/25 of the solar flux. Historically, most missions this far out in the solar system have required nuclear power, as solar panels were not efficient enough at this distance to sustain high-power missions, or they would require panels too large to be practically launched. Juno, a recent mission to Jupiter, has taken advantage of more modern solar panel technology to successfully operate at such extreme distances from the sun. However, its panels are still very large, and would be unable to fit into an aeroshell during the aerocapture event. This trade is discussed further in section 5.6.

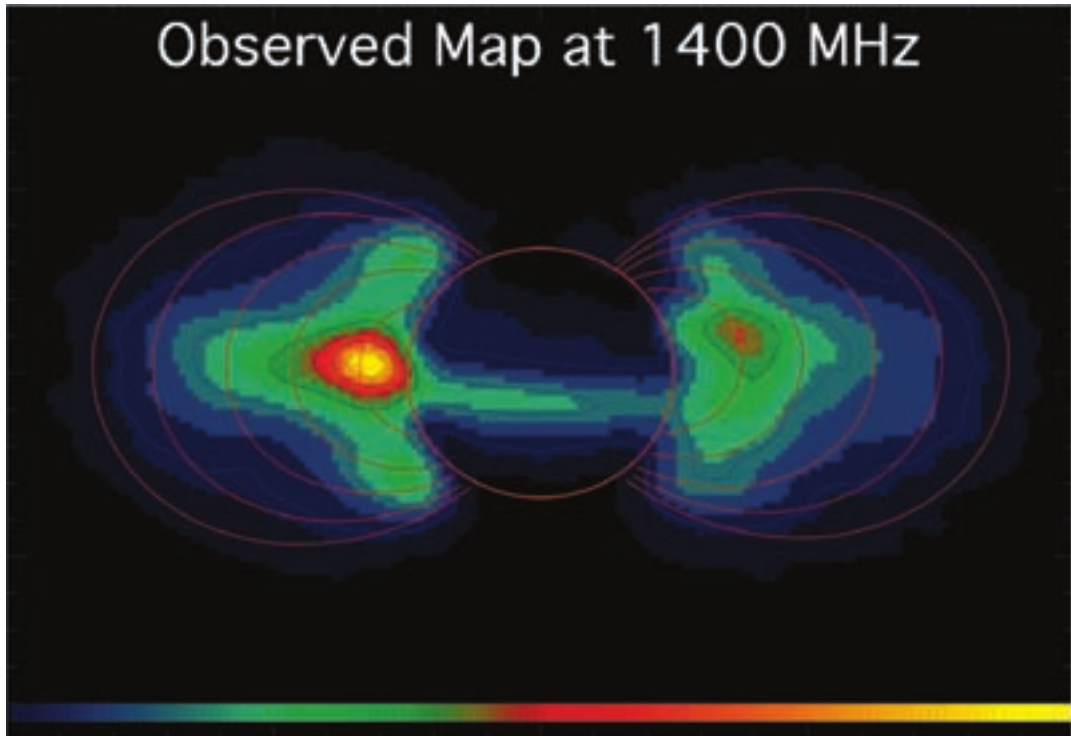


Figure 21: Microwave radiation distribution around Jupiter. In addition to charged particles, EM radiation is emitted in all spectra, up to and including gamma radiation. Figure from [5]

5.3.2 Magnetic and Radiation Fields

Jupiter has an intense magnetic field, the source of which is hypothesized to be a combination of the planet's very short rotational period and metallic hydrogen forming under the extreme pressures of its interior.

This magnetic field is extremely large, with a magnetopause at $75 R_J$ [6]. The field traps charged particles from the sun, nearby space, and orbiting moons, subsequently accelerating them to relativistic speeds. These particles present a significant hazard for any spacecraft in the vicinity of Jupiter.

When compared to other planets, Jupiter's particle makeup consists of more high-energy electrons, though heavier particles are also present. One of the closest moons, Io, has substantial volcanic activity and spews 1000 kilograms per second of material, mostly sulfur dioxide, into Jovian orbit [6]. This material contributes substantially to the ion distribution around Jupiter as it becomes ionized. Because these particles travel in arcs along the magnetic field lines, they emit synchrotron (gamma) radiation, which is a secondary source of danger for spacecraft components and may cause radio interference.

5.3.3 Radiation Doses

Direct calculation of the radiation dose in the near-Jupiter environment is highly dependent on the precise orbit, with the most detailed information about doses being related to the surface of the moons. The inner Jovian moons can receive multiple hundreds of rems per day, and a spacecraft in the vicinity will likely receive a similar dose. Previous estimates for a Europa orbiter probe discussed radiation doses as high as 2.9 Mrad through 100 mil of aluminum shielding over the course of the mission [7]. This is approximately an order of magnitude more radiation than Juno is predicted to receive, and it bears consideration in both the operation and many aspects of the design phase of the program.

The RAD750 computer selected is tolerant to high levels of radiation, and according to the manufacturer, immune to transistor latchups. However, semiconductor components which must necessarily be outside of the avionics vault, such as star trackers, may require their own shielding.

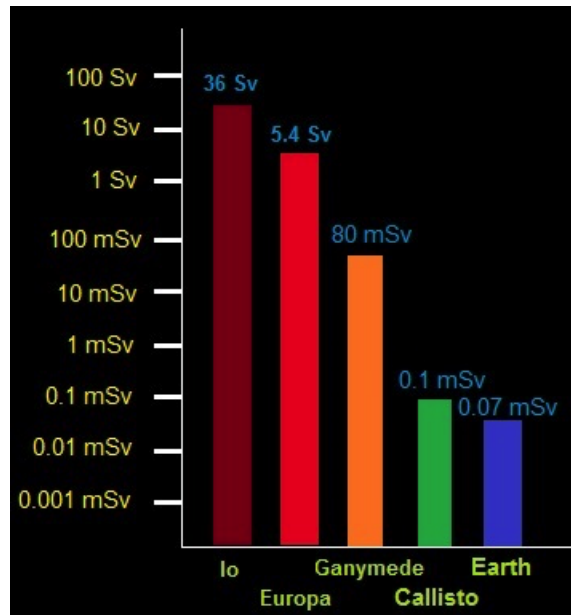


Figure 22: Radiation dosage on the surface of Jupiter’s moons. Values from [8], and converted from rem

Many more issues exist at the post-PDR level with regards to radiation tolerant design. For example, plasma charging from aerocapture, photoelectric effects, or ion bombardment may electrically charge the spacecraft, which in turn may affect instruments or cause the spacecraft to collect dust. Differential charging could cause arcing between components if common grounds are not available, which could cause severe damage. Arcing across reaction wheel bearings could cause pitting in the bearing races and premature failure. Heavy radiation doses are almost guaranteed to degrade certain surfaces, such as wire insulation, kapton surface treatments, and potentially even optical components such as treatments applied to the lenses of the cameras.

5.4 Structure and Mechanical System

5.4.1 Structure subsystem Level IV Requirements

Table 18: Structure Subsystem Requirements

Req. No.	Requirement	Rationale	Verification
STR-01	The structure shall maintain a center of mass (COM) to +/- 0.05 (m) with respect to the main axis.	Allows for proper pointing stability for the mission operating phases.	Verified by SolidWorks analysis
STR-02	The structure shall have the capacity to attach and detach from the launch vehicle and to survive the launch environment.	Critical for mission success	Accounted for in selection of launch vehicle
STR-03	The structure shall provide sufficient radiation protection for electronic components in the Jupiter atmosphere environment.	This requirement will drive structural design of a 'radiation vault' in which electronic systems and other radiation-sensitive equipment will be installed.	Accounted for by design of the radiation vault
STR-04	The structure shall survive the aerocapture event (up to loads of 575,000 N).	Necessary to enable the survival of spacecraft during the aerocapture event.	Verified through SolidWorks Simulation
STR-05	The structure shall contain the proper mechanisms to separate from orbital spacecraft.	Necessary to enable the orbital stage mission.	Accounted for in selection of separation mechanism

5.4.2 Aerocapture Method Trade Study

The method of aerocapture is of paramount importance to the success of the mission. For such an unprecedented mission to be successful, the parts used on this mission have to be resilient, particularly to age and the environment. The aerocapture maneuver was considered with three primary methods: rigid aeroshell, inflatable aeroshell, and trailing ballute. A table outlining the trade study that was performed on the three methods may be viewed in Table 19. Each method was analyzed in terms of the device's mass, heritage, peak tolerable heat dissipation, and maximum tolerable speed when in use. Flight heritage and maximum speed were determined to be the most important properties between the three methods, owing to the unprecedented and costly nature of this mission. With such considerations, only the best hardware that is sure to work should be used. The peak heating and mass were important, but only considered half as important as the other two metrics. This is because the component's masses and heating would be irrelevant if the components could not function correctly in the high speed environment

Table 19: Aerocapture Trade

Aerocapture Method Trade	Mass	Heritage	Peak Qdot (W/m^2)	Max Speed (Mach)	Score
Weight	5	10	5	10	N/A
Rigid Aeroshell	300	10	30	20	40
Inflatable Aeroshell	200	2	30	5	55
Trailing Ballute	40	0	1	5	80

Each method's score was determined by assigning ranks to each method for each metric. In this way, the methods could be compared with relative weights despite the highly dissimilar categories. The components were ranked in each category by a 1-2-3 scale, where rank 1 represents the most

desirable value, rank 2 represents the middle value, and rank 3 represents the least desirable value. For the mass, the rigid aeroshell is heaviest, and therefore least desirable. Conversely, the trailing ballute is the lightest and most desirable, leaving the inflatable aeroshell in the middle. When looking at heritage, only the rigid aeroshell has multiple flights demonstrating its flight-readiness, therefore being most desirable. The inflatable aeroshell has been demonstrated on a test flight to re-enter Earth, but never an interplanetary mission. Unfortunately, the trailing ballute concept had never been applied to a spacecraft, and thus has no heritage.

The peak heating that can be dissipated is equal between the two types of aeroshell, at approximately 30 W/m^2 . However, the trailing ballute is only able to dissipate 1/30th of this heat, most likely because it trails the spacecraft instead of attaching to the front of it. Therefore, the two aeroshells tie for desirable and the ballute is highly undesirable, particularly in a heating-intensive environment like Jupiter's atmosphere.

Finally, the max tolerable speed to each method was considered, as SPACEJAM will enter the atmosphere at extremely high speeds. Both the inflatable aeroshell and ballute are only known to be rated up to Mach 5, while rigid aeroshells are known to be viable until at least Mach 30. As such, the rigid aeroshell has the most desirable max speed, with the other two methods tying for second. When every rank is multiplied by the metric's weight, and each product is summed together, the final score for each method is produced. In this trade study, lower scores are more desirable, owing to the 1-2-3 ranking system described earlier. Therefore, the rigid aeroshell was plainly shown to be the best of the three options to operate within the high-performance constraints of SPACEJAM's mission.

5.4.3 Material Selection

Aluminum 7075-T6 has been used on many previous deep-space missions. It is a very high-strength material and subsequently suitable for use in a highly-stressed structure. Moreover, the mass of aluminum 7075-T6 is relatively low compared to other materials that provides approximately the same strength. Aluminum 7075-T6 is also relatively inexpensive.

Titanium has been previously used to build vaults in order to protect electronic components in Jupiter's heavy radiation environment. The reason for using titanium as the vault material is that the radiation absorption rate of titanium is particularly low, which means that the internal components are well-protected from radiation damage. For the purposes of this mission, a 2-cm thick Ti-13Nb-12Zr titanium alloy was chosen for the hardware vault.

Carbon Phenolic is a material available for use in high heat fluxes and high pressure conditions. Moreover, Carbon Phenolic TPS has been flight-proven for entry into Jupiter's atmosphere during the Galileo mission. Therefore, carbon phenolic was chosen as the ablative heat shield material.

SSE Missions	Existing Materials	Sample Return Missions			Direct Entry					Aerocapture						
		Lunar SR	Comet/Asteroid SR	Mars SR	Mars	Titan	Venus	Saturn	Neptune	Jupiter	Mars	Titan	Venus	Saturn	Neptune	Jupiter
Ablative TPS Material Classes																
Low-density silicones	SLA-561V, SRAM17	X	X	X	● ¹	▶	X	X	X	X	▶	▶	X	X	X	X
Low-density phenolics	PICA PhenCarb	●	● ¹	▶	●	○	▶	X	X	X	▶	○	▶	X	X	X
Mid-density phenolics	Densified-PICA, BPA(?), C-P, PhenCarb	▶	▶	▶	○	○	▶	X	X	X	○	○	▶	X	X	X
Carbon-based multilayer	Carbon-carbon /Fiberform® (Genesis)	▶	● ¹	▶	○	○	▶	X	X	X	○	○	▶	X	X	X
High-density phenolics	Carbon phenolic	● ²	● ²	● ²	○	○	● ²	● ²	● ²	● ³	○	○	○	○	○	○

●¹ Limited Mission Capability
 ●² Fully capable
 ●³ Test Facility Limits Qual/Cert.
 X Not applicable; conditions too severe

▶ Potentially capable
 Low TRL/Not Demonstrated

Figure 23: Ablative Material Trade

Other... (drag skirt, aeroshell, RTG shield board)

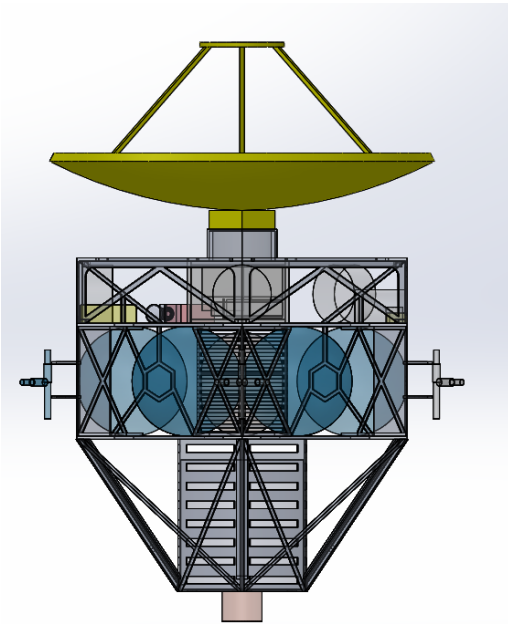


Figure 24: Telecomm Deck Location, Front

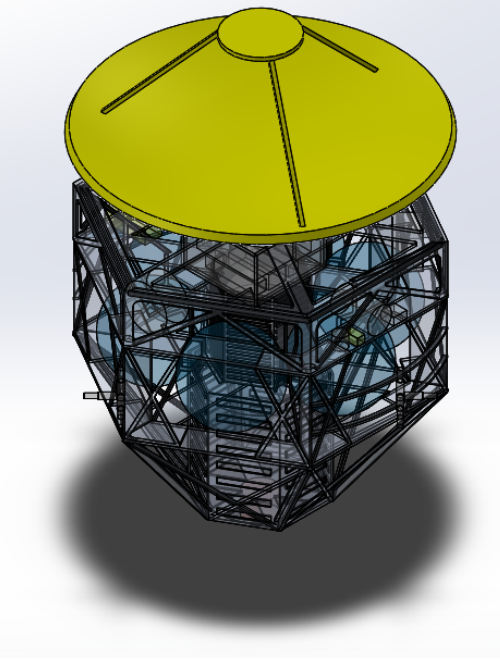


Figure 25: Telecomm Deck Location,
Isometric

5.4.4 Orbital Stage Design

The orbital stage of the spacecraft houses the scientific payload instruments, as well as a propulsion, guidance, power, telemetry, and command and data handling systems. This stage is connected to the heat shield, aeroshell, and drag skirt via a pyrotechnic separation mechanism that is actuated at the appropriate time in aerocapture. The stage is arranged in four decks partitioned by hexagonal platforms to be discussed in further detail below. The decks lie on the x-z plane, with the y-axis referred to interchangeably with "main axis."

5.4.4.1 Telecomm Deck

The Telecomm deck is the top-most deck of the Orbital Stage. This deck lies outside of the thermal insulation and consists solely of the high-gain antenna (HGA). The location of the Telecomm deck is highlighted in Figures 24 and 25

5.4.4.2 Science Deck

The Science deck (Figures 26, 27), protected from the environment by an equipment enclosure, consists of electronic and scientific equipment. Two reaction wheels are oriented vertically with respect to the plane of the deck such that their moment vectors coincide with the x- and z-axes. A star tracker, as well as a sun sensor and the visible imager optical head, are oriented optical-end facing outwards in order to operate appropriately. The previously-discussed radiation vault is centered between these components, close to the main axis. A third reaction wheel, oriented with a moment vector coincident with the main axis, sits on top of the radiation vault. Other equipment situated on this deck include the EPC and transfer switch, the ultraviolet spectrometer, and an IMU. The deck is supported structurally by radial struts that connect the center of the platform to the equipment enclosure, perimeter struts that run around the enclosure, and strengthening bars on the underside of the top of the equipment enclosure.

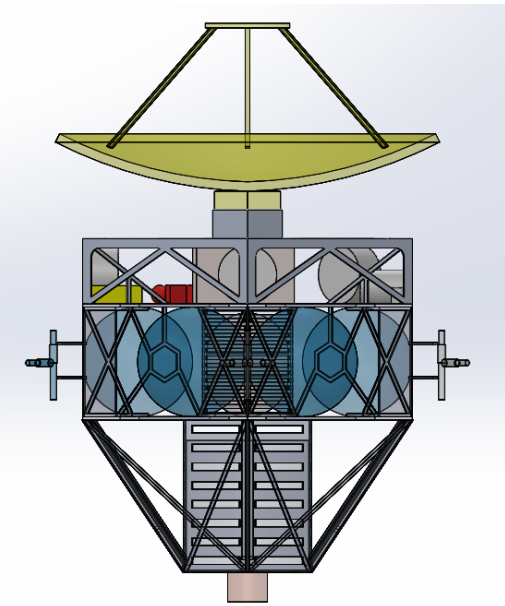


Figure 26: Science Deck Location, Front

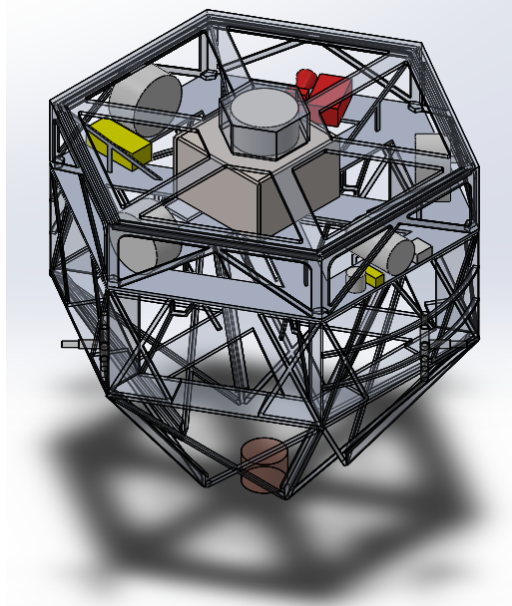


Figure 27: Science Deck Location, Isometric

5.4.4.3 Vault

In order to protect sensitive electrical equipment from both the radiation-heavy environment about Jupiter as well as radiation emitted from the RTG, a radiation vault will be constructed out of 2 cm-thick Ti-13Nb-13Zr as discussed above. A similar structure was used on the Juno spacecraft (Figure 28). Components within the radiation vault will include the transponder, the traveling wave tube amplifier, the sun sensor electronics components, the flight board, and the power distribution unit.

The vault will be positioned on the top side of the upper hex platform, between the reaction wheels and scientific equipment (Figure 29). Electrical wiring will run out of the vault via shielded conduits and all wiring outside of the vault will be insulated with radiation and EMI shielding.

5.4.4.4 Propulsion Deck

The Propulsion deck supports the propulsion system, whose proximity to the RTG will assist in keeping the fuel at an appropriate temperature. The fuel system consists of a centrally-located helium pressurant tank surrounded by six evenly spaced propellant tanks (see Figures 30 and 31). The propulsion deck is supported by main struts and support trusses running radially about the spacecraft, as well as by side trusses about the perimeter.

Four thruster quads, each containing three mutually orthogonal 1N thrusters and a 20N thruster opposing the (+) y-oriented thruster, are centered on the x-z plane on which the y-coordinate of the COM resides. The thruster quads are placed as far from the COM as possible in order to minimize thrust required for spacecraft orientation. They are also spaced 90° apart from each other so that pitch, yaw, and roll operations can be made with equal and opposing magnitude thrusts about the respective axes for increased stability. Translational movement can also be made in the positive and negative direction of all three axes with this configuration, an example of which is shown in Figure 32.

5.4.4.5 RTG Deck



Figure 28: Juno's radiation vault being lowered, Credit: NASA webpage

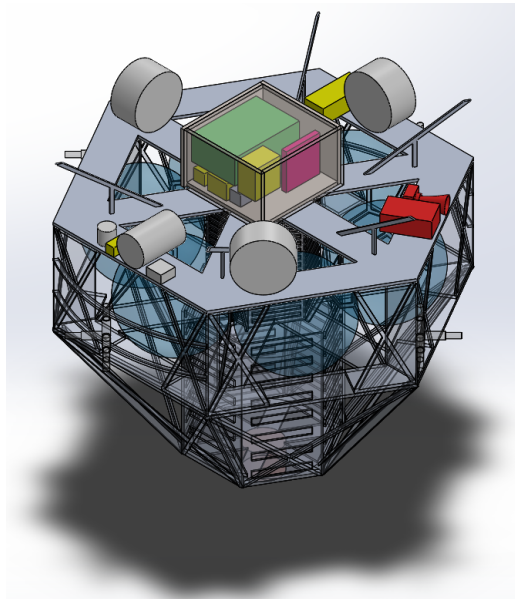


Figure 29: Vault Location Within Science Deck

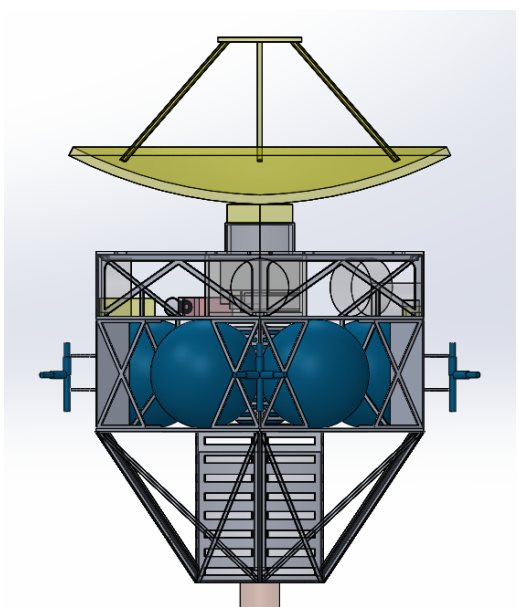


Figure 30: Propulsion Deck Location, Front

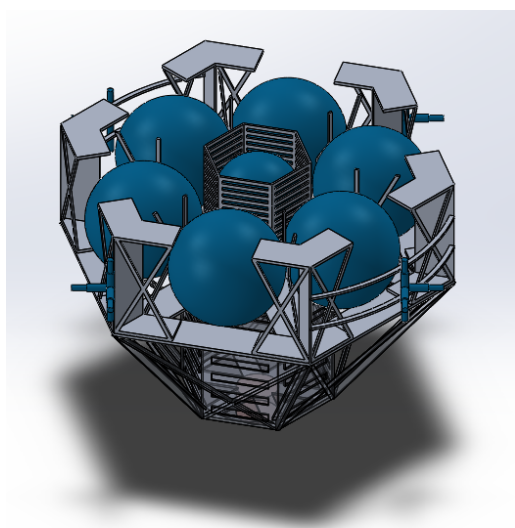


Figure 31: Propulsion Deck Location, Isometric

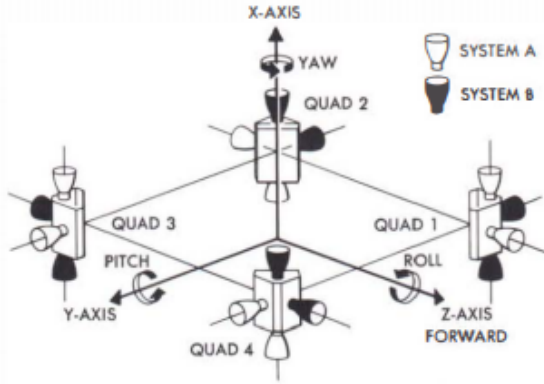


Figure 32: Thruster Quad Schematic [9]

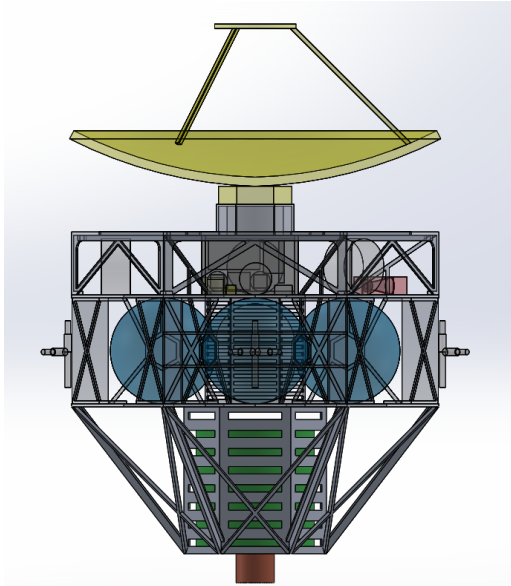


Figure 33: RTG Deck Location, Front

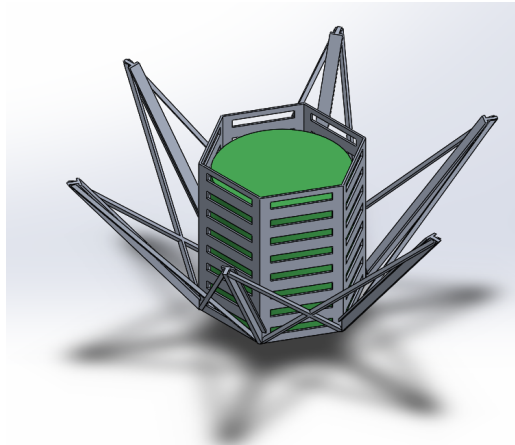


Figure 34: RTG Deck Location, Isometric

The RTG deck (Figures 33 and 34) houses the RTG and its protective structural sheath, as well as structural trusses that support the spacecraft. As the RTG emits large amounts of heat and radiation, it will be strategically placed as far away from the scientific and electric hardware as possible in order to preserve the required environment of the spacecraft. A counterweight is affixed to the bottom end of the RTG sheath in order to shift the COM to lie on the main axis. The spacecraft's COM is located at a point along the main axis within the limits of the propellant tanks so that propellant use does not cause the COM to shift over time, as it is burned and mass is expelled from the spacecraft.

5.4.4.6 Bolt

Fixtures within the orbital stage will be joined by double-bolted countersunk socket-head cap screws (SHCS) wherever possible. Double-bolting will provide security against heavy vibration and redundant protection in the event of a fixture failure. Countersinking bolts will facilitate the construction of the stage, as removing the head of the bolt from the work space will reduce the likelihood of incidental damage occurring during construction should tools get caught.

Where it is not possible to use countersunk bolts, safety wire can be implemented as an added defense against screws backing out. If one bolt loosens, the wiring ensures that the redundant bolt tightens.



Figure 35: Safety wiring mechanism

5.4.4.7 Orbital Stage Data

Relevant information about the orbital stage is shown in Table 20 below. All masses account for 20% margin on top of dry mass values.

Table 20: Orbital Stage Data

Item	Property	Unit	Notes
Dry Mass	924.1	kg	
Wet Mass, Orbital	1,171.0	kg	Contains fuel for orbital stage
Wet Mass, Cruise	1,343.4	kg	Contains fuel for cruise stage and orbital stage
Length	3.08	m	along main axis
Diameter	2.05	m	at HGA
Diameter	2.37	m	at thruster quads
COM_x	0	m	centered on main axis
COM_z	0	m	centered on main axis
COM_y	1.29	m	From bottom of spacecraft

5.4.5 Entry Stage Design

The entry stage consists of the aeroshell, the drag skirt, and the orbital-wet orbital spacecraft. The "aeroshell" refers to the heat shield and back shell, while the drag skirt is its own entity. These components surround the orbital spacecraft during the aerocapture maneuver. The entry stage is displayed in Figures 36 and 37

5.4.5.1 Heat Shield Design

Using heritage missions as a baseline for design, the heat shield was designed as a shallow cone with a diameter greater than that of the HGA. The cone is angled at 70° and tapers from a carbon phenolic thickness of 40 mm at the nose to 30 mm at the edges. The cone connects to the back shell and drag skirt at its rim. The heat shield will attach to the equipment enclosure of the orbital stage via a separation mechanism. The majority of the loading experienced during aerocapture will act on the heat shield and be transferred to the orbital stage through these connections.

5.4.5.2 Back Shell Design

The back shell's function is to protect the orbital stage during aerocapture, as well as to provide a surface for drag to act on during the latter part of the aerocapture maneuver. The back shell

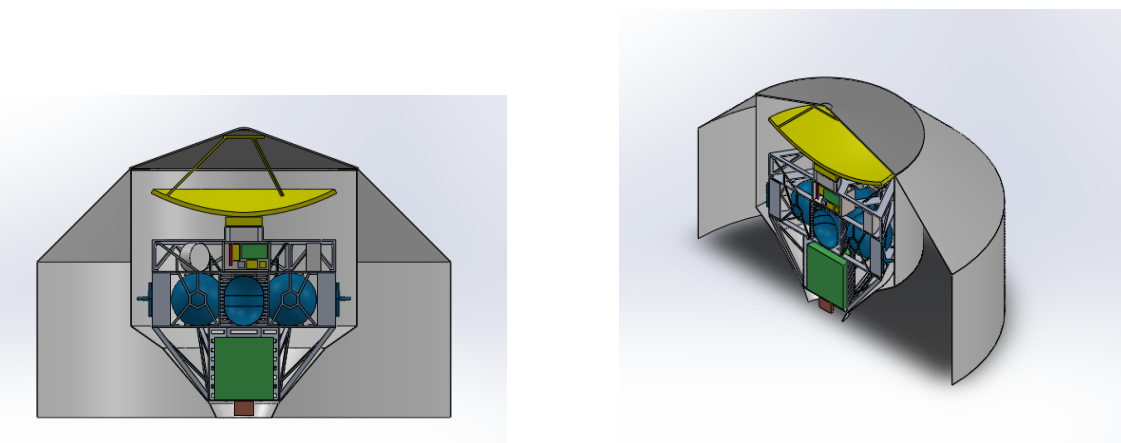


Figure 36: Entry Stage, Front

Figure 37: Entry Stage, Isometric

is made from carbon phenolic for similar reasons as the heat shield, and is designed to occupy a sleek, narrow profile around the orbital stage. It will connect to the orbital stage via separation mechanisms at the top of the equipment enclosure as well as at each deck support plate.

5.4.5.3 Drag Skirt Design

The drag skirt will also be made of carbon phenolic. It will be designed to taper away from the interface with the heat shield at a 45° angle in order to provide a surface for drag as well as aerial stability. At a diameter of 4.56 m, the drag skirt will cease to taper and transform into a cylindrical shape in order to fit within the launch vehicle fairing.

5.4.5.4 Entry Stage Data

Relevant information about the entry stage is shown in Table 21 below. All masses account for 20% margin on top of dry mass values.

Table 21: Entry Stage Data

Item	Property	Unit	Notes
Entry Mass	1,891.8	kg	Aeroshell and orbital wet mass
Mass, Heat Shield	121.2	kg	
Mass, Drag Skirt	276.3	kg	
Length	3.20	m	along main axis
Diameter	2.50	m	at back shell
Diameter	4.56	m	at drag skirt

5.4.6 Cruise Stage Design

The cruise stage (Figures 38 and 39) houses rudimentary telemetry, guidance, and propulsion systems. It is connected to the drag skirt via a separation mechanism and is jettisoned just before the aerocapture maneuver.

5.4.6.1 Propulsion Deck

The propulsion deck of the cruise stage consists of a series of 1N thruster quads arranged in a similar manner to those of the orbital stage. No 20 N thrusters are needed, as maneuvers necessary during

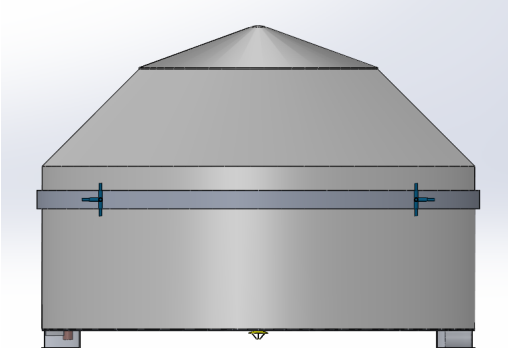


Figure 38: Cruise Stage, Front

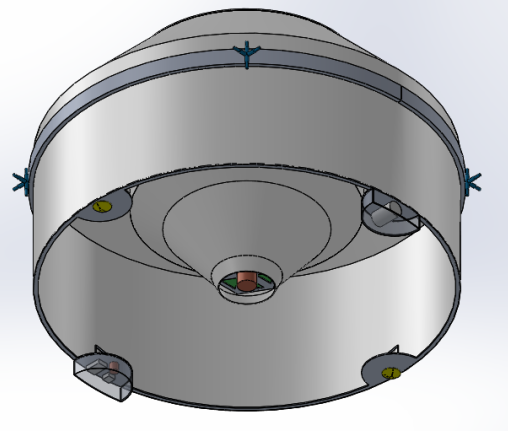


Figure 39: Cruise Stage, Isometric

the cruise stage will be small TCMs. The thruster quads are attached to a small deck taking the shape of a ring, which will detach via a separation mechanism at the appropriate time. The deck is located at the COM of the main axis so that the thrusters remain close to the COM as it shifts as propellant is expended.

5.4.6.2 Science Deck

The science deck of the cruise stage consists of a small ring located at the base of the drag skirt. It has four nodes, two of which house LGAs, and the other two of which house a star tracker and sun sensor. An additional MGA will be placed atop the heat shield so that the spacecraft will be in communication with ground control under multiple orientations. This MGA will be attached to the spacecraft via a separable boom that extends from the propulsion deck - it will not be affixed to the heat shield. The science deck will be expelled from the entry stage via a separation mechanism initiated just before the aerocapture maneuver.

5.4.6.3 Cruise Stage Data

Relevant information about the cruise stage is shown in Table 22 below. All masses account for 20% margin on top of dry mass values.

Table 22: Cruise Stage Data

Item	Property	Unit	Notes
Dry Mass	2,244.7	kg	Orbital wet mass
Wet Mass	2,417.1	kg	Launch mass
Length	3.49	m	along main axis
Diameter	5.00	m	at propulsion deck
COM_x	0	m	centered on main axis
COM_z	0	m	centered on main axis
COM_y	1.57	m	From bottom of spacecraft

5.4.7 Separation Mechanism

Separation mechanism are used for jettison cruise stage and aeroshell. Low shock separation system which is flight heritage from RUAG Space has been selected to perform separation. The diameter range of separation target can be between 381 to 2624 mm.



Figure 40: Separation Mechanism [10]

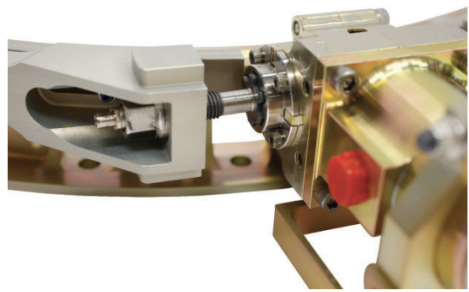


Figure 41: Separation Mechanism Installed View [11]

5.4.8 Simulation Results

A loading simulation was performed using SolidWorks to verify that the structure of the orbital stage would survive the aerocapture maneuver at Jupiter. The maximum loading expected was estimated at around 30 Earth gs, which multiplied by the entry mass of around 1,900 kg gives a force that was rounded up to 575,000 N. This force was applied evenly around the top edge of the equipment enclosure. The results of the study are shown in Figures 42 and 43.

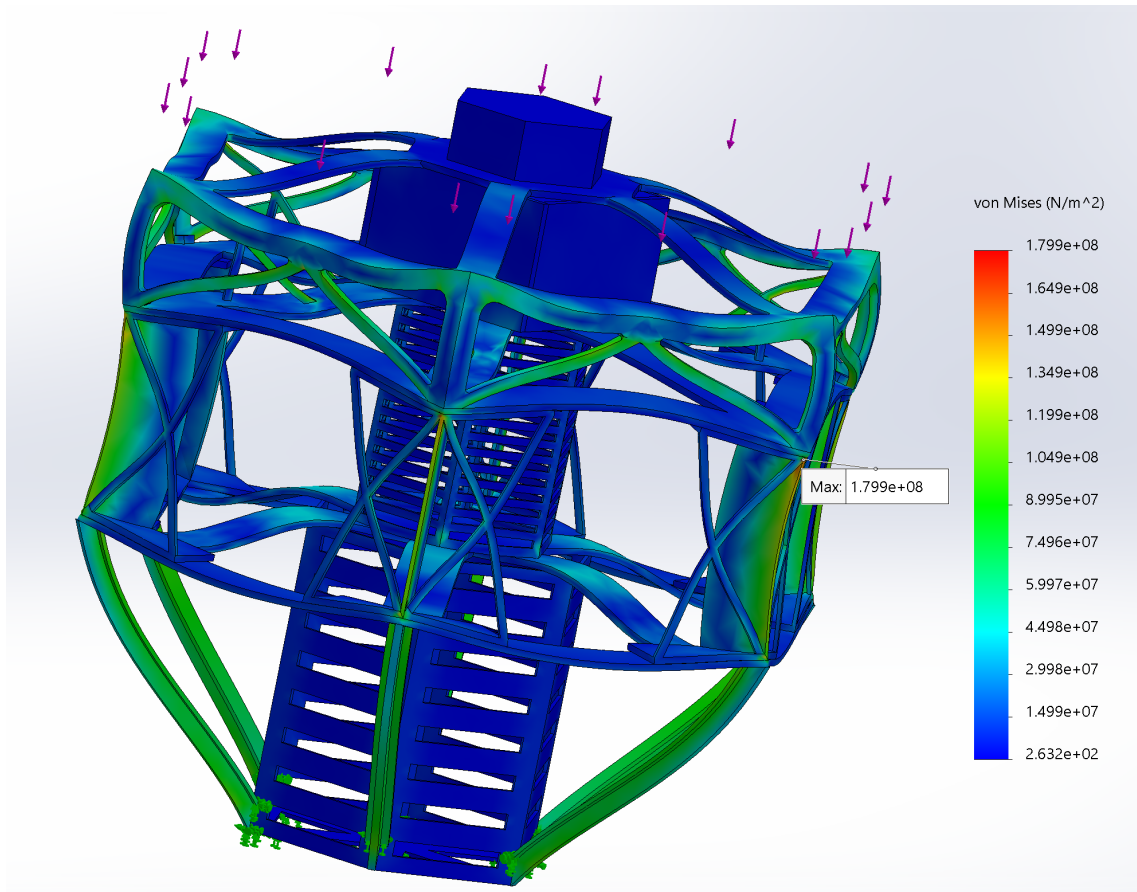


Figure 42: Load Simulation Stress

The maximum stress the structure is expected to undergo under this loading is about 194 MPa. As the yield stress of Al-7075 is 503 MPa [12], this grants a safety factor of roughly 2.6, well within an acceptable engineering limit. To further the conclusion that the spacecraft is adequately structurally designed, the SolidWorks simulation was unable to accommodate the radial struts on all three decks, meaning the actual safety factor is likely higher.

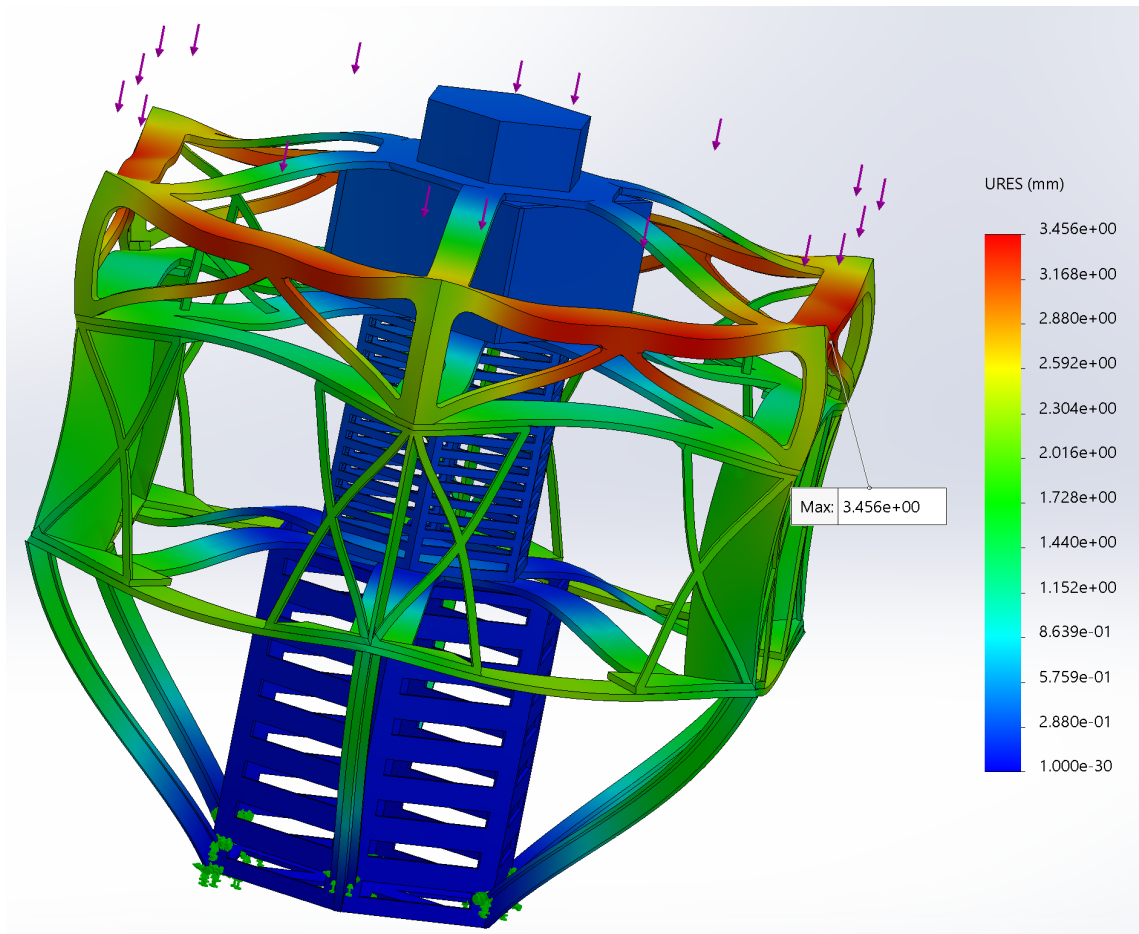


Figure 43: Load Simulation Deflection

The maximum deflection that the structure is expected to undergo is 3.6 mm. This deflection occurs over a span of 1.01 m, and is acceptable, especially under low expected stresses.

5.4.9 Risk

The structures subsystem faces several imminent risks pertaining to the aerocapture maneuver as well as the spacecraft environment (Figure 44). There is a small chance that, despite thorough loading analysis, the spacecraft fails structurally during the aerocapture maneuver. There is also a minimal risk that the separation events do not complete successfully and the spacecraft remains attached to the launch vehicle, to the Cruise stage, or to the Entry stage. As these risks are unlikely, they are tolerable. There is also the risk that the spacecraft's electronics will decompose due to the radiation in the environment around Jupiter. If this were to occur, it would likely be at a slow enough pace for the mission to remain successful.

5.5 Thermal System

Thermal control of the spacecraft is essential for proper operation. Maintaining a reasonable operating temperature will allow the equipment, instrumentation, and mechanisms to operate efficiently and properly. A consistent temperature will also aid in structural stability as differing material coefficients of thermal expansion will not respond positively to large temperature fluctuations. This could result in structural failure if not controlled.

Consequence (Expected Impact to the Mission)	Severe (5)	Separation mechanisms do not actuate, vehicle remains fixed to LV/Aeroshell	Heat shield/Orbital Stage does not survive aerocapture maneuver			
	Significant (4)	Micrometeoroid impact		Radiation vault does not shield sensitive components from environment		
	Moderate (3)					
	Minor (2)					
	Negligible (1)					
Likelihood (Qualitative)		Very Unlikely (1)	Unlikely (2)	Possible (3)	Likely (4)	Very Likely (5)
Acceptable Tolerable Intolerable						

Figure 44: Structures Risk Matrix

5.5.1 Thermal Level IV Requirements

The Thermal Control Requirements are as follows:

Table 23: Thermal Subsystem Requirement

Req. No.	Requirement	Rationale	Verification
TPS-01	The TPS shall maintain scientific (payload) equipment between -20° and +60°C. (TBR)	This is the maximum and minimum operational temperature of payload.	Analysis and Test
TPS-02	The TPS shall maintain operational equipment between -20° and +50°C. (TBR)	This is the maximum and minimum operational temperature of all the components.	Analysis and Test
TPS-03	The TPS shall include MLI blankets as insulative material to retain heat.	This will ensure the spacecraft does not exceed the operational temperature.	Analysis and Test
TPS-04	The TPS shall include a system of louvers to jettison excess heat.	This will allow for proper internal heat dissipation within the spacecraft vault.	The spacecraft design includes louvers
TPS-05	The rigid aeroshell shall include 4cm thick (TBR) of carbon phenolic ablative material.	This will ensure the aeroshell ablative material will not be at zero thickness when the aerocapture event is over.	Analysis and Test
TPS-06	The rigid aeroshell shall be capable of withstanding $40MW/m^2$ peak heat.	This will ensure the spacecraft does not exceed the operation temperature.	Analysis
TPS-07	The rigid aeroshell shall be capable of withstanding $40MW/m^2$ integrated heat load	This will ensure the spacecraft does not exceed the operational temperature.	Analysis and Test
TPS-08	The TPS shall include a rigid aeroshell to protect the spacecraft during aerocapture.	This will ensure the spacecraft does not exceed the operational temperature during the aerocapture event.	The spacecraft design includes a rigid aeroshell

5.5.2 Operating Temperature

The operating temperature of the spacecraft will be between -20° and 50° Celsius. We will include a 20° margin so the analyzed temperature range will be 0° to 30° Celsius. This was determined by creating a thermal budget outlining the operational temperatures of the components in the spacecraft and finding the warmest low end temperature and the coolest high end temperature to set the bounding range. This budget is shown in the table below:

5.5.3 Thermal Environment

The thermal environment for the spacecraft will vary for the different stages of flight. The primary cases for thermal considerations are cruise near Venus (hot), Jupiter eclipse (cold), and aerocapture (hot heatshield). With the exception of the aerocapture stage, the primary form of heat transfer between the spacecraft and its environment will be radiation. This will be in the form of direct solar radiation, albedo radiation (solar radiation reflected from nearby planets), planetary radiation, RTG radiation, and radiation from the spacecraft to deep space.

The main contributor to the thermal environment will be radiation from the sun. There will be two primary solar irradiance values to consider in the preliminary analysis of the spacecraft. One at Venus orbit and the other at Jupiter orbit. These values are $2601.3 W/m^2$ and $50.26 W/m^2$ respectively. A secondary contributor will be planetary radiation. For the limiting thermal load cases (hot and cold) the planetary radiation fluxes will vary. The hot case will use Venus's planetary

Telecom	Low Temperature (C)	High Temperature (C)
Small Deep Space Transponder	-40	60
IRIS Transponder V2.1	-20	50
Waveguide Transfer Switch x 2	-20	50
X-Band Diplexer	-20	50
High Gain Antenna (Orbiter)	-160	170
Medium Gain Antenna (Cruise)	-160	170
Low Gain Antenna (Cruise)	-160	170
Traveling Wave Tube Amplifier (TWTA)	-40	60
C&DH	Low Temperature (C)	High Temperature (C)
RAD750 SpaceVPX SBC	-55	125
ADCS	Low Temperature (C)	High Temperature (C)
Sun Sensor x 2: Digital Sun Sensor ($\pm 32^\circ$)	-20	65
Star Tracker x 2	-20	65
4 Reaction Wheels - Assume RSI 45	-20	65
IMU - LN-200S	-54	71
Operation Temperature	-20	50

Figure 45: Operational Temperature Budget

radiation and the cold case will conservatively assume no planetary radiation since the spacecraft will be far enough from any planets for that portion to be considered negligible.

Tertiary effects will be from planetary albedo and RTG radiation/spacecraft radiation. Albedo radiation is calculated using the formula $J_a = J_s a F$ where a is the planetary albedo (Venus: $a = 0.6$, Jupiter: $a = 0.465$) and F is the visibility factor (For purposes of this assessment we will conservatively assume $F = 1$ which would be a low altitude direct angle case).

5.5.4 Thermal Design

The spacecraft will use both active and passive thermal controls. The primary form of thermal control will be the passive control of surface finish and insulation. Our spacecraft will be painted in such a way to limit the ratio of α/ε . MLI blankets are strategically placed to provide additional radiative insulation to the spacecraft. Additionally, the spacecraft design has been adjusted in such a way to consider conduction paths and desirable heat dissipation within the vault. The surface coating and insulation will be discussed in more detail in the thermal analysis section.

The MLI blankets used for the spacecraft will include three primary types of layering. The outer cover, reflective layers, and separator layers. NASA/TP-1999-209263 (Multilayer Insulation Material Guidelines) was used as a guide to the MLI blanket design. For the outer layer Kapton was selected as the material due to its favorable absorptance to emissivity ratio and its proven record in spaceflight.

[1] Kapton			
Thickness, cm (mil)	gm/cm ² (lb/yd ²)	a	e
0.0013 (0.5)	0.0019 (0.034)	0.41	0.50
0.0025 (1.0)	0.0036 (0.66)	0.44	0.62
0.0051 (2.0)	0.0071 (0.131)	0.49	0.71
0.0076 (3.0)	0.011 (0.20)	0.51	0.77
0.0127 (5.0)	0.019 (0.34)	0.54	0.81
0.0191 (7.5)	-		
0.0254 (10.0)	-		

Figure 46: Kapton Radiative Properties

For the reflective layers, Alumized reflective Mylar will be used also for its absorptance to emissivity ratio and historical usage.

[3] Mylar, single aluminized		
Thickness, cm (in.)	a	e
0.00064 (0.00025)	0.16	0.33
0.0013 (0.0005)	0.16	0.46
0.0025 (0.001)	0.19	0.57
0.0051 (0.002)	0.23	0.72
0.0076 (0.003)	0.25	0.77
0.0127 (0.005)	0.27	0.81

Figure 47: Mylar Radiative Properties

The separators layer will be made from Dacron netting. This due to its proven record in spacecraft and availability. The separator layer serves no insulating purpose.

For active control, the design incorporates louvers within the pressure sealed vault to encourage heat dissipation via conduction and convection. For the cold Jupiter eclipse case, active heater control will be used.

The heaters used in the spacecraft will be thermostatically controlled resistive heaters. In particular Polyimide Film Insulated Flexible Heaters. These are a good choice due to their simplicity and excellent outgassing properties in a vacuum. Any required heat output can be achieved with the right electrical input.

The heatshield material is addressed in the structures section. Carbon phenolic will be used as the ablative material for the heat shield. It will experience a maximum 400 MW/m^2 heat flux during aerocapture for roughly 3 minutes. The initial estimation for heat shield thickness is 4cm in the center and 3cm on the edge. This is based on test data for a carbon phenolic heat shield for a lower heat flux with 1.5cm thickness. The thickness was scaled up to the maximum thickness that will accommodate the mass requirements. The final thickness will be determined after detailed analysis at the CDR level.

Detailed finite element thermal analysis will be completed post-PDR and risks associated will be addressed in the risks and mitigation plan. For the purposes of a PDR-level review, simplified geometry and basic assumptions will be made for the thermal analysis.

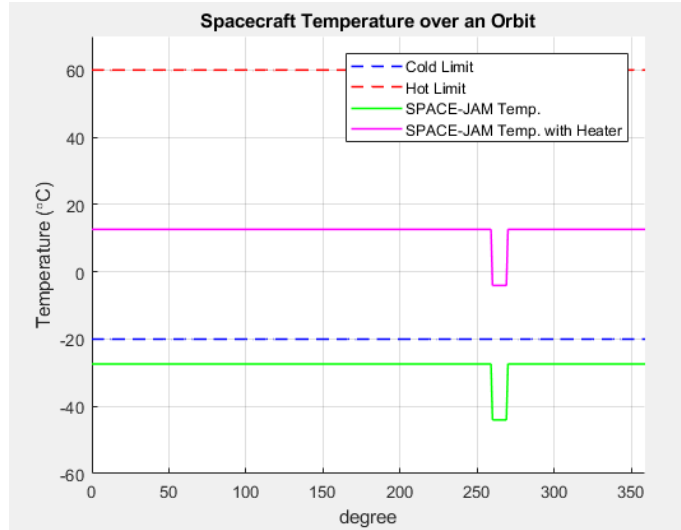
5.5.5 Thermal Analysis

An initial thermal analysis was completed to determine the temperature of the spacecraft. This was done using the thermal environments described earlier. A basic energy balance was completed assuming the spacecraft is a sphere. Using this balance, a matlab script was created to calculate

$$Q_{in,solar} + Q_{in,albedo} + Q_{in,internal} = Q_{out,space} + Q_{out,earth}$$

the balance and use it to determine temperature. The resulting table from that analysis is shown below:

Detailed finite element thermal analysis will be completed post-PDR and will be finalized for CDR.



5.5.6 Thermal Risks and Mitigation Plan

The primary risk from a thermal perspective is loss of mission due to improper thermal control. This is mitigated by the combination of active and passive thermal control on the spacecraft. As mentioned in the thermal design section, the spacecraft will utilize surface coating and insulation as a passive control, and heaters and louvers as an active control. Another risk is the failure of the active systems such as the louvers and heaters. Both of these systems, and especially the heaters are extremely simple components with few opportunities for failure. Quality control is essential to ensure the products are coming from a reliable supplier with historical reliability in the spacecraft industry. The thermal systems implemented on our spacecraft have been used for decades on a multitude of different missions. The methods used are well tested and verified. The failure of the thermal system is at low risk.

5.6 Electric and Power System

5.6.1 Requirements

Req. No.	Requirement	Rationale	Verification
EPS-01	The EPS shall provide operational current and voltage power to all subsystems	Ensures all subsystems have required power.	Sizing power modes and ground testing.
EPS-02	The EPS shall provide protection to all subsystems from voltage and current transients.	Ensures components and systems are not damaged due to power transients.	Ground testing.
EPS-03	The EPS shall have the capability to switch power on or off to individual subsystems.	Ensures that the spacecraft power draw does not exceed the desired power or total power available.	Ground testing.
EPS-04	The spacecraft battery shall allow at least 12 hours of continuous downlink once the RTG has degraded below peak downlink power requirements.	Avoids bottlenecks in science data retrieval.	Day-in-the-life simulations and ground testing of battery capability.
EPS-05	The spacecraft battery depth of discharge shall not exceed 80% over the mission life.	Helps preserve battery life.	Day-in-the-life simulations.
EPS-06	The power system shall be able to perform power reset of the spacecraft.	System recovery.	Ground testing

Table 24: Level IV EPS Requirements

5.6.2 Power Selection

With an average orbit radius of 5.2 AU, the solar flux at Jupiter is roughly 3.7% of that at Earth. As such, any solar powered spacecraft operating at Jupiter must have solar panels which are considerably larger than required at Earth for the same power. Juno's are 72m^2 and generated only 480W at the start of the mission. An aerocapture mission requires two sets of panels, one for the cruise stage and one for the orbiter which would unfold after the aeroshield jettison event.

The other option for spacecraft power is to use an RTG which provides a constant source of power through radioactive decay. RTGs have been used in multiple missions but incur extremely high cost and produce several kilowatts of waste heat most of which must be radiated into space.

A preliminary trade study was conducted to determine the feasibility of solar vs RTG power for SPACEJAM based on projected spacecraft power demands. The study assumed a cruise stage requiring 100W and orbiter requiring 200W. The estimated parameters of a solar-powered spacecraft are shown in Fig 25.

	Cruise	Orbiter	Totals
SC Power (W)	100	200	
Degradation	15%	15%	
Margin	20%	20%	
Effective Power (W)	138	276	414
Area (m²)	20.73	41.45	62.18
Mass (kg)	97.75	195.50	293.25
Volume (m³)	1.04	2.07	3.11
Cost	\$1,868,750.00	\$3,737,500.00	\$5,606,250.00

Table 25: Preliminary Solar Power Study

A similar study was conducted for an RTG powered spacecraft assuming a 200W power requirement at end of mission, Fig 26. While an RTG powered spacecraft is considerably more expensive, the savings in mass, volume, and complexity are substantial.

Power EOM (W)	200
Power BOL (W)	343.58
Mass (kg)	123.69
Volume (m³)	0.594
RTG Cost	\$168M
Launch Provider Costs	\$28M
Total Cost	\$196M

Table 26: Preliminary RTG Power Study

In addition to mass, volume, and cost comparisons, the power system decision also factored in complexity concerns which ultimately drove the decision for RTG. Following aerocapture the spacecraft has a limited time (potentially just a few days, see the mission design and aerocapture sections, found in 5.1) to jettison the aeroshell and begin using the orbiter GNC system to calculate the spacecraft's Jovian orbit and compute and perform the perijove raise maneuver. Any delays in this process could result in the spacecraft failing to complete an acceptable perijove raise and re-entering Jupiter's atmosphere on its initial orbit causing a complete mission failure. Requiring solar panel deployment and orientation immediately following aerocapture adds additional complexity and potential for mission failure if the panels do not deploy correctly. This concern swung the spacecraft power decision in favor of using an RTG. The overall trade-study results are shown in Fig. 27. Since the overall cost of a 200W end of life (EOL) RTG is substantial effort was made to reduce the overall spacecraft power consumption considerably to reduce the size of the RTG which would also reduce the thermal load on the spacecraft.

	Weight	RTG		Solar	
		Score	Total	Score	Total
Volume	2	1	2	2	4
Mass	1	1	1	2	2
Cost	3	2	6	1	3
Reliability	4	1	4	2	8
Complexity	5	1	5	2	10
Total			18		27

Table 27: RTG-Solar Trade Study (Lower is better)

5.6.3 RTG Performance

The RTG utilizes plutonium-238, which decays rapidly with a half-life of just 87 years. This results in a power decline of 4.8% per year after assembly of the RTG, known as beginning of life (BOL). This mission is designed for an RTG with a BOL of 203 We. The decline in performance over the

mission is shown in Fig. 48 assuming BOL is one year prior to launch. This decay leads to an EOL RTG output of 120 W approximately 10.7 years after assembly on the RTG.

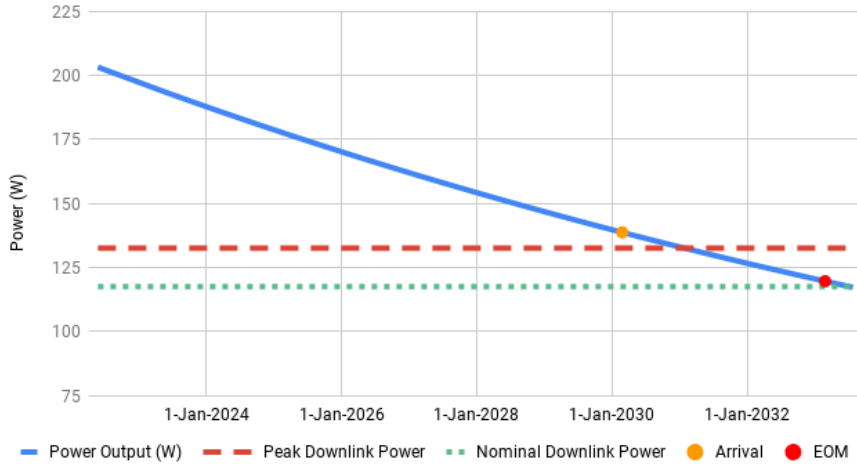


Figure 48: RTG Lifetime Power Decay

5.6.4 System Overview

The electrical and power system is responsible for the distribution and regulation of power on-board the spacecraft. The spacecraft is powered by an RTG based on the multi-mission radioisotope thermoelectric generator, which is contained within the orbiter section of the vehicle and powers both the orbital and cruise sections for the duration of the mission. This RTG is connected to a shunt regulator unit, which dissipates the waste heat by-product from the device. The RTG then connects to a power distribution unit. This PDU is connected to separate bus boards that provide power to spacecraft components with different voltage requirements. The main busses that are connected to the PDU provide power at voltages of 5 V, 15 V, and 28 V. The power system also include a 400Wh lithium ion battery to provide extra power during downlink and emergency power in case of a power interruption to one of the busses. Regulation of the battery charge and temperature is conducted by the battery management unit (BMU), battery charge regulator (BCR), and battery discharge regulator (BDR). Battery temperature is regulated using waste heat from the RTG.

5.6.5 Power Distribution Unit

The power distribution unit used on this spacecraft is TBD (Pending reduced power consumption on new PDU). The PDU regulates the flow of power from the RTG to the components and battery, as well as the rails to each of the voltage busses. This layout may be viewed in the power system's functional block diagram in Fig. 49. Additionally the PDU functions to switch subsystem power on and off as directed by CDH and flight software depending on the operational mode of the spacecraft. The PDU monitors the power draw by each subsystem and component and can shutdown and reset systems in the event of a malfunction. This function also protects subsystem components from transient over/under voltage conditions. To recover the spacecraft in the event of a failure mode, the PDU can also perform a spacecraft power reset.

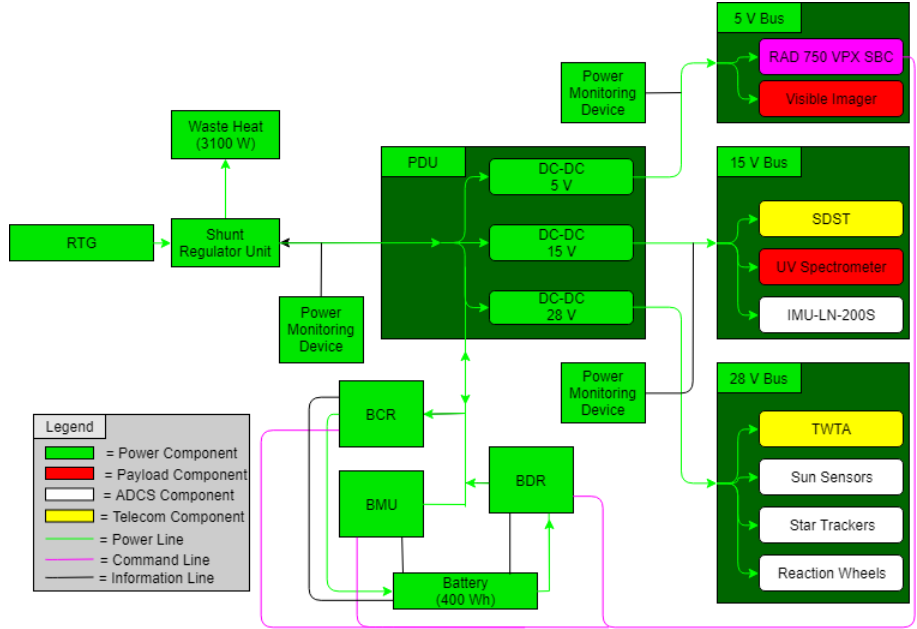


Figure 49: Power System Functional Block Diagram

5.6.6 Power Budget

The spacecraft power draw by subsystem and allocated contingency power to account for power transients and aging components is shown in Table 28. Subsystem components are then broken down and powered on or off in one of five main submodes: Science, Downlink, Cruise, Aerocapture, and Safe Mode. The PDU is responsible for directing power to each subcomponent as commanded by the flight software. With the exception of downlink, the spacecraft is power positive in all modes. Downlink requires the use of a battery to support the gap in power provided by the RTG after it decays beyond 133W (see battery sizing).

System	Nominal Power	Contingency	Peak Power	Components
Telecom				
Small Deep Space Transponder	12.9 /19.5 54	20% 5%	12.9 54	1 1
C&DH				
Flight Computer	10	30%	11	1
EPS				
PDU	5	20%	5	1
Propulsion				
Thruster	5	20%		4
ADCS				
Sun Sensor	1	5%	1	2
Star Tracker	8	5%	8	2
Reaction Wheels	2	20%	2	4
IMU	12	20%	12	1
RCS Thrusters	1	20%	0	16
Payload				
Visible Imager	6	20%	6	1
UV Spectrometer	18	20%	18	1

Table 28: Subsystem Power Draw

System	Science		Downlink		Cruise	
	Nominal	Peak	Nominal	Peak	Nominal	Peak
Telecom						
Small Deep Space Transponder	12.9	15.48	19.5	23.4	12.9	15.48
TWTA	0	0	54	56.7	0	0
C&DH						
Flight Computer	10	13	10	13	10	13
EPS						
PDU	5	6	5	6	5	6
Propulsion						
Thruster	0	0	0	0	20	24
ADCS						
Sun Sensor	1	1.05	1	1.05	1	1.05
Star Tracker	8	8.4	8	8.4	8	8.4
Reaction Wheels	8	9.6	8	9.6	8	9.6
IMU	12	14.4	12	14.4	12	14.4
RCS						
Thrusters	0	0	0	0	8	9.6
Payload						
Visible Imager	6	7.2	0	0	0	0
UV Spectrometer	18	21.6	0	0	0	0
Total Power	80.9	96.73	117.5	132.55	84.9	101.53

Table 29: Spacecraft Power Modes - Science, Downlink, Cruise

System	Aerocapture		Safe Mode	
	Nominal	Peak	Nominal	Peak
Telecom				
Small Deep Space Transponder	12.9	15.48	12.9	15.48
TWTA	0	0	0	0
C&DH				
Flight Computer	10	13	10	13
EPS				
PDU	5	6	5	6
Propulsion				
Thruster	0	0	0	0
ADCS				
Sun Sensor	0	0	1	1.05
Star Tracker			8	8.4
Reaction Wheels	0	0	15	18
IMU	12	14.4	12	14.4
RCS Thrusters	0	0	0	0
Payload				
Visible Imager	0	0	0	0
UV Spectrometer	0	0	0	0
Total Power	39.9	48.88	63.9	76.33

Table 30: Spacecraft Power Modes - Aerocapture, Safe Mode

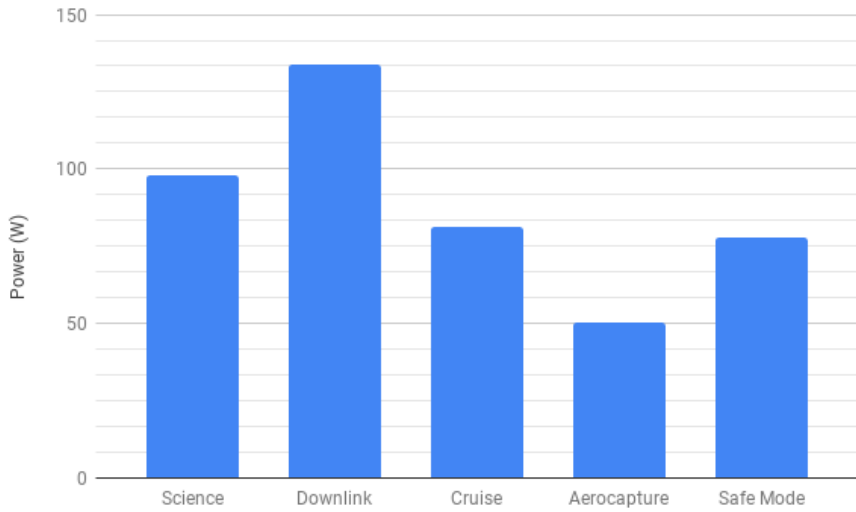


Figure 50: SPACEJAM Power Budget

5.6.7 Battery Sizing

Due to a negative net power when the spacecraft is transmitting science data back to the Earth, a lithium-ion battery is used to overcome the gap in power. The max net power loss is 13W based on the projected RTG performance at EOM and the peak downlink power. As the spacecraft is power positive when not transmitting, the battery depth of discharge can be allowed to be greater than in a solar powered spacecraft. Starting with a 400Wh battery and allowing for margin and battery degradation, the battery can support a discharge time of 19.8 hours and 11.2 hours to recharge assuming the spacecraft is in the science power mode while recharging. If the instruments are switched off, recharge can be accomplished faster.

RTG GPHU	13
Power BOL (W)	203.13
Power Launch (W)	193.38
Power EOM (W)	119.61
Max Bus Power (W)	132.55
Net Power (W)	-12.94
Heat Load Launch (W)	3094
Battery Size (Wh)	400
Battery Degradation	20%
Max Drawdown	80%
Effective Battery Size (Wh)	256
Battery Discharge Time (h)	19.78
Recharge Net Power (W)	22.88
Battery Recharge Time (h)	11.19

Table 31: Spacecraft Battery Sizing

5.6.8 Risk

The power system in coordination with CDH and flight software provides the necessary logic and control to protect the spacecraft in the event of power transients or interruptions and to attempt a recover of the spacecraft by conducting a power reset. These functions will be tested and verified on the ground prior to launch. The largest risk to the spacecraft comes from the radiation environment which the PDU and electronics vault must be able to tolerate for the duration of the

mission. In the event of a power interrupt, the battery can provide temporary emergency power to the spacecraft; however due to the limited battery capacity and lengthy communications time, the spacecraft power system must be able to self-recover into safe mode without human intervention. The power risk matrix is shown in Figure 51.

Consequence (Expected Impact to the Mission)	Severe (5)			Critical Bus Failure (Ground testing)			
	Significant (4)						
	Moderate (3)				Radiation Damage (Shielding and fault tolerance)		
	Minor (2)			Battery Overheat (Battery charge regulation & temp monitoring)	Power Interrupt (Battery backup / power reset)		
	Negligible (1)				Transient Power Exceedance (Battery backup / PDU switching logic)		
			Very Unlikely (1)	Unlikely (2)	Possible (3)	Likely (4)	Very Likely (5)
		Acceptable	Tolerable	Intolerable	Likelihood (Qualitative)		

Figure 51: Power Risk Matrix

5.7 Command and Data Handling

Command and data handling is responsible for keeping the spacecraft operational throughout the mission from take-off to decommissioning. The subsystem must be able to continuously monitor all of the subsystems, send commands to the subsystems if necessary, and store the science data until it can be sent to the ground. These responsibilities are shared with the ground crew, but command and data handling must be able to handle any issue autonomously until the ground crew can contact the spacecraft.

5.7.1 Requirements

The following requirements are derived from the high level science objectives of the mission and are meant to define the capabilities of the command and data handling subsystem. From these requirements, a list of possible solutions can be determined. The baseline for the numerical values in the requirements came from Juno's capabilities and research into the current technology.

Table 32: Command and Data Handling Requirements

Req. No.	Requirement	Rationale	Verification
CDH-01	Command and data handling shall provide at least 512 megabytes of non-volatile flash memory.	There must be enough memory to store data and flight software throughout the mission.	Selected a radiation hardened flash memory.
CDH-02	Command and data handling shall be capable of operating between -50 to +100 degree Celsius temperature range.	Electronics must be able to operate in a wide range of conditions that may occur.	Ground thermal testing.
CDH-03	Command and data handling shall continuously monitor internally for data anomalies during the mission.	The spacecraft needs to be able to diagnose and correct problems autonomously because of the large distance to Jupiter.	Ground testing of software.
CDH-04	Command and data handling shall provide a master clock for the spacecraft.	Because there will be limited communication, the spacecraft needs to be able to coordinate its in-flight actions and communication with the ground team.	Ground testing of software.
CDH-05	Command and data handling shall monitor the spacecraft location and orientation.	The spacecraft must be able to correct its orientation or trajectory autonomously.	Ground testing.
CDH-06	Command and data handling shall provide at least 128 Megabits per second of on-board data transfer capabilities.	Based on capabilities of Juno with similar instruments.	Ground testing.

The following image shows the functional inputs and outputs of the command and data handling subsystem.

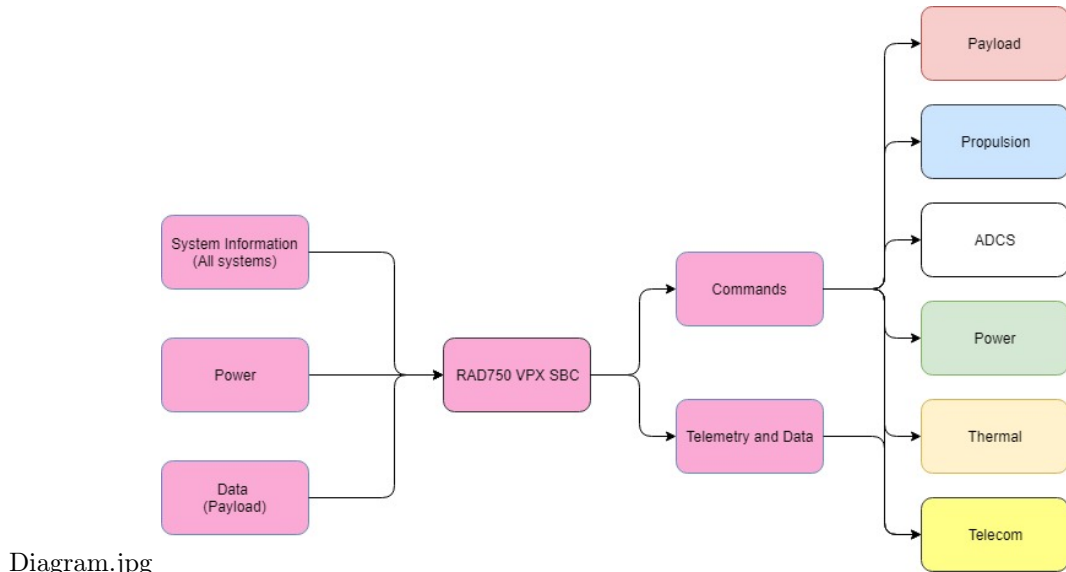


Diagram.jpg

Figure 52: Command and Data Handling Functional Block Diagram

5.7.2 Trade Study

The requirements listed above define the selection criteria for necessary components of the command and data handling subsystem. Two initial possibilities were considered: selecting a processor, the computer board, and flash memory storage separately to get the best components possible, or selecting a single board computer that had already integrated these parts. Ultimately the decision was to go with a single board computer. Although this decision limited some options, it nearly eliminates the time necessary to ensure selected parts will work together. Using that time for fault testing and making the launch date was determined to be more important than getting a high performance configuration. Once this decision was made, three single board computers were selected for further consideration. Two were from BAE Systems, the RAD750 VPX and RAD5545 VPX, and one from IBM and Motorola, the PowerPC 603e TM.

Each of these three single board computers is capable of satisfying the requirements with minimal or no additions. The IBM/Motorola computer does not meet the memory requirement, but an additional storage unit could have been added. However, power consumption, unit size, voltage, current, operational temperature range, processing capability, and flight heritage were the major factors in the trade study process. Cost was a factor as well, but was not heavily weighted in the initial decision process. In most areas the computers were very similar, so the decision came down to three major factors, power consumption, available memory, and data processing capabilities, shown in the following table.

Command and Data Handling Trade Study			
Computer	Power(W)	Memory	Processor Ability
RAD750 VPX	10.9	128MB RAM, 512MB Flash	500DMIPS
RAD5545 VPX	35	16GB SDRAM, 8GB Flash	3.7GFLOPS
PowerPC 603e TM	12.5	4MB SRAM, 4MB EEPROM	152 DMIPS

From the table, the PowerPC 603e TM offers the least memory and processing capability, and has higher power consumption than the RAD750 VPX. The RAD5545 VPX offered significant advantages in memory and processing ability, but power consumption was too high to be feasible for this mission. The RAD750 VPX was left as the most desirable option, using the least power but still offering enough memory and processing capability to meet the requirements. A similar computer was flown on Juno which only bolstered confidence that this computer would work well for this mission.

5.7.3 Memory Allocation

Memory will be limited on this mission so it must be decided early on how much memory is allocated for science data. Starting with 512 Megabytes, 10% is immediately taken off for a margin. This leaves 460.8 Megabytes of usable space. At this point, 15 Megabytes have been allocated for whichever operating system is ultimately chosen, such as VxWorks. An additional 25 Megabytes have been allocated for the application software and backup copy of the software. This leaves 420.8 Megabytes of storage for science data and any other currently unknown storage needs. Built in to the allocation estimates for the operating system and software is a margin of roughly 20%. It is likely that the code will grow over time, even after launch, so some margin will remain even as the launch date approaches.

5.7.4 Risk Assessment

On this mission, one of the largest risk factors is the radiation that will be encountered by the spacecraft. It can affect the on board memory resulting in loss of data, loss of spacecraft, and loss of mission. Radiation hardened components were selected to mitigate the possibility of these outcomes and some storage has been bookmarked for backup data.

There is significant risk in flying only one computer. If it malfunctions and cannot be restored, then the mission is over. However, adding a backup computer adds significant complexity to the design and subsequently that computer must also be tested during flight to ensure functionality. The two biggest factors in this decision were determined to be longevity and radiation. The computer will need to survive operating for around ten years minimum, at least three of which will be in a very high radiation environment. Two recent missions using the RAD750 processor, Juno and the Van Allen probes, have been in operation for 7.5 and 6.5 years respectively. This builds confidence in the ability of the computer to perform for the length of the mission, and because of the high radiation environments these missions operate in, it also builds confidence in the radiation resistance capability. Because bringing a second computer does not necessarily protect the system from radiation hazards, and because the electronics will be enclosed in a vault similar to Juno's to guard against radiation, one computer was determined to be sufficient for this mission. Some additional factors that were considered in this decision were cost, complexity, ground testing time, and failure modes. It was determined that the risk of flying one computer was low enough to offset the extra time and money needed to integrate a second computer that may also fail.

5.8 Attitude Determination and Control System

The ADCS system is used to determine a spacecraft's position in space and assess the need for using any combination of actuators to maneuver the spacecraft into the desired orientation. During SPACEJAM mission cruise and science operations, RCS and reaction wheel control will be provided to maintain telemetry connections with Earth, obtain proper pre-TCM attitude and stabilize the spacecraft as needed for data collection. Guidance and control throughout the aerocapture maneuver will also rely heavily on ADCS sensor feedback to provide additional TCM capability to compliment control provided by aeroshell geometry for accurate post-aerocapture positioning.

5.8.1 ADCS Requirements

Table 33: ADCS Cruise Stage and Aerocapture Event Requirements

Req. No.	Requirement	Rationale	Verification
ADCS-CR-01	The spacecraft shall maintain pointing accuracy necessary to communicate with Earth based radio stations	High gain antennas usually have very small beam widths and need to be pointed accurately.	Accuracy of sensors and RWA
ADCS-CR-02	Attitude must be known to a sufficient level where any desired TCM can be performed within required error margin	Unnecessary TCM corrections waste spacecraft fuel.	Monte Carlo analysis
ADCS-CR-03	Attitude must be correctable to a sufficient level where any desired TCM can be performed within required error margin	Unnecessary TCM corrections waste spacecraft fuel.	Monte Carlo analysis
ADCS-AC-01	The spacecraft control system shall ensure a final apogee error of less than 10,000 km post aerocapture.	This requirement will ensure the spacecraft will exit aerocapture maneuver within correctable limits for final desired orbit and minimize dV associated with TCMs.	Monte Carlo Analysis
ADCS-AC-02	The control system shall maintain a stable flight configuration throughout the duration of the aerocapture event	Any non-characterized form of spacecraft tumbling during the aerocapture maneuver has a high probability of causing loss of mission	Entry sequence simulation

Table 34: ADCS Subsystem Orbiter Stage Requirements

Req. No.	Requirement	Rationale	Verification
ADCS-OO-01	The spacecraft shall slew at a rate greater than 38 urad/s to allow for science collection at 7.5 km resolution.	Ensures that the spacecraft will be capable of completing primary science objectives	Monte Carlo analysis
ADCS-OO-02	The ADCS system shall sufficiently maintain desired attitude for long enough to maintain a clear image of prescribed region at desired resolution.	Improved data quality	Monte Carlo analysis
ADCS-OO-03	Spacecraft attitude shall be known to within a 1 mrad error	This will ensure accuracy of attitude corrections	Monte Carlo analysis
ADCS-OO-04	Spacecraft shall have authority to control the spacecraft attitude to within a prescribed 6 mrad error.	Collecting science data at multiple locations will require an assortment of possible camera angles	

Due to the complexity of the JAC science mission and aerocapture maneuver, some of the requirements for this particular ADCS system are unique when compared to other missions in a similar class. The unique aspects of the JAC ADCS system are touched on briefly below because they have notable effects on cruise, aerocapture and science collection procedures and could have significant implications toward the design of the spacecraft bus as a whole.

Getting to Jupiter is never an easy feat, but it can be made simpler by using certain control methods. For example, deep space missions like Juno have maintained stability during the long distances covered between TCM maneuvers by using spin stabilization, which is highly effective and easy to maintain if the mission requirements are conducive to doing so. Although the JAC mission will likely use this technique during transit to Jupiter, the pointing requirements associated with the plume characterization photo collection made spin stabilization difficult to use once the science phase has begun. Additionally, spin stabilization of the Juno spacecraft was assisted by the large inertia associated with the extensive solar panels. As discussed in other sections of this report, an RTG was selected for the JAC mission for many reasons, but one large byproduct of this decision was the diminished effectiveness of using spin stabilization during all phases of the JAC mission.

Due to the extreme environments associated with the aerocapture maneuver, a major subsystem requirement for the JAC mission is to minimize hardware outside the aeroshell until after the maneuver has been completed. For this reason, the ADCS system will need to accommodate the capability to maintain lift or drag modulation as the primary control technique during aerocapture. As some RCS and associated fuel will be required during cruise but the associated hardware and mass would complicate aerocapture, this requirement was also a primary argument behind the use of an expendable cruise stage.

Pointing requirements associated with the JAC mission are not in themselves atypical for this type of deep space mission, but the science requirements for this particular mission do dictate atypical conditions under which the pointing requirements will be met. The science requirements dictate that the JAC spacecraft will visit the Jovian moons at various mission stages. Therefore, the spacecraft will be required to provide significant attitude adjustments with relatively high frequency and must be able to slew with precision to get the necessary data. This is a role which reaction wheels are generally able to fulfill, but common secondary and desaturation mechanisms

like magnetometers will not be useful for this particular mission due to the inconstant and generally poorly characterized nature of the Jovian magnetic field, which also yields implications toward the use of magnetometers in attitude determination. Similarly, other common attitude determination mechanisms like sun sensors, earth horizon sensors, and GPS will be difficult to employ for this mission due to the immense distances from Earth and the sun.

5.8.2 Design Options and Trades

To meet the requirements outlined above, a number of solutions were proposed. Decisions were then brought to the PDR level by use of similar trade metrics to previous subsection decision making processes. These particular options were compared using many metrics, but the most heavily weighted were system reliability, mass, power and heritage status. Although many of the important trades discussed by the ADCS subsystem will also be discussed within other subsections, important aspects of the JAC spacecraft design as they pertain to the ADCS subsystem are outlined below.

One of largest trade performed by the JAC ADCS sub team was whether to use reaction wheels or RCS thrusters as the primary control mechanism for the SPACEJAM spacecraft. Both actuator types have distinct advantages and disadvantages ranging from power or fuel usage to pointing precision and settling speed. This decision was also coupled with the discussion of using a detachable cruise stage because the added mass and mission phase-dependent geometry associated with flying an additional stage complicated calculations, control algorithms and energy/data supply (fuel lines, data lines and electricity could have to be fed through an umbilical, etc). Within the cruise stage trade, the discussion also arose as to whether any resultant cruise stage should be uncontrolled or minimally controlled, and, if minimal control was necessary, should there be redundancy in the ADCS system to span the stages or could a central computing location with an umbilical system be sufficient? This sub-discussion primarily arose from the realization that cruise stage pointing metrics are primarily driven by low gain antenna pointing whereas the orbit stage requirements are driven by image stability and high gain pointing for science transmission.

After extensive discussion and research into commercially available hardware, the decision was made to place reaction wheels on the orbiter stage to be used in parallel with small RCS systems on both the cruise stage (outside the aeroshell) and the orbiter stage (inside the aeroshell; only to be used for post-aerocapture TCMs and perijove alteration maneuvers). Such an arrangement would enable multiple degree of freedom control of the spacecraft at all mission phases within prescribed pointing and detumbling requirements and would also reduce the amount of mass to be decelerated during aerocapture by jettisoning the unnecessary structural mass of the empty fuel tank and other related hardware. This configuration was also most readily managed from a computation and control standpoint because it enabled the use of a single array of signal wires to span spacecraft segments instead of having a completely redundant ADCS computation systems which could lead to unnecessary complexity and conflicts. This outcome is discussed in greater detail below.

Providing attitude determination and control throughout the aerocapture maneuver proved to be a technical task with solutions requiring trade. The primary discussions began as whether or not to provide active control during the maneuver and what form passive control would take if it arrived at the top of the trade space. Outlined further in the next subsection, the decision was made to pursue passive control during the aerocapture maneuver with the ADCS primarily used to monitor changes in attitude for accurate post-aerocapture TCM determination. The additional mass and complexity associated with using lift or bank angle modulation coupled with the lack of aerocapture heritage swayed the decision toward using a naturally stable rigid aeroshell configuration instead of other options like a deployable drag skirt or other mechanisms associated with an algorithm akin to Apollo-style lift modulation. It is also worth noting that control surfaces were bypassed for this particular mission due to the hypersonic velocities at which the maneuver will begin.

The last major trades addressed by the ADCS sub team concerned sensor selection, spacecraft power generation, processing/filtering , and subsequent control algorithms. As mentioned briefly above, many common sensor packages like magnetometers, GPS, earth horizon sensors and solar sensors are difficult to use for SPACEJAM for various reasons. The trade space therefore focused great detail on which sensors would be relevant in particular stages of flight and whether or not they

could be coupled for more effective attitude determination. Trading these instruments resulted in the decision to move forward with using star trackers and solar sensors as the primary navigation and attitude determination instruments with an inertial measurement unit (IMU) as required. The star trackers would be weighted more heavily in the attitude determination algorithm as a function of their greater accuracy at cruise and Jovian distances from the sun, but the solar sensor allowed a relatively easy to integrate redundancy and notable post-detumble reference point if such a scenario is ever encountered. The IMU would be used for confirmation of the other two systems until a contingency situation like detumble occurs, at which point the IMU would become the primary attitude determination system until system rates return to a desirable range. If the magnetic field becomes better understood prior to the SPACEJAM launch date, it is also worth noting that a magnetometer could also be highly useful for attitude determination of the orbiter after arriving at Jupiter, but the general perception still leans toward a lack of usefulness with our current Jovian magnetic field models.

Although power source is primarily within the EPS subsystem domain, the ADCS subteam heavily pushed for the use of an RTG because the massive solar panels required to power a mission like SPACEJAM would be very difficult to control. After deployment, the inertia values would be very high (JUNO solar panels are $2.7 \times 8.9\text{m}$ with a combined mass nearing 340 kg), which has implications toward improved spacecraft stability once a spin has started, but also implies difficulty in altering the spacecraft pointing vector. As primary science requirements dictate a capability to modify the pointing vector with great frequency, such a mass distribution would dramatically complicate the completion of primary science objectives. Additionally, assuming that the solar panels would be designed to minimize required mass, it is logical to assume a general lack of rigidity and stiffness which could allow undesired jitter or other dynamic modes that would not be present if an RTG is used. It is also worth noting that having a deployable subsystem also increases the complexity of ADCS control systems by introducing additional modes and configurations under which the system must maintain positive controllability, so it is desirable to avoid such situations where ever possible.

5.8.3 ADCS PDR Configuration

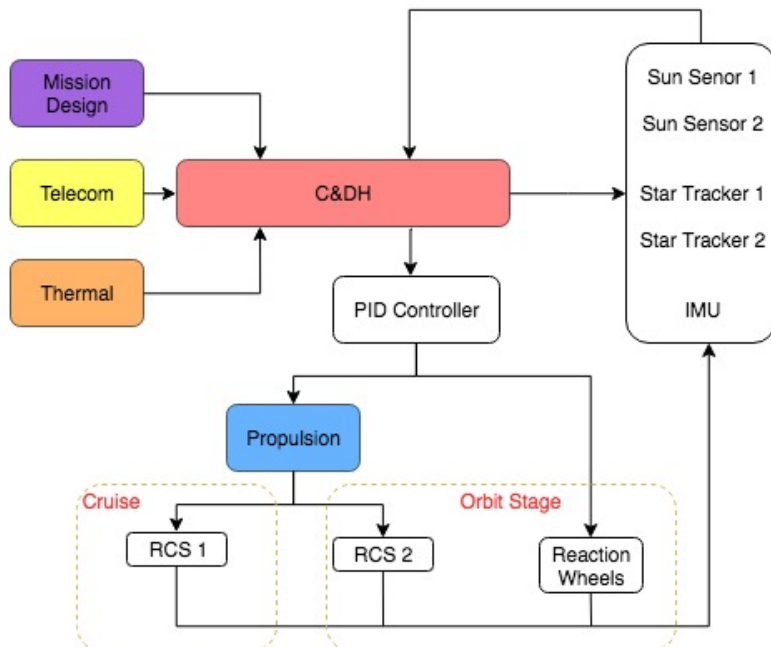


Figure 53: ADCS Block Diagram

At the time of PDR, the SPACEJAM team has elected to fly the mission in the operational configuration described above. The sensors were chosen to maintain redundant measurements with different failure or inoperative modes. Star trackers are incredibly accurate and have ever increasing heritage use, and sun sensors are highly effective and well understood means of navigation. Both are shown in duplicate as a function of the expendable cruise stage. The second set of sensors will not be used until after deployment of the rigid aeroshell as they would interfere with or become damaged by the loads and environments associated with the aerocapture maneuver. The currently selected sun sensor is the Adcole Two-Axis Fine Sun sensor. This instrument has a 64 degree FOV and can be accurate between 0.05 and 0.01 degrees. Current star tracker specs reference the Ball Aerospace High Accuracy Star Tracker (HAST) unit. With an 8x8 degree FOV, this star tracker can acquire and track rates between $\pm 8^\circ/\text{sec}$ and accelerations between $\pm 8^\circ/\text{sec}^2$.

Each Star Sensor Head (SSH) has >99 percent chance of finding at least one star, and each HAST has two SSHs. The HAST can track approximately 8 stars at 60 Hz or less, or 4 start near 100 Hz if higher data rates are needed. It was also selected because it can be customized for a particular mission and heritage missions have demonstrated 0.04 arcsec of pointing knowledge, which is more than sufficient for the SPACEJAM mission. Images of both units are shown below.



Figure 54: Adcole 2 Axis Fine Sun Sensor [13]

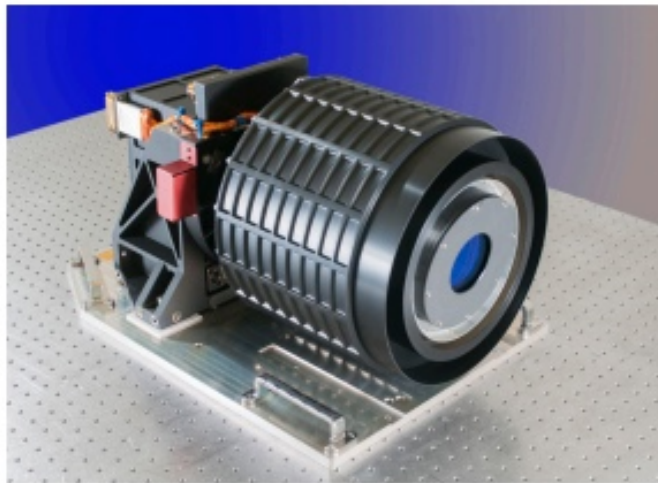


Figure 55: Ball HAST Star Tracker [14]

The SPACEJAM trade studies also determined that use of an IMU was necessary on the spacecraft for de-tumbling and contingency in an eclipse situation where the sun sensor would not be useful. The Northrop Grumman LN-200s has extensive heritage on programs including Shuttle, ISS, Spirit, Opportunity and an extensive list of others. It is built from three solid state fiber optic gyros

and three solid state Micro Electro-Mechanical Systems (MEMS), which makes it a particularly robust candidate for the Jovian radiation environment [15]. It uses a digital serial output to relay incremental velocity and acceleration, which should interface well with the SPACEJAM CD&H system. The LN-200s consumes relatively low power with a nominal draw around 12 W and weighs only 1.65 lb. The LN-200s is shown below.



Figure 56: Northrop Grumman LN-200s IMU [16]

Actuators were selected on criteria that most readily enabled efficient arrival at Jupiter as well as effective completion of the primary science mission. The block diagram displays a combination of reaction wheels and RCS. Both RCS systems will be setup in the RCS quad configuration (see propulsion subsection for a diagram). Assuming all lines of action pass through or near the overall spacecraft center of mass, the quad configuration enables effective translation through use of mutually oriented, diametrically opposed thrusters and pure rotation for attitude control by using oppositely oriented diametrically opposed thrusters (see propulsion section for more information). The cruise stage RCS will be used for all pre-aerocapture TCMs, detumbling and spin stabilization maneuvers, and will be assisted by the Orbiter stage reaction wheels on an as-needed basis. The cruise stage RCS will be jettisoned before initialization of the aerocapture maneuver.

During the cruise portion of the mission, the spacecraft will be spin stabilized about its cylindrical axis. This spin will be enabled by the symmetric cruise stage design, and will be maintained by the RCS thrusters. This constant, slow rotation will allow the spacecraft to maintain stability without active station-keeping from the reaction wheels.

5.8.4 Pointing Control

Reaction wheels will be employed by SPACEJAM to provide exceptional pointing accuracy and spacecraft slew authority during science collection mission phases. The SPACEJAM spacecraft is currently designed to use a modified version of the reaction wheel quad configuration in which the three primary wheels are mutually orthogonal to each other for extensive 1D control. With a fourth wheel oriented at an equal angle to all three primary spacecraft axes. SPACEJAM will orient the three primary wheels along the spacecraft primary axis to maintain mutual orthogonality, but the fourth wheel shall be gimbaled to allow further customization of coupled angular momentum vectors in the event that one reaction wheel becomes inoperative during flight. The common reaction wheel quad configuration is shown below along with one of the four New Space Systems 10 mNs reaction wheels to be used. A table of expected operation scenarios is also displayed below to demonstrate expected spacecraft operation modes and their respective primary actuators.

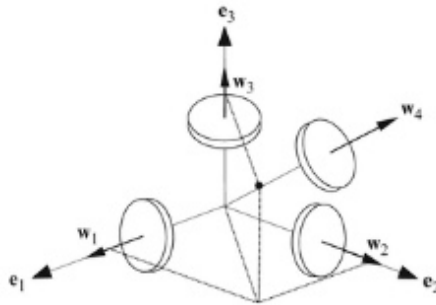


Figure 57: Reaction Wheel Quad Configuration

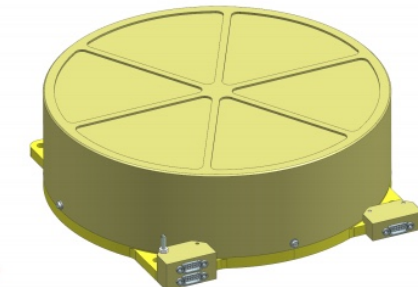


Figure 58: New Space Systems 10 mNs Reaction Wheel [17]

Operation Mode	Goal	Primary Actuator
Detumble	Force angular velocities to zero	RCS
Gravity assist & TCM prep	Orient spacecraft to desired pre-TCM orientation	RCS or RWS
TCM adjustment	Correct for disturbance torques during TCM	RCS
Cruise	Spin stabilize	RCS/RWS
Aerocapture	Maintain trajectory	Drag skirt
Downlink	Maintain telemetry connection	RWS
Safe	Force angular velocities to zero, reorient antenna toward Earth	RCS then RWS
Science	Maintain sufficient stability to accomplish science requirements	RWS

Figure 59: Expected ADCS Operational Modes and Primary Actuators

Using NSS 10mNs reaction wheel capabilities and inertia values about each axis of the spacecraft in 1D angular momentum analysis, it can be seen below that the SPACEJAM spacecraft as currently designed can slew on the order of $2^\circ/\text{sec}$ per axis with angular accelerations of approximately $0.04^\circ/\text{sec}^2$.

I_{xx}	307.68 kg m²
I_{yy}	265.61 kg m²
I_{zz}	302.95 kg m²

Figure 60: Spacecraft Inertia Values

ω_x	0.03445 rad/sec	1.974 deg/sec
ω_y	0.03991 rad/sec	2.287 deg/sec
ω_z	0.03499 rad/sec	2.005 deg/sec

$\dot{\omega}_x$	0.00068 rad/sec ²	0.039 deg/sec ²
$\dot{\omega}_y$	0.00079 rad/sec ²	0.045 deg/sec ²
$\dot{\omega}_z$	0.00069 rad/sec ²	0.040 deg/sec ²

Figure 61: Expected Maximum Slew Rates and Angular Accelerations

5.8.5 Pointing Error

Based on heritage values from Juno [18] and Cassini [19] [20], SPACEJAM was designed to hold a pointing accuracy of 6 mRad at 3 sigma for use in Mission Design dV budgets. To ensure the system was capable of achieving this metric, a monte carlo test is in work to capture system statistics. The high-fidelity version of this simulation will account for, among other things, predicted sensor accuracies, reaction wheel angular velocity precision, estimated mechanical assembly precision, sensor fusion, mission phase, desired time window (more for stability characterization, but it is associated with this simulation as well) and the optimized version of the SPACEJAM PID controller gains. Predicted sensor accuracies will be taken directly from the spec sheet of a particular component unless a more refined number is available from the manufacturer at time of purchase. This number will be fed into the downstream monte carlo simulation by using a random number generator in Matlab to arrive at a number within the expected accuracy range of the component. This will be done for each component at the start of each monte carlo run. The total attitude determination sensor influence will then be calculated using a weighted sum or an unscented Kalman filter. The statistical status of each sensor or actuator will then be combined with other system components and the system controller behavior to provide the final statistical description of the system at a given mission phase assuming a total number of simulation runs on the order of 5000.

Estimated assembly position error will be taken directly from NASA heritage and project documents, although it will also still be fed in to the monte carlo simulation in a similar fashion as the sensor and hardware accuracies before sensor fusion is performed. It is worth noting however the angular velocity of the reaction wheel must be treated slightly differently than other components of the system. This is because even though the angular velocity could be within its dictated range at any given time, because this inaccuracy will eventually result in a system attitude change once the resultant slew pushed the craft beyond the deadband limits, it must be re-simulated each time the deadband limits are reached. This is because the reaction wheel system is designed to hold a position, and the resultant slew associated with an inaccuracy in angular velocity will eventually trigger a response from the controller. Subsequently, the pointing error as it pertains to the reaction wheel subsystem is directly related to the amplitude of PID controller gains. These gains are expected to be optimized before the coming CDR, so the resultant pointing error should be well characterized at that time.

5.8.6 Detumbling

If a tumbling scenario is ever encountered by the SPACEJAM craft, the RCS thruster quads are expected to enable recovery to a zero rate state. A tumble of sufficient magnitude will trigger an automated detumble response using a Bang-Off-Bang controller design. The controller will pull accelerometer and gyroscope data from the LN-200s IMU to determine spacecraft rates and angular accelerations. As SPACEJAM will not require solar panels to stay operational during a safe mode, the primary driver behind the aggressiveness with which the spacecraft approaches a zero rate state will be dominated by overall spacecraft and payload safety. Therefore, moving forward to CDR would see another monte carlo simulation to optimize system settling time and yield a total expected fuel usage for a detumbling event.

5.8.7 Entry Guidance

The goal of aerocapture is to utilize a single pass through a planet's atmosphere in order to decrease the spacecraft's orbital energy about the central body to achieve a captured orbit. There are two main modes of guidance during aerocapture: lift modulation and drag modulation. Each case is further split into either discrete-event or continuously-variable control. While lift modulation provides ample control authority and increase final orbit accuracy, this method requires additional mass to offset the vehicle center of mass to allow it to fly at an angle of attack. Lift modulation also relies on complex guidance and control laws in order to steer the vehicle through the atmosphere.

Due to the uncertainty of the Jovian atmosphere and flexibility in final apogee accuracy, lift modulation was deemed unnecessarily complex for the mission requirements.

Alternatively, drag modulation is a desirable guidance method, as the vehicle can enter the atmosphere in a ballistic configuration at zero angle-of-attack, and the control inputs directly affect the vehicle's ballistic coefficient. Within drag modulation, continuous and discrete methods were considered. However, due to the mechanical complexity of a continuous drag modulation schema, the discrete modulation method was ultimately chosen for this mission.

Table 35: Scoring: The higher the number, the more positive and appealing the method is. I.e. a 3 for mechanical complexity means that this method is simple and reliable.

Entry Guidance Methods & Scores					
	Weights	Continuous Lifting	Discrete Lifting	Continuous Drag	Discrete Drag
Accuracy	1	3	2	3	2
Cg Offset? (y/n)	2	1	1	2	2
Fuel Cost	3	2	1	3	3
Mechanical Complexity	4	3	1	1	3
Total:		23	11	20	27

5.8.8 Entry Guidance Block Diagram

The proposed algorithm for entry guidance is based on a Newton Raphson 4th order predictor-corrector. In order to ensure guidance accuracy and linear dynamic propagation, the dynamics loop will be called at a frequency that is an order of magnitude higher than the guidance loop. The algorithm calculates the jettison time at each guidance call by predicting the final apoapsis and adjusted it using the Newton Raphson method and an estimate of the localized slope of the optimization function.

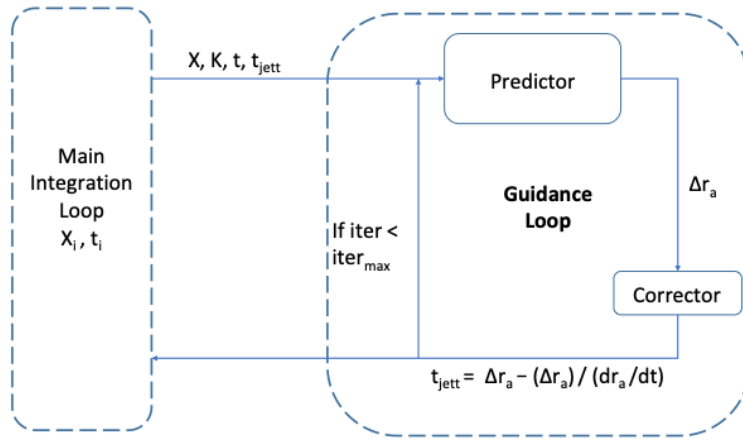


Figure 62: The NPC block diagram for SPACEJAM entry guidance and control.

It is noteworthy that this method of control does not allow for any corrections post-jettison maneuver. However, through simulation and tests, it was shown that all successful aerocapture passes A Monte Carlo simulation was run with noise dispersions injected into the Jupiter atmospheric model in order to quantify the final accuracy in apoapsis. This study and its results are discussed further in the mission design simulations in section 5.1.

5.9 Propulsion System

5.9.1 Propulsion Subsystem Level IV Requirements

Table 36: Propulsion Subsystem Requirements

Req. No.	Requirement	Rationale	Verification
PROP-01	The spacecraft propulsion system shall comprise a pressure-regulated monopropellant	Allows for simplicity and constant mass flow rate.	Fulfilled by design
PROP-02	The spacecraft shall contain a 3-axis RCS capable of providing 20 N of thrust	Control over pitch, yaw, roll, and translation is required.	Fulfilled by design
PROP-03	The structure shall provide 141 m/s ΔV with 10% ΔV margin (TBR) for the Cruise Stage.	Driven by mission design.	Verified by design and calculation
PROP-04	The structure shall provide 378 m/s ΔV with 20% ΔV margin (TBR) for the Orbital Stage.	Driven by mission design.	Verified by design and calculation
PROP-05	The propulsion system shall contain a propulsion (pressurant) tank of sufficient size to store required fuel (pressurant) and a plumbing system that feeds fuel to the RCS system.	Necessary for the operation of the propulsion subsystem.	Fulfilled by design

5.9.2 ΔV Requirements

The ΔV requirements for the propulsion subsystem are driven by mission design. There are several maneuvers under which ΔV must be expended, which are tabled in chronological order in Table 37:

Table 37: ΔV Sequencing and Budget

Maneuver	Nominal ΔV (m/s)	$3\sigma \Delta V$ (m/s)	Stage
Launch Error		5	Cruise
TCMs	92	136	Cruise
Margin		10%	Cruise
Total Cruise		155.1	Cruise
Perijove Raise	98	94	Orbit
Station Keeping	1	50	Orbit
Contingency	100	100	Orbit
Disposal	113	114	Orbit
Margin		20%	Orbit
Total Orbit		429.6	Orbit
Total		584.7	

The TCMs will occur while the spacecraft is en route to Jupiter. These maneuvers will occur while the spacecraft is in the cruise configuration. The perijove raise maneuver will occur following aerocapture, after the aeroshell have been jettisoned and the spacecraft is in its final orbital configuration. Station keeping and spacecraft disposal apply only to the orbital stage. A large amount of additional margin has been built into the orbital stage under the 'contingency' category.

5.9.3 Propellant Selection

A variety of propellants were considered for the main propulsion system, with the most relevant design trades being propellant storability, system simplicity, and thrust capability to perform the periapsis raising maneuver. Electric propulsion systems were quickly eliminated from the selection process, as an ion or hall-effect thruster would not be able to provide the acceleration required to raise the spacecraft's periapsis out of Jupiter's atmosphere inside of the relatively short planned orbital period. In addition, the electrical power requirements of such a propulsion system would overwhelm the power generating capabilities of the spacecraft. Alternatively, a very high thrust engine such as an RL-10 LH₂/LOX engine could not store its propellants for long enough to reach Jupiter, as both liquid oxygen and liquid hydrogen are cryogenic, and would evaporate over the course of the cruise. The engine itself also posed a large mass and volume cost, and might not even fit under the planned aeroshell.

After the more extreme choices were eliminated, hypergolic propellants were considered, most of which are hydrazine blends. Hydrogen peroxide monopropellant thrusters were considered, but the propellant does not store as well as hydrazine and may degrade over the mission duration. These would be utilized either as a monopropellant or bipropellant with dinitrogen tetroxide as an oxidizer. Hydrazine systems have many decades of heritage on interplanetary missions, and are almost exclusively the propulsion system of choice for this regime. Due to the aerocapture maneuver, the spacecraft's propulsion system will be utilized far less than a standard interplanetary mission. The largest single maneuver post-aerocapture will be the periapsis raise. As a result, the final ΔV requirement is approximately half of most comparable missions.

Initial sizing estimates were based on the propulsion systems of previous spacecraft, such as Juno, Galileo, MRO, and MAVEN. Typical bipropellant propulsion systems reached Specific Impulse (I_{sp}) values of 280 seconds, while monopropellant systems were closer to 180 seconds.

However, many of these spacecraft were required to perform extensive orbital maneuvers and insertion burns, and consequently, they typically devoted about half of their launch mass to propellant. In comparison, this spacecraft needs far less propellant, so while I_{sp} was considered, neither a

monopropellant or bipropellant system's propellant load would substantially affect the mass of the spacecraft. Therefore, the final design selected a monopropellant for reliability reasons. While the periapsis raise maneuver is comparatively small, it is a critical event where a failure of the main engine would end the mission quickly. The simplest system gives the best chance of performing this maneuver correctly.

5.9.4 Propellant and Tank Sizing

The propellant and tank sizing used an iterative approach to converge upon a final mass figure and tank selection. An estimate for the dry mass of the orbital and cruise stages as well as the aeroshell assembly were used to calculate a preliminary propulsion mass value, from which a propulsion volume was found. A tank was selected based on this estimated volume. As mass values became more accurate over the course of the modeling stage of design, the propulsion volume requirement was monitored and the tank selection was updated as necessary.

Based on the geometry of the orbital stage, it was decided that six spherical tanks spaced evenly about the COM would house the propellant volume (Figure 63). These tanks will be drawn from at equal rates during ΔV maneuvers in order to keep the position of the COM coincident with the main axis over time. A manifold will connect each propellant tank to a single pressurant tank, positioned at the center of the circle formed by the propellant tanks. Six tanks provides sufficient redundancy in case of a single failure, although such a failure would severely limit mission duration.

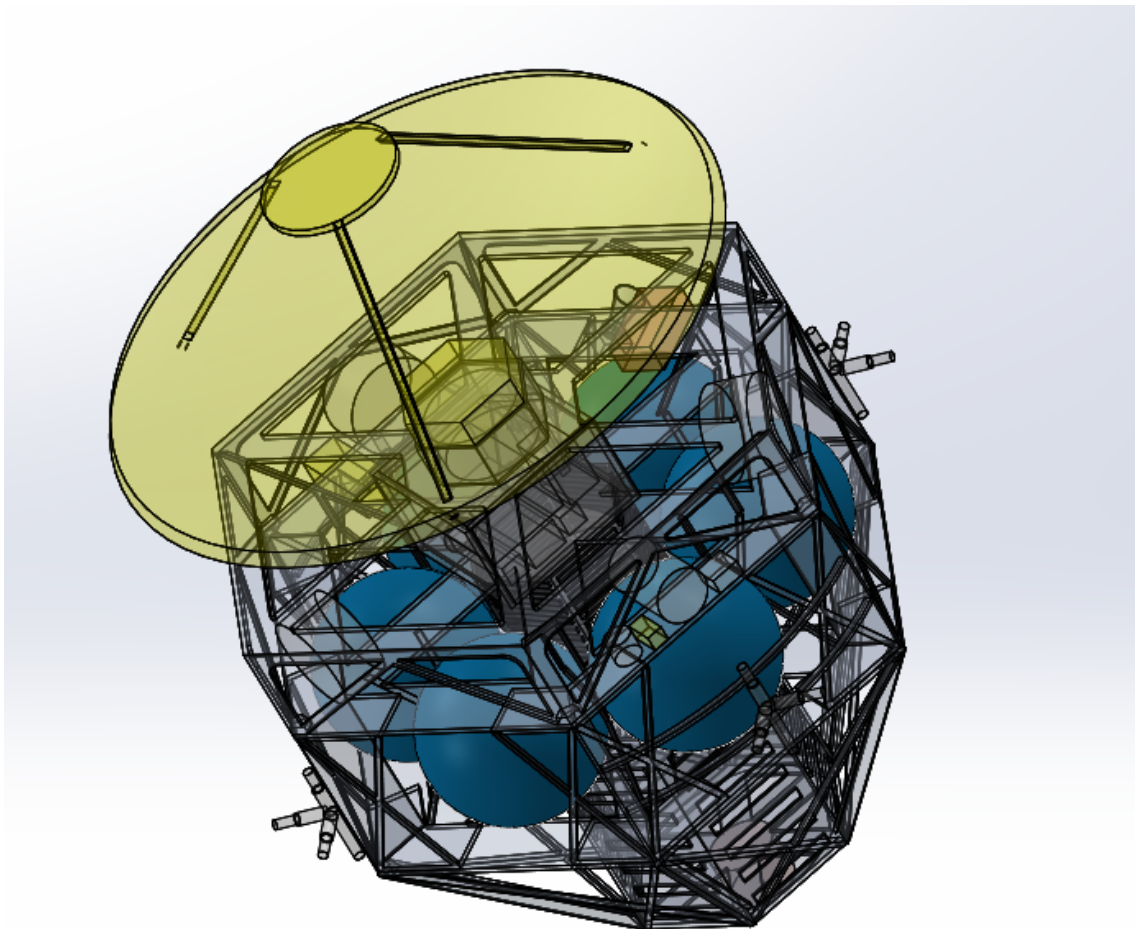


Figure 63: Propulsion Tanks within SPACEJAM structure

The propellant tank was sized using a bottom-up, iterative approach. Knowing the dry masses of the various spacecraft stages and configurations as well as the ΔV requirements and fuel type, the required fuel volume was settled, after several iterations, at $21,984 \text{ in}^3$, or $3,664 \text{ in}^3$ per tank. Northrop Grumman provides a wide variety of titanium propellant tanks with extensive flight heritage. Their 80259-1 tank is capable of holding $4,167 \text{ in}^3$, sufficient for the requirements and margin of this application, and was therefore selected. This tank operates at a pressure of 375 psig, driving the pressurant tank selection discussed below.

After the propellant tank was selected, a top-down approach was used to calculate the actual ΔV margin. Each tank will be filled to capacity with propellant at launch: six 80259-1 tanks are capable of storing 414.2 kg of hydrazine. Estimating 2 kg of hydrazine filling the plumbing system gives a total propellant mass of 416.2 kg. The amount of propellant consumed by each maneuver and usable propellant left are listed in Table 38 below:

Table 38: Propulsion Consumption and Margin

Item	Value	Unit
Thruster p	362.7	psia
Est. I_{sp}	227.4	s
Total m_{prop}	416.2	kg
Unusable m_{prop}	10	kg
Launch Error m_{prop}	5.41	kg
Launch Error ΔV	5	m/s
TCM m_{prop}	142.6	kg
TCM ΔV	136	m/s
Cruise Margin m_{prop}	14.3	kg
Cruise Margin ΔV	14.1	m/s
Periapsis Raise m_{prop}	48.7	kg
Periapsis Raise ΔV	94	m/s
Station Keeping m_{prop}	25.1	kg
Station Keeping ΔV	50	m/s
Contingency m_{prop}	48.5	kg
Contingency ΔV	100	m/s
Disposal m_{prop}	52.7	kg
Disposal ΔV	114	m/s
Orbital Margin m_{prop}	61.7	kg
Orbital Margin ΔV	141.3	m/s
Total ΔV	654.4	m/s

There is a trade between propellant margin during the Cruise stage and the Orbital stage. Since the Cruise stage is about twice as massive as the Orbital stage, 1 m/s of margin given to the Cruise stage detracts about 2 m/s of margin from the Orbital stage. An optimal figure of 10% margin was given to the Cruise stage to meet Req. PROP-3, resulting in a 14.1 m/s ΔV margin for the Cruise stage and a 39.5%, 141.3 m/s ΔV margin for the Orbital stage. This trade is displayed in Figure 64 below.

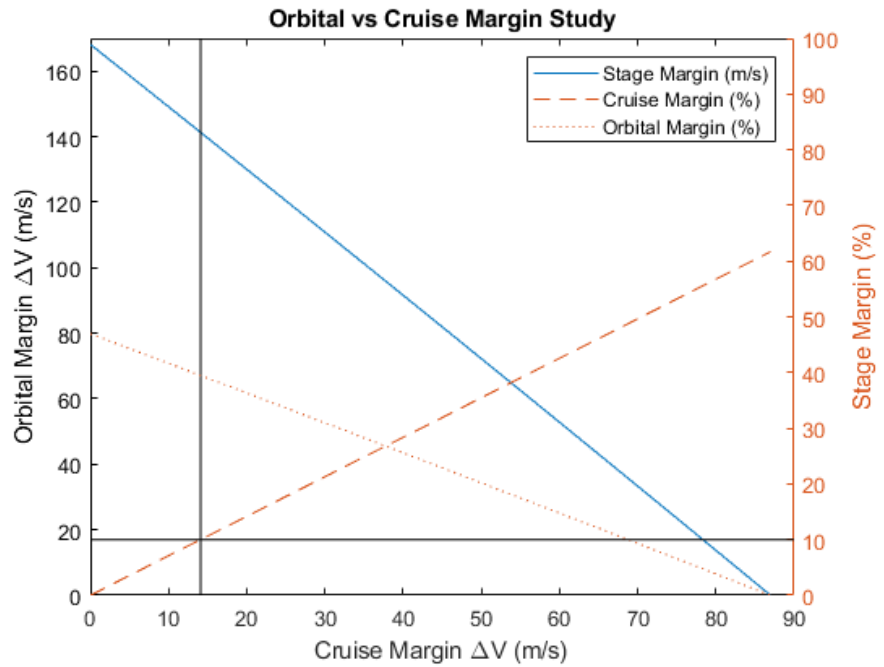


Figure 64: Propellant Stage Margin Study

The high amount of ΔV margin left over for the Orbital stage will make an extended mission possible. The cruise stage should aim to use as little margin as it can, as doing so will lengthen the duration of an extended mission due to the high amount of propellant margin and ΔV left over.

5.9.5 Pressurant and Tank Sizing

The propellant tanks will be operated at a constant pressure by a pressure-regulated system. A pressure-regulated propulsion system offers several advantages over a blowdown system. Constant I_{sp} values depend on constant fuel pressures, which a blowdown system is unable to provide. Constant pressure also results in a constant and controlled mass flow rate of propellant to the thrusters, which will simplify maneuvers. The location of the pressurant tank, displayed in Figure 65, is centrally oriented between the propulsion tanks on the main axis.

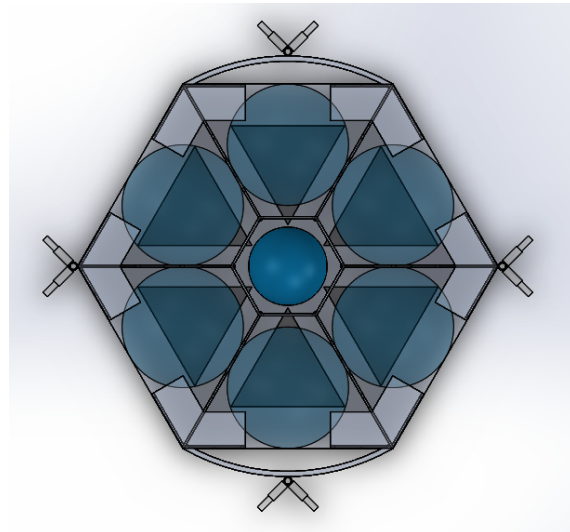


Figure 65: Pressurant Tank Location Within Propulsion Deck

The pressurant tank was selected iteratively based on the operating pressure of the propulsion tanks, as alluded to above. The total volume of the propulsion tanks, as well as the pressure of the system, were known. A pressurant tank was selected, and from its data sheet the initial volume and final volume of propellant was calculated based on tank total volumes and propellant volumes. Assuming a constant pressurant temperature, as well as constant mass, the initial pressure in the pressurant tank was calculated. This process was iterated until the initial pressure was within the operating limits of the pressurant tank, according to its data sheet. The pressurant tank selected is a Northrop Grumman 80548-1 unit, providing $3,173 \text{ in}^3$ of volume and capable of withstanding 4,500 psig. The calculated initial pressure within the pressurant tank was 4,356 psia, and the mass of the helium pressurant within the system is 2.721 kg.

5.9.6 Thruster Selection

The SPACEJAM team has decided to design around the use of multiple small thruster arrays instead of a main engine/RCS thruster combination. As discussed previously, this decision was influenced by a multitude of factors, but the most notable involve the lack of a need for extreme instantaneous ΔV . Because SPACEJAM is able to rely heavily on gravity assist maneuvers, only a minor amount of thrust is needed at any given time for the PRM, preparation of a TCM, or even a detumble scenario.

The Ariane group has a COTS family of monoprop hydrazine thrusters that appear to fit well with the SPACEJAM mission at the time of PDR. They have extensive heritage on many generations of satellite flights and also a commendable record of reliability on high-visibility missions, as would be the case of the eventual SPACEJAM flight. A combination of the 1N and 20N thrusters will be arranged in the RCS quad configuration in such a way that optimizes the trade between thruster burn time, post TCM precision and overall system mass. Effectively, a larger thruster capable of delivering a greater instantaneous ΔV to the spacecraft would contribute to an efficient TCM by minimizing the width of the time integration step, but a smaller thruster could incrementally improve the resultant post-TCM error by delivering the TCM in smaller quantities. It is also worth noting that the 20N thrusters have a mass on the order of 2.5 times that of the 1N thruster, so the use of 20N thrusters will be limited to locations which will directly impact the TCM time step trade in a favorable way. At this time, this particular trade is TBR but will be resolved by PDR. The Ariane 1N and 20N thrusters are shown below.



Figure 66: Ariane 1N Hydrazine Thruster [21] (L) and 20N Hydrazine Thruster [22] (R)

Characteristics	
Thrust Nominal	1 N
Thrust Range	0.320 ... 1.1 N
Specific Impulse, Nominal	220 s
Pulse, Range	200 ... 223 s
Mass Flow, Nominal	0.44 g/s
Mass Flow, Range	0.142 ... 0.447 g/s
Inlet Pressure Range	5.5 ... 22 bar
Minimum Impulse Bit	0.01 ... 0.043 Ns
Nozzle Expansion Ratio	80
Mass, Thruster with valves	290 g
Propellant	Hydrazine (N_2H_4), High-Purity Grade
Qualification	
Total Impulse	135,000 Ns
Cycle Life	59,000 cycles
Propellant Throughput	67 kg
Single Burn Life	12 h
Accumulated Burn Life	50 h
No of Cold Starts <10°C	10

Figure 67: Ariane 1N Hydrazine Thruster Specs [21]

Characteristics	
Thrust Range	7.9 ... 24.6 N
Supply Pressure Range	5.5 bar - 24 bar
Nominal Mass Flow Range	3.2 g/s ... 10.4 g/s
Nominal Specific Impulse Range	222 s ... 230 s
Minimum Impulse Bit Range	0.238 ... 0.685 Ns
Nozzle area ratio	60
Mass	= 650 g (with 1.5 m flying leads)
Propellant	Monopropellant grade Hydrazine (N_2H_4)
Environmental Loads	16.2 grms
Qualification	
Total Impulse	> 517,000 Ns
Total number of pulses	> 93100
Total hydrazine throughput	> 290 kg
Total operating time	10.5 h
Longest steady state burn	1.5 h
Number of cold starts < 20°C	36
Number of cold starts at 0°C	12

Figure 68: Ariane 20N Hydrazine Thruster Specs [22]

5.9.7 Propulsion Plumbing

The propulsion system will include dual lines from each tank to the thruster quads to provide redundant protection. A series of shutoff valves upstream from each thruster will control the operation of each thruster. Pressure gauges located inside the tanks and along the fuel lines will update the ship's computer about the status of the propulsion system, allowing it to calculate

how much fuel needs to be burned by which thrusters for ΔV maneuvers. A filter will be placed between the pressurant and the propulsion tanks. Heavy thermal insulation will be applied to the fuel lines to keep the propellant from freezing.

Fuel lines will be extended from a shutoff valve within the Orbital stage through the aeroshell to the Cruise stage in order to provide propellant for its thrusters. The fuel lines for the Orbital thrusters will remain closed until the Cruise stage and aeroshell are jettisoned. The fuel lines that provide propellant to the Cruise stage thrusters will be closed and jettisoned as well. All valves, pressure gauges, and thrusters will be connected to the EPS and C&DH systems. The C&DH system will work in accordance with ADCS and MD in order to operate the shutoff valves and thrusters as needed for appropriate RCS maneuvers.

The plumbing system is visualized in the propulsion subsystem block diagram, displayed in Figure 69.

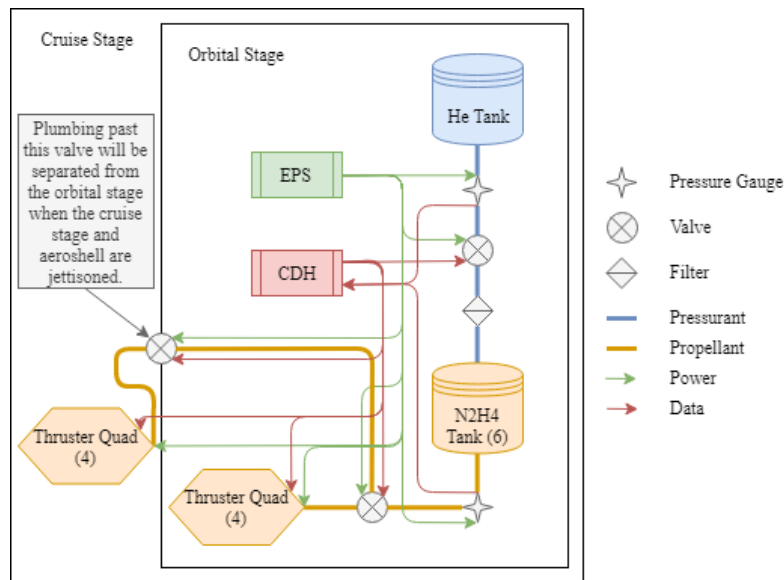


Figure 69: Propulsion Subsystem Block Diagram

5.9.8 Risk

The largest risks that the propulsion subsystem faces are the relatively high freezing temperature of hydrazine, the loss of functionality of the fuel tank or plumbing system, and an incorrect Periapsis Raise Maneuver. The freezing potential of hydrazine will be mitigated to very unlikely by insulation around the fuel lines and heaters on the propulsion deck. The loss of tank functionality is mitigated by redundant design, where six propulsion tanks are used and parallel lines and valves are in place along the plumbing system. A maneuver error by a faulty thruster is considered very unlikely, if they are installed correctly and operate properly given commands from other subsystems (Figure 70).

Consequence (Expected Impact to the Mission)	Severe (5)	PRM error	Loss of tank functionality			
	Significant (4)	Thruster quads damaged during separation events	Multiple propulsion tanks redundant plumbing lines	Hydrazine fuel freezes		
	Moderate (3)		Partial loss of tank functionality			
	Minor (2)					
	Negligible (1)					
		Very Unlikely (1)	Unlikely (2)	Possible (3)	Likely (4)	Very Likely (5)
Likelihood (Qualitative)						
Acceptable		Tolerable	Intolerable			

Figure 70: Propulsion Subsystem Risk Matrix

5.10 Telecommunications

The SPACE-JAM telecommunications system is designed to satisfy requirements TELECOM-01 through 07 as described in Table 39.

Table 39: Level IV Telecommunications Requirements

Req. No.	Requirement	Rationale	Verification
TELECOM-01	The carrier link margin shall be greater than 3 dB for all phases of flight.	3 dB is common for carrier link budgets	HGA and MGA Link Performance
TELECOM-02	Recorded aerocapture acceleration data shall be downlinked within 3 hours after aerocapture.	Assumes aerocapture data will be downlinked before perijove raise maneuver.	HGA allows for 1 MB of downlink in less than 2 minutes.
TELECOM-03	Adjustments to the perijove raise maneuver shall be uplinked to spacecraft within 1 day (TBR) of the perijove raise maneuver.	Gives sufficient margin for the spacecraft to prepare for perijove raise maneuver	HGA allows for 1 MB of uplink in less than 2 minutes.
TELECOM-04	The spacecraft shall provide telemetry ranging data and health status to the Deep Space Network ground stations during the cruise and orbital phases, besides phases of flight constrained by science operations.	Telemetry ranging data and health status are necessary and standard for all interplanetary missions.	MGA will be Earth-pointing during cruise, besides periods constrained by TCMs. HGA antenna will be Earth-pointing in orbit during periods other than science operations. Both have carrier margins above 3 dB to provide telemetry and health status.
TELECOM-05	The spacecraft shall provide sufficient time for downlink for at least 1 day of science data (68 MB).	68 MB is the minimum memory needed for 1 Vis and 1 UV Image every 0.8 hours for 1 day.	HGA data rate allows for downlink of 68 MB of data in less than 2 hours.
TELECOM-06	The spacecraft shall provide sufficient time for uplink to receive at least 256 MB of commands.	Assume commands will never take up more than half of available memory.	Commands can be uplinked during science downlink using the X-band diplexer. Assuming 6 days of continuous science data (battery limiting case), this data can be uplinked in less than 6 hours.
TELECOM-07	The spacecraft will establish link with NASA's DSN 5 minutes (TBR) following spacecraft separation at launch.	Initial link with NASA's DSN must be established as soon as possible.	Heritage LGA's will establish link after spacecraft separation at launch.

5.10.1 Component Overview

Components are chosen and sized to supply sufficient link to the various phases of flight. Much of the telecommunications hardware is chosen from heritage interplanetary missions, such as Juno [18], for simplicity and cost-effectiveness. As is typical with interplanetary missions, an X-band carrier will be utilized for communications in all phases of flight. The Small Deep Space Transponder (SDST) will provide transmission and reception in the X-band at 8.4 GHz. The signal is amplified using a Traveling Wave Tube Amplifier (TWTA) in order to supply sufficient transmit power. Each antenna utilizes a mechanical Waveguide Transfer Switch (WTS). An X-band Diplexer (XD) is utilized to allow the spacecraft to transmit signals at one frequency and receive at another (a second is added for redundancy). The diplexer transmits at 8.29–8.545 GHz and receives at 7.1–7.23 GHz. A redundant SDST, TWTA, and XD is flown in order to mitigate the risk of failure of each necessary component.

Table 40: Telecommunications Components [18]

Component	Number of Units	Phases of Flight	Flight Heritage
High Gain Antenna (HGA)	1	Orbital	None
Medium Gain Antenna (MGA)	1	Cruise	None
Low Gain Antenna (LGA)	2	Cruise	Juno, MRO
Toroidal Low Gain Antenna (TLGA)	1	Cruise	Juno
Small Deep Space Transponder (SDST)	2	All	Juno, Cassini
Traveling Wave Tube Amplifier (TWTA)	2	All	Juno, MRO
Waveguide Transfer Switch (WTS)	6	All	Juno, MRO
X-Band Diplexer (XD)	2	All	Juno, MSL

Figure 71 shows the telecommunications system and each component in a block diagram.

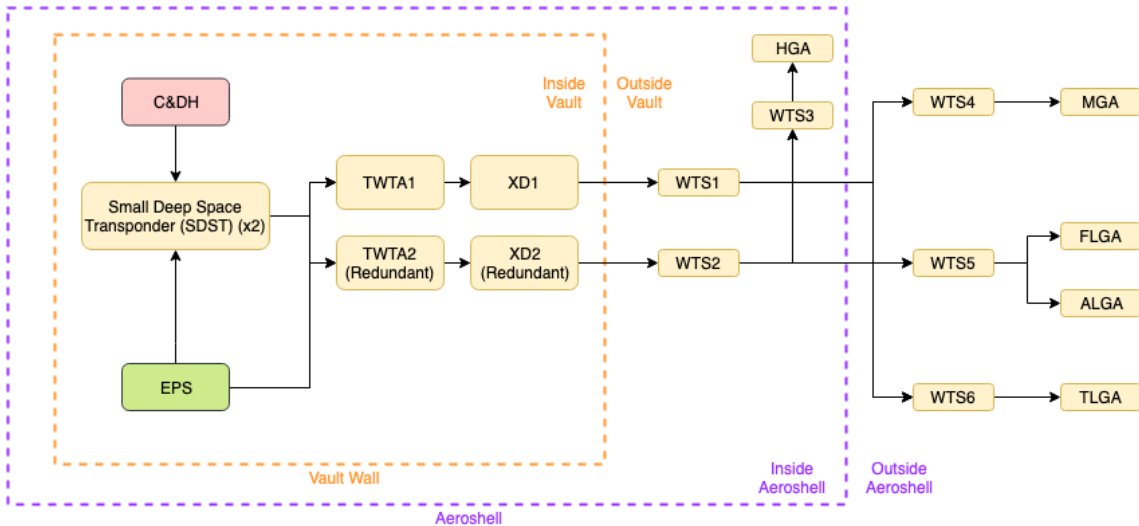


Figure 71: Telecommunications Block Diagram

5.10.2 Cruise Phase Operations

The cruise phase will utilize 4 antennas: the MGA, two LGAs, and the TLGA. After separation at launch, link to the DSN station in view will be established with the appropriate LGA (forward or aft). Once the MGA is pointed toward Earth, the MGA will support the majority of telemetry operations during cruise. The TLGA was added to the cruise stage to support TCMs where the spacecraft may not be Earth-pointing. The directivity of the TLGA is -90 and 90 degrees off-boresight, ensuring telemetry coverage during the TCMs.

5.10.3 Orbital Phase Operations

The orbital phase will use the HGA for all communications during the 3-year science mission at Jupiter. The antenna is sized to provide a data rate of approximately 12 kbps to support large amounts of science data (see HGA Link Performance).

After aerocapture, the spacecraft will immediately point toward Earth in order to downlink the recorded aerocapture accelerometer data while providing ranging data for orbit determination. If necessary, changes to the pre-planned perijove raise maneuver can be uplinked during the coast to apoJove.

Due to power restrictions during downlink at end of life (EOL), the spacecraft cannot downlink science data at its maximum data rate indefinitely. A possible concept of operations for science downlink was identified assuming six continuous days of science operations, in which 2 photos (one Visible, one UV) are taken every 0.8 hours. The total amount of data recorded during this phase would be approximately 408 MB, leading to a total downlink period of less than 9.3 hours at the maximum data rate. In the proposed week-long operations cycle, science data is recorded for 6 days using pre-planned maneuvers, while the last day would be reserved for downlink, orbit determination, and uplink of the next week's science operations.

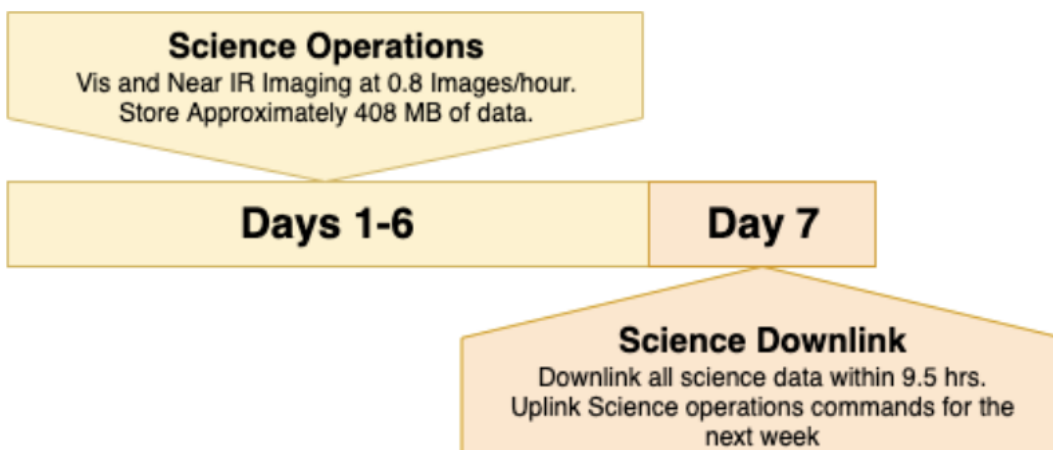


Table 41: Potential Science Downlink Parameters

Parameter	Unit	Value
Days of Operations	images	6
Total Number of Images	images	204
Total Image Data	MB	408
Downlink Time	hrs	9.26
Battery Capacity	Whr	400
Downlink Energy Usage (EOL)	W	19.51
Battery Margin at End of Downlink	Whr	219.26
Battery SOC at End of Downlink	%	54.81%

Note that the proposed science downlink timeline is one of many possible operational schemes that can be used to fulfill the imaging requirements at EOL based on battery limitations. For example, if it's determined that orbital perturbations over 6 days will cause the orbital predictions to be insufficient, this time can easily be shortened. Longer times are also possible, but will be limited by battery SOC requirements which can affect a potential mission extension.

5.10.4 HGA Link Performance

This section presents the carrier link margin and data rate associated with the HGA. Further detail is provided in section 9.2.

HGA Link Parameters

Transmit Frequency (GHz)	8.4
Antenna Diameter (m)	2
Antenna Efficiency (%)	0.70
Range (AU)	6.4588
Range (m)	9.6622E+11
DSN Antenna	34-m

HGA Carrier Downlink Budget

	Parameter	Unit	Value
1	Transmit Power	dBm	43.98
2	Antenna Gain	dB	43.36
3	Line Losses	dB	-0.50
4	EIRP (1+2+3)	dBm	86.84
5	Free Space Path Loss	dB	-290.63
6	Pointing Loss	dB	-0.10
7	Waveguide Loss	dB	-0.25
8	DSN Antenna Gain	dB	68.41
9	DSN Station Line Loss	dB	-0.50
10	SDST Noise	dB	-2.8
11	DSN Receiver Sensitivity	dBm	-160.00
12	Carrier Suppression	dB	-10.00
13	Total Received Power (4+5+6+7+8+9)	dBm	-136.23
14	Carrier Link Margin (13+10+12-11)	dB	10.97

HGA Downlink Data Rate

	Parameter	Unit	Value
15	Ground System Temperature	K	53.00
16	System Noise	dB	-17.24
17	Required Eb/N0	dB	3.00
18	Data Rate (Using 13,16,17)	bps	16,314
19	Data Rate (With 25% Margin)	bps	12,235

5.10.5 MGA Link Performance

MGA Link Parameters

Transmit Frequency (GHz)	8.4
Antenna Diameter (m)	0.8
Antenna Efficiency (%)	0.70
Range (AU)	6.4588
Range (m)	9.6622E+11
DSN Antenna	34-m

MGA Carrier Downlink Budget

	Parameter	Unit	Value
1	Transmit Power	dBm	43.98
2	Antenna Gain	dB	35.40
3	Line Losses	dB	-0.50
4	EIRP (1+2+3)	dBm	78.88
5	Free Space Path Loss	dB	-290.63
6	Pointing Loss	dB	-0.10
7	Waveguide Loss	dB	-0.25
8	DSN Antenna Gain	dB	68.41
9	DSN Station Line Loss	dB	-0.50
10	SDST Noise	dB	-2.8
11	DSN Receiver Sensitivity	dBm	-160.00
12	Carrier Suppression	dB	-10.00
13	Total Received Power (4+5+6+7+8+9)	dBm	-144.19
14	Carrier Link Margin (13+10+12-11)	dB	3.01

MGA Downlink Data Rate

	Parameter	Unit	Value
15	Ground System Temperature	K	53.00
16	System Noise	dB	-17.24
17	Required Eb/N0	dB	3.00
18	Data Rate (Using 13,16,17)	bps	2,610
19	Data Rate (With 25% Margin)	bps	1,958

5.10.6 Telecommunications Risk

Figure 72 presents a visualization of the risks identified in the telecommunications subsystem.

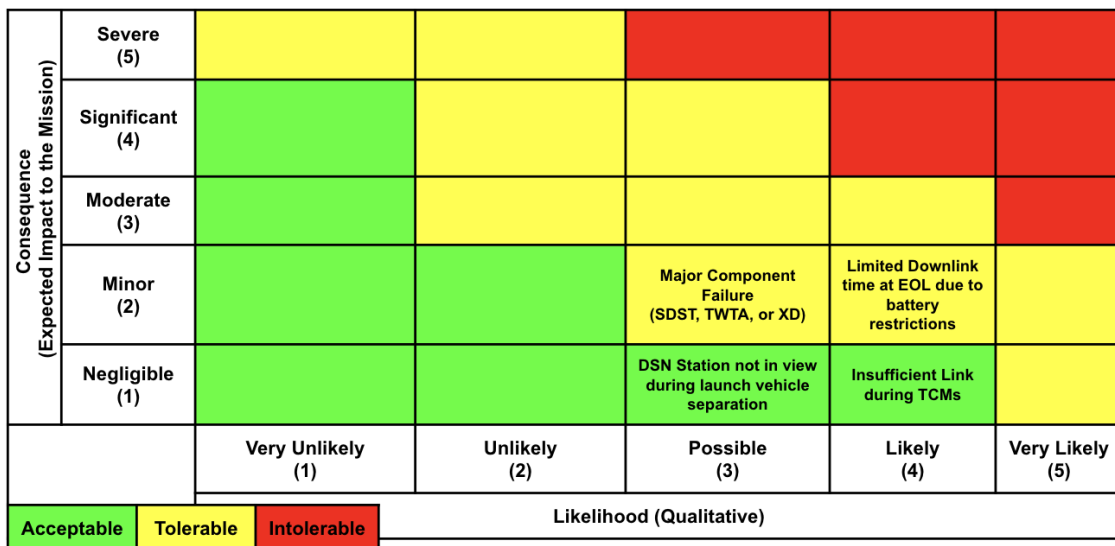


Figure 72: Telecommunications Risk Overview

The "Major Component Failure" risk is possible over the 10 year lifetime, but the risk is mitigated by including a redundant SDST, TWTA and XD.

Downlink during EOL could potentially become an issue if continuous link is needed for an extended period of time (> 10 hours) due to power constraints. This risk could be mitigated if a TWTA with a lower required power is replaced with the current TWTA. This would of course need to be traded with a larger antenna or lower data rates in order to account for the lower transmit power.

5.11 Operations and Ground Support

Ground Support

This mission expects to have at minimum a team of three ground operators on rotation while the spacecraft is in flight. During launch and critical maneuvers (such as flybys, TCMs, and JOI) the full team, including flight system engineers, mission design, operations, and mission manager, is expected to be present.

DSN Time

As is discussed in section 5.10, the science orbit will have a period of roughly 7 days. Six of these days will be used for orbit planning and analysis of the previous week's data, while the seventh day will be used for uplink and downlink with the DSN.

System Autonomy

Due to the nature of the time lag between Earth and Jupiter, it is expected that critical events will have full autonomy. For example, following the aerocapture maneuver, it is expected that the spacecraft will be able to raise periapsis regardless of whether or not link is established during that first apoapsis pass. However, ground link will be necessary in order to determine the spacecraft's final orbit. Link will also ensure that the spacecraft is able to raise periapsis by the correct amount to achieve the desired science orbit.

Mission Extension

Throughout design, mission extension was kept in mind in order to ensure that if required, the spacecraft would be able to continue collecting science data following the 3 year mark.

6 System-level Risks and Mitigation Plan

This section provides a risk assessment of each of the major, system-level risks identified. Table 73 presents a visualization of each risk discussed in this section.

	Severe (5)		Aerocapture Failure			
Consequence (Expected Impact to the Mission)	Significant (4)	Launch Failure				
	Moderate (3)	Failure to Raise Perijove Post-aerocapture	Aerocapture Apojove Target Failure		RTG Cost	
	Minor (2)					
	Negligible (1)					
		Very Unlikely (1)	Unlikely (2)	Possible (3)	Likely (4)	Very Likely (5)
Likelihood (Qualitative)						
Acceptable		Tolerable	Intolerable			

Figure 73: System Level Risks

6.1 Red Risk Items

Red items are defined by being unresolved, likely, imminent and/or severe in effect. These are risks which can compromise mission success, cost and schedule, with little to no mitigation plan currently in place. All red risk items for the SPACEJAM mission have been retired or mitigated to a lower risk classification.

6.2 Yellow Risk Items

Yellow items represent risks that can have potentially severe effects on mission success and/or risks which are growing in likelihood.

6.2.1 RTG Cost

As is discussed later in section 7, the cost of the RTG runs a risk of causing the project to go over-budget. However, as is discussed during the trade studies in section 5.6, the risk of total mission failure due to the use of solar panels was determined to be great enough that the design team was willing to accept the risk of going over budget.

6.2.2 Aerocapture Failure

The viability of aerocapture at Jupiter is currently identified as the highest risk to mission success as there are many possible points of failure during the event. The event itself, while short in duration, will result in a mission failure if not executed successfully. Aerocapture in general has yet to be demonstrated as a viable option for orbital insertion for interplanetary missions, so there is currently no flight heritage in determining potential risks.

Perhaps the greatest risk to the success of the event is not having a high-fidelity model of Jupiter's atmosphere. Much of the research on aerocapture has focused on missions to Mars or Venus, where higher fidelity models exist. While flight software will adjust the aeroskirt jettison time based on accelerometer readings, there is no mitigation if the spacecraft encounters lower or higher density atmosphere outside of the expected range. In addition, wind gusts on Jupiter are high velocity and occur frequently; further modeling is needed to understand the effects of wind gusts on the aerocapture event. These factors could lead to a premature ablation of the heat shield, causing overheating, or extremely high drag which would plummet the spacecraft into Jupiter, resulting in a complete mission failure.

6.2.3 Aerocapture Apojove Target Failure

This risk represents the event in which the apojove of the post-aerocapture transfer orbit is outside of the expected 3-sigma value. The ADCS algorithms used for apoapse targeting using an aeroskirt has yet to be demonstrated for interplanetary missions, so it is possible that the system is less robust than once thought. An apojove which is too low may be beyond the the delta-V capabilities of the spacecraft, and an apojove too high may not be able to meet resolution requirements, in addition to cases in which the spacecraft exists aerocapture in an escape trajectory. Even in the event in which a stable Jupiter orbit can not be recovered due to delta-V constraints, the mission will be considered a partial success as it is assumed that the aerocapture accelerometer data can still be downlinked.

6.3 Green or Grey Risk Items

Green or grey items represent risks of small likelihood and/or effect on the mission.

6.3.1 Failure to Raise Perijove

This risk represents the event in which the spacecraft fails to raise perijove and enter a stable Jupiter orbit. The outcome of this event is similar to that of the Apojove Target Failure risk, but is much less likely to occur based on the heritage of similar flight operations, as aerobraking Mars missions (such as MRO) perform multiple periapse correction maneuvers. In addition, commands are uplinked to the these spacecraft in a much shorter allowable time window when compared to SPACEJAM due to the difference in orbital period.

6.3.2 Launch Failure

Launch vehicle failure is a risk that must be accepted for every spacecraft. This risk is mitigated by selecting a launch vehicle with a long flight history and through launch insurance.

7 Development Cost and Schedule

7.1 Cost Breakdown

This mission falls under the category of a Discovery Class mission, and subsequently has a total mission budget of \$500 million. The overall budget is broken down as follows:

SPACEJAM Total Budget Breakdown		
Allocation	\$m	% of Total Budget
Spacecraft Design Contract	200	40
Reserve	150	30
Project Management	50	10
Payloads	50	10
Phase E	50	10
Science	25	5

The scope and focus of this document is within the \$200m reserved for the spacecraft contract. This allocation is then broken down further:

Spacecraft Contract Breakdown		
Category	\$m	% of Total Budget
LV Integration	1	0.6
Ground System	5	2.6
Planning and Mission Design	10	5
Structural	16	8
Thermal	20	10
ADCS	16	8
C&DH	4	2
EPS	2	1
RTG*	191	95
Telecommunications	4	2
Propulsion	2	1
Software	4	1.9
Harness	1	0.5
GSE	2	1.1
GFE	2	1
Systems Engineering	3	1.6
Product Assurance	2	1.1
Parts	4	2
Contamination	< 1	'0.1
Integration and Test	6	3.2
Reserve	20	10
Total	258	129.2

7.1.1 Discussion of Cost Estimate Methods

The cost estimates for this mission were based on a number of factors. Previous work on estimating science spacecraft uses historical data and averages for small to mid-sized spacecraft that have a budget of \$200m.[\[23\]](#) The values listed above are based on these averages; however, there are some notable differences. As this is strictly the spacecraft contract budget, the launch vehicle provider costs are not listed in this budget. Likewise, the science operations and components are rolled up into the science allocation of the overall Discovery Class budget.

Individual subsystem allocations have been adjusted based on the specifics of this mission. For example, because this mission is utilizing aerocapture as the method of orbit insertion, the propellant savings for this mission come out to 70% of the mass required for propulsive insertion. This leads to subsequent savings from the propulsion cost of the spacecraft contract.

This is likewise seen in the Telecommunications, Software, and C&DH subsystems. However, this savings is due to the heritage and use of flight proven technology from the Juno and Mars Science Laboratory missions.

As this mission is not a lander and will have a plan in place for end-of-life disposal, the costs for sterilization and contamination are subsequently lower than analogous lander missions.

Other subsystems, such as Thermal and Structures, instead saw an increase in cost when compared to the averages from spacecraft of similar sizes. This is due to the multiple spacecraft stages that the mission will utilize, as well as the costs of the TPS material and testing.

The exception to this method of pricing was the RTG, which is discussed in following sections.

7.1.2 Discussion of Labor Costs

In the cost roll-up above, labor costs are included within each subsystem. From pre-phase a through the end of phase A, the design team will consist of a total of ten engineers. In total, the salary per fiscal year of this team will not exceed \$4m. As the project proceeds through CDR and subsequently phase B, the team will expand to grow at each subsystem level to relieve overlap in

responsibilities. Other teams, such as V&V, flight test, operations, and technicians will be added through the project's lifespan.

7.1.3 Discussion of RTG Cost

As was discussed in the power section, the decision to use an RTG over solar panels was a choice based on the added complexity, mass, and critical risk of post-aerocapture solar panel deployment. This mission stands in the unique design space of an orbiter and a probe, as the spacecraft must travel to Jupiter encased within an aeroshell that will then be jettisoned post-aerocapture. As a result, the solar panels would have had to either be deployed during cruise and then somehow stowed during aerocapture, and then re-deployed. The alternative was to use two redundant sets of solar panels: one set on the cruise stage, and the other folded within the aeroshell. This would effectively double the required solar panel mass, as the cruise stage panels would still need to be sized for the Jupiter environment.

One set of solar panels would have added nearly 1000kg of mass to the mission, and required complex stowage and deployment post-aerocapture. While costly, an RTG is mechanically fail-safe, will save hundreds of kilograms of weight, and will not result in mission failure due to deployment failure.

The RTG cost estimate is based off of standard pricing of plutonium-fueled generators and the cost of launch provider testing that will be required in order to launch a radioactive payload from Cape Canaveral. Ultimately, this comes out roughly to \$840k per watt generated by the plutonium and \$28m for the additional launch costs.

7.1.4 Discussion of Cost Risk

However, due to the decision to proceed with the RTG design, a significant cost was added to the mission due to the additional launch verification tests and the raw cost of the plutonium. While it is clear that this choice will place the mission at least 30% over-budget, the decision ensures that other mission-ending failure modes are not present.

7.2 Schedule

After PDR, there will be three major milestones to accomplish before the spacecraft will be launched. Immediately after PDR, the Critical Design will begin. This phase will include the verification of the launch vehicle as well as final spacecraft design. Thorough simulations of the spacecraft's structural integrity will be run, and each subsystem will be checked for validation. The CDR milestone demonstrates that the design is sufficient to commence full-scale fabrication and assembly of the spacecraft, and reviews the final design of the spacecraft. This phase is expected to take approximately one year.

The next stage will be the Flight Readiness phase. This phase includes the procurement of hardware and equipment that will compose the spacecraft, as well as assembly and testing. Towards the FRR, a performance prediction as well as launch operations procedures will be put together. The FRR will determine that the system is prepared for a successful launch and operation. This phase is expected to take about two and a half years.

The last stage before launch is the Launch Readiness phase. Upon completion of the FRR, the spacecraft will be shipped to the launch site and integrated into the launch vehicle. A thorough set of flight simulations will be made and presented during the LRR. The launch vehicle and the spacecraft will be given a final check for integrity before the launch is green-lit, which is scheduled for May 2023.

After launch, there will be a Post-Launch Assessment Review (PLAR), which will consist of a summary of the launch as well as the project budget [24].

An image of the schedule is displayed in Figure 74.

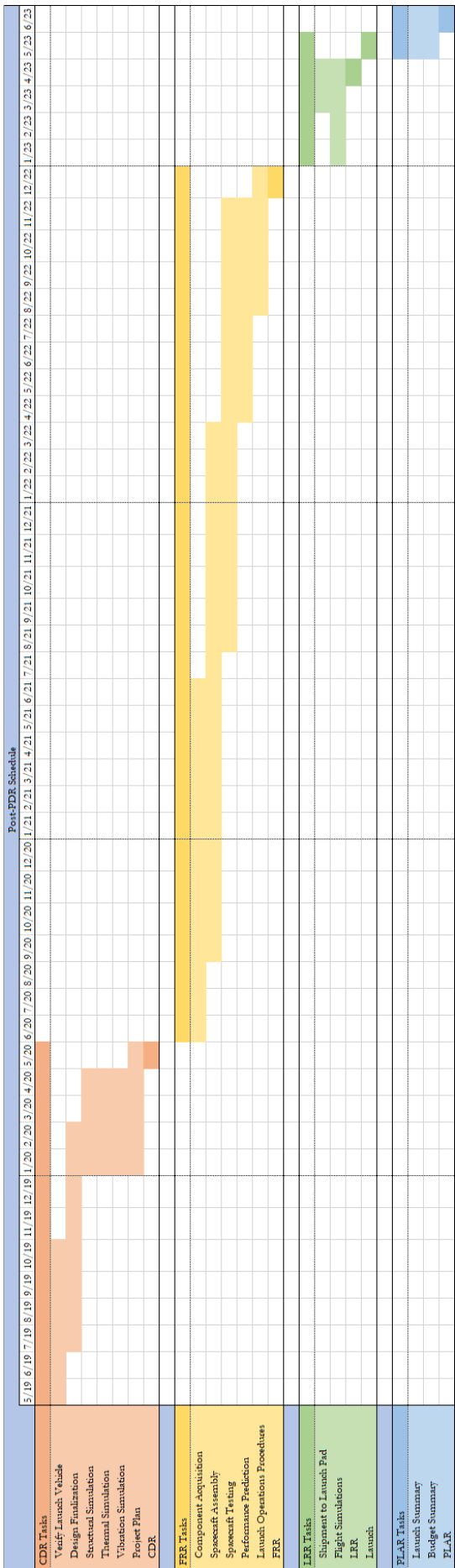


Figure 74: Post-PDR Schedule

8 TBR Requirement Resolution

Table 42 presents a path forward for each requirement for each requirement labeled as "To Be Revised" (TBR).

Req. No.	Requirement	Path Forward
PROP-03	The structure shall provide 141 m/s ΔV with 10% ΔV margin (TBR) for the Cruise Stage.	Better understanding of mission uncertainties needed for sufficient margin.
PROP-04	The structure shall provide 378 m/s ΔV with 20% ΔV margin (TBR) for the Orbital Stage.	Better understanding of mission uncertainties needed for sufficient margin.
TPS-01	The TPS shall maintain scientific (payload) equipment between -20° and +60°C. (TBR)	Thermal requirements of every spacecraft component not fully understood.
TPS-02	The TPS shall maintain operational equipment between -20° and +50°C. (TBR)	Thermal requirements of every spacecraft component not fully understood.
TPS-05	The rigid aeroshell shall include 4cm thick (TBR) of carbon phenolic ablative material.	Higher fidelity thermal models of the aerocapture event required in order to properly size aeroshell.
TELECOM-03	Adjustments to the perijove raise maneuver shall be uplinked to the spacecraft within 1 day (TBR) of the perijove raise maneuver.	Minimum time to perijove raise is greater than 3 days, more information needed on orbit determination processes on the ground.
TELECOM-07	The spacecraft will establish link with NASA's DSN 5 minutes (TBR) following spacecraft separation at launch.	Determine minimum possible time to establish link after LV separation

Table 42: TBR Requirements

9 Appendix

9.1 Imaging Frequency calculations

The duration of a plume t_d , is equivalent to the end time minus the start time.

$$t_d = t_e - t_s \quad (1)$$

The resolution of each of these measurements is equivalent to the reciprocal of the imaging frequency. For example, taking two images an hour is equivalent to a resolution of 30 minutes.

$$\text{resolution} = \frac{1}{f} \quad (2)$$

The uncertainty in each of the start and end time is equivalent to half the resolution. For example, an imaging resolution of 30 minutes gives an uncertainty of plus or minus 15 minutes, and the actual event is assumed to have started or ended in the exact middle of the window.

$$\delta t_e = \delta t_s \equiv \pm \frac{\text{resolution}}{2} \quad (3)$$

Therefore:

$$\delta t_e = \delta t_s = \pm \frac{1}{2f} \quad (4)$$

The uncertainty in the duration time is then:

$$U_{t_d} = \sqrt{\left(\frac{\partial t_d}{\partial t_e} \delta t_e\right)^2 + \left(\frac{\partial t_d}{\partial t_s} \delta t_s\right)^2} \quad (5)$$

where:

$$\frac{\partial t_d}{\partial t_e} = 1 \quad (6)$$

and:

$$\frac{\partial t_d}{\partial t_s} = -1 \quad (7)$$

Therefore:

$$U_{t_d} = \sqrt{\left(\frac{1}{2f}\right)^2 + \left(\frac{-1}{2f}\right)^2} \quad (8)$$

$$U_{t_d} = \sqrt{\frac{1}{4f^2} + \frac{1}{4f^2}} \quad (9)$$

Finally:

$$U_{t_d} = \sqrt{\frac{1}{2f^2}} \quad (10)$$

Therefore, for $U_{t_d} = 1$ hour, $f = \sqrt{1/2} \approx 0.707$ images per hour.

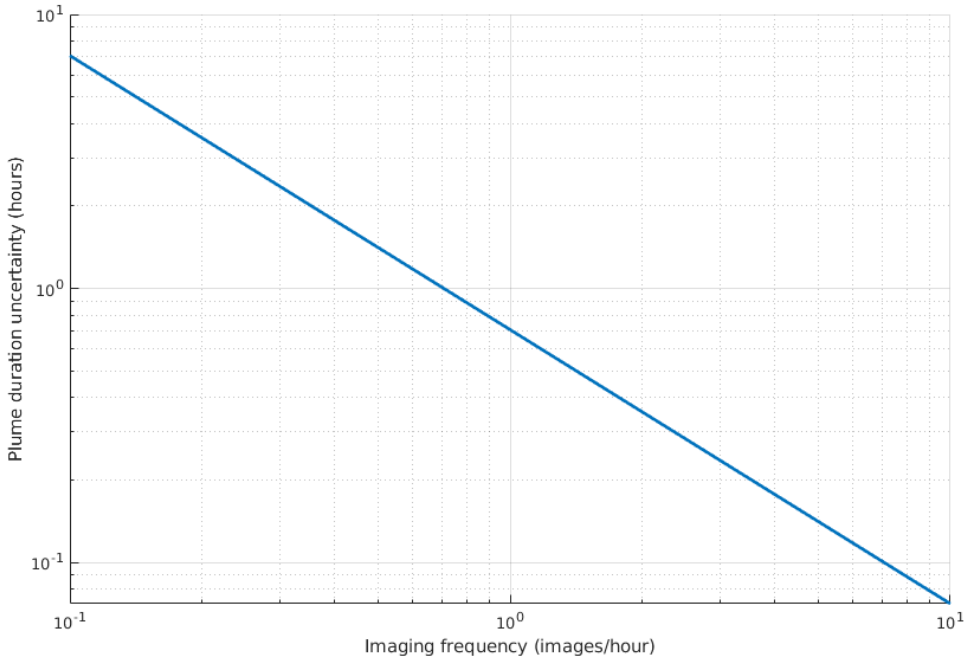


Figure 75: The frequency that images need to be taken in order to achieve a certain plume duration uncertainty.

9.2 Carrier Link and Data Rate Calculations

Carrier Link Margin for each antenna is calculated in dB using the following equation:

$$M = EIRP + G_r - L_{fs} - L_p - L_l - DSN_s - SDST_n - C_l \quad (11)$$

where:

M	Margin (dB)
$EIRP$	SPACEJAM EIRP (dBm)
G_r	DSN Antenna Gain (dB)
L_{fs}	Path Loss (dB)
L_p	Total Pointing Loss (dB)
L_l	Line losses (dB)
DSN_s	DSN Receiver Sensitivity (dBm)
$SDST_n$	SDST Noise Value (2.8 dB)
C_l	Carrier Suppression (10 dB)

Data rates were estimated using the following equation:

$$R = 10^{(P_r + 228.6 - P_n - \frac{E_b}{N_o})/10} \quad (12)$$

where:

R	Data Rate (bps)
P_r	Total Received Power (dB)
P_n	Noise Figure (dB)
$\frac{E_b}{N_o}$	Required $\frac{E_b}{N_o}$ (3 dB)

10 Acknowledgements

References

- [1] NASA, “NASA Systems Engineering Handbook: Rev 1,” .
- [2] Fortescue, S. and Stark, “Spacecraft Systems Engineering, Fourth Edition,” 2011.
- [3] Petropoulos, A. E., Longuski, J. M., and Bonfiglio, E. P., “Trajectories to Jupiter via Gravity Assists from Venus, Earth, and Mars,” *Journal of Spacecraft and Rockets*, Vol. 37, No. 6, 2000, pp. 776–783.
- [4] NASA, “Mars Science Laboratory Entry Descent and Landing Instrument (MEDLI),” .
- [5] Garrett, H. B., Levin, S. M., Bolton, S. J., Evans, R. W., and Bhattacharya, B., “A revised model of Jupiter’s inner electron belts: Updating the Divine radiation model,” 2005.
- [6] Marshall, R., “Module 8: Comparative Environments: Jupiter,” 2018.
- [7] Clark, K. B., “EJSM/Jupiter Europa Orbiter Design and Status,” January 18, 2010.
- [8] Ringwalkd, F. A., “SPS 1020 (Introduction to Space Sciences). California State University, Fresno,” February 29, 2000.
- [9] NASA, “Reaction Control Quick Reference Data,” .
- [10] Space, R., “Separation Mechanism,” .
- [11] Space, R., “Separation Mechanism Installed View,” .
- [12] “Aluminum 7075-T6,” .

- [13] Corp., A., “2 Axis Fine Sun Sensor System,” .
- [14] Aerospace, B., “High Accuracy Star Tracker,” .
- [15] Girard, Morana, L. R. M. B. M. P. C. M. O. B., “Recent advances in radiation-hardened fiber-based technologies for space applications,” August 2018.
- [16] Corp., N. G., “LN-200s Inertial Measurement Unit (IMU),” .
- [17] Systems, N. S., “10 Nms Reaction Wheel,” .
- [18] Mukai, Hansen, M. T. D., “Juno Telecommunications,” October 2012.
- [19] Allen Y. Lee, E. L. B., “Pointing Stability Performance of the Cassini Spacecraft,” 2014.
- [20] Mittelsteadt, C. O., “Cassini Attitude Control Operations – Guidelines Levied on Science To Extend Reaction Wheel Life,” 2014.
- [21] Group, A., “1N Monopropellant Hydrazine Thruster,” .
- [22] Group, A., “20 N Monopropellant Hydrazine Thruster,” .
- [23] Sarsfield, L. P., “The Cosmos on a Shoestring: Small Spacecraft for Space and Earth Science,” 1998.
- [24] NASA, “2019 NASA Student Launch Handbook and Request for Proposal,” 2019.